Summer 8-13-2010

A Study of the Ebola Virus Glycoprotein: Disruption of Host Surface Protein Function and Evasion of Immune Responses

Joseph R. Francica
University of Pennsylvania, jfrancica@gmail.com

A Study of the Ebola Virus Glycoprotein: Disruption of Host Surface Protein Function and Evasion of Immune Responses

Abstract
The Ebola virus (EBOV) is a member of the family, Filoviridae, and is the etiological agent of Ebola hemorrhagic fever (EHF). This disease causes significant morbidity and mortality in humans and non-human primates, with human fatality rates reaching 90% during outbreaks of the Zaire subtype. Currently, there are no licensed vaccines or antivirals for EBOV and our understanding of viral pathogenesis is limited. Therefore, further studies examining the pathogenic mechanisms of EBOV are necessary to fully understand and effectively treat EHF. The main Ebola virus glycoprotein (GP) is the only viral protein found on the surface of the Ebola virion and is therefore responsible for mediating attachment and entry of the virus into host cells. However, expression of GP independently of other viral proteins induces dramatic morphological changes including cell rounding and detachment in those cells expressing GP. This phenomenon is referred to as GP-mediated cytopathology and is the focus of the work described herein. We have undertaken studies to identify the mucin domain, a highly glycosylated domain within GP, as sufficient to cause this cytopathology. We then have used a cell-biological approach to elucidate the mechanism by which this cytopathology occurs. The mucin domain forms a glycan shield at the plasma membrane, disrupting the function of host proteins in the vicinity of GP. We then show that GP-mediated shielding of major histocompatibility complex class I at the cell surface prevents the activation of CD 8+ T cells. Additionally, GP can sterically shield its own epitopes at the cell surface. This model of steric hindrance was also found to apply to the surface of pseudoviral particles, where access to a neutralizing epitope on GP is affected. Our data indicate that the EBOV GP forms a glycan shield with the ability to block antibody binding and disrupt protein function at the cell and virion surface. This study describes a novel viral mechanism for the disruption of surface protein function and suggests a possible mechanism for the evasion of host humoral and cellular immune responses.

Degree Type
Dissertation

Degree Name
Doctor of Philosophy (PhD)

Graduate Group
Cell & Molecular Biology

First Advisor
Paul Bates, Ph.D.

Keywords
Ebola virus, glycan shield, MHC I, mucin, adhesion, viral glycoprotein

Subject Categories
Virology

A STUDY OF THE EBOLA VIRUS GLYCOPROTEIN: DISRUPTION OF HOST SURFACE PROTEIN FUNCTION AND EVASION OF IMMUNE RESPONSES

Joseph Richard Francica

A DISSERTATION

in

Cell and Molecular Biology

Presented to the Faculties of the University of Pennsylvania

in Partial Fulfillment of the Requirements for the Degree of Doctor of Philosophy

2010

Dissertation Supervisor:

_____

Paul Bates, Ph.D., Associate Professor of Microbiology

Graduate Group Chairperson:

_____

Daniel S. Kessler, Ph.D., Associate Professor of Cell and Developmental Biology

Dissertation Committee:

Jeffrey M. Bergelson, M.D., Associate Professor of Pediatrics
Robert W. Doms, M.D., Ph.D., Professor of Pathology and Laboratory Medicine
Michael S. Marks, Ph.D., Associate Professor of Pathology and Laboratory Medicine

I would like to dedicate this dissertation to my grandfather, Robert Gauthier. His persistence in his scientific career, the integrity with which he lives his life, and his encouragement of me from a young age has been a guiding influence in my life.

ACKNOWLEDGMENTS

I would like to thank Paul Bates for his mentorship throughout my graduate career. Paul encouraged me to further investigate the initial observations that led to this dissertation, while allowing me the freedom to take my studies in whichever direction interested me. His enthusiasm for scientific discovery and the creativity in his experimental approach has made a deep impression on me as a new scientist.

I would like to thank Jeffrey Bergelson, Robert Doms and Michael Marks for their service on my thesis committee and for the genuine interest they have taken in my work. Their advice has helped me focus and streamline my studies, which has undoubtedly condensed the time of my graduate career. I would especially like to acknowledge the mentorship of my program director, Robert Doms, who took personal interest not just in my work, but also in my well being as a graduate student, and who gave me valuable advice in seeking postdoctoral positions.

I would like to thank the past and present members of the Bates lab, who have made both direct and indirect contributions to this work. Also, a special thanks to the members of the Doms lab, with whom sharing technical advice, reagents and matters less scientifically related was a daily occurrence.

I would like to thank Marisa Bartolomei, Richard Schultz, and Robert Doms for appointing me to the Cell and Molecular Biology and Emerging Infectious Diseases training grants, which financially supported me through my graduate career and allowed me to present my research at several domestic and international meetings.

Finally, I would like to thank my family and friends for their constant love and support throughout the highs and lows of my graduate career.

ABSTRACT

A STUDY OF THE EBOLA VIRUS GLYCOPROTEIN: DISRUPTION OF HOST SURFACE PROTEIN FUNCTION AND EVASION OF IMMUNE REPSONSES

Joseph Richard Francica

Dissertation Supervisor: Paul Bates

The Ebola virus (EBOV) is a member of the family, *Filoviridae*, and is the etiological agent of Ebola hemorrhagic fever (EHF). This disease causes significant morbidity and mortality in humans and non-human primates, with human fatality rates reaching 90% during outbreaks of the Zaire subtype. Currently, there are no licensed vaccines or antivirals for EBOV and our understanding of viral pathogenesis is limited. Therefore, further studies examining the pathogenic mechanisms of EBOV are necessary to fully understand and effectively treat EHF. The main Ebola virus glycoprotein (GP) is the only viral protein found on the surface of the Ebola virion and is therefore responsible for mediating attachment and entry of the virus into host cells. However, expression of GP independently of other viral proteins induces dramatic morphological changes including cell rounding and detachment in those cells expressing GP. This phenomenon is referred to as GP-mediated cytopathology and is the focus of the work described herein. We have undertaken studies to identify the mucin domain, a highly glycosylated domain within GP, as sufficient to cause this cytopathology. We then have used a cell-biological approach to elucidate the mechanism by which this cytopathology occurs. The mucin domain forms a glycan shield at the plasma membrane, disrupting the function of

host proteins in the vicinity of GP. We then show that GP-mediated shielding of major histocompatibility complex class I at the cell surface prevents the activation of CD 8^+ T cells. Additionally, GP can sterically shield its own epitopes at the cell surface. This model of steric hindrance was also found to apply to the surface of pseudoviral particles, where access to a neutralizing epitope on GP is affected. Our data indicate that the EBOV GP forms a glycan shield with the ability to block antibody binding and disrupt protein function at the cell and virion surface. This study describes a novel viral mechanism for the disruption of surface protein function and suggests a possible mechanism for the evasion of host humoral and cellular immune responses.

TABLE OF CONTENTS

LIST OF FIGURES

CHAPTER 1

CHAPTER 2

CHAPTER 3

CHAPTER 4

CHAPTER 1 – EBOLA VIRUS LITERATURE REVIEW AND INTRODUCTION TO EBOLA GLYCOPROTEIN-MEDIATED CYTOPATHOLOGY

1.1 Identification of the Ebola virus

The first documented outbreak of Ebola virus (EBOV) began on September 5th, 1976, at the Yambuku Mission Hospital near Bumba in northern Zaire (now the Democratic Republic of Congo, DRC). A 44-year-old patient had presented himself to the hospital 10 days earlier with a febrile illness and was given an injection of chloroquine for presumptive malaria, which alleviated his fever. However, febrile symptoms returned on September 1st; 3 days after being admitted to the hospital, the patient died. By October 24th of that year, 280 fatal human cases of an unknown viral hemorrhagic fever had been documented around Yambuku, and later Kinsasha, along with only 38 serologically-confirmed survivors [1].

In the weeks after this index case was reported, an international team of doctors deployed to the effected region with the following goals: to surveil and contain the disease, to conduct an epidemiological analysis of its spread, and to begin investigating the microbial agent behind this novel syndrome. They found that patients often presented with general symptoms such as fever, headache and sore throat, but showed more critical signs as the disease progressed such as diarrhea, vomiting and bleeding [1]. Initially, the disease was thought to be one of the other viral hemorrhagic fevers known at the time, such as Crimean Congo hemorrhagic fever or Marburg disease [2]. Indeed, initial characterization by electron microscopy revealed particles similar in morphology to Marburg virus (MARV) [3,4,5]. However, the virus isolated from the Yambuku outbreak

was found to be serologically distinct from MARV and was given the name, Ebola virus, after the nearby Ebola River [1].

It is interesting to note that almost concomitantly to this outbreak of what would later be identified as the Zaire subtype of EBOV, an outbreak of a genetically distinct subtype had begun just months earlier in Sudan. (The Sudan outbreak would be investigated slightly after the Zaire outbreak, as a World Heath Organization team was only dispatched to Sudan in late October of 1976 [6].) The Sudan outbreak occurred primarily in the villages of Nzara and Maridi, only a few hundred kilometers northeast of the Bumba region in Zaire (Figure 1-1). The approximately 4 day journey between Nzara, Sudan and Bumba, Zaire was occasionally made by residents of that region, and so at the time it was considered a possibility that an infected individual had traveled from Nzara to the Yambuku hospital to initiate that outbreak [1,6]. Subsequent genetic analysis of the viruses from these first two EBOV outbreaks confirmed their distinct phylogeny, thereby disproving this theory; nevertheless, the temporal and geographic coincidences remain.

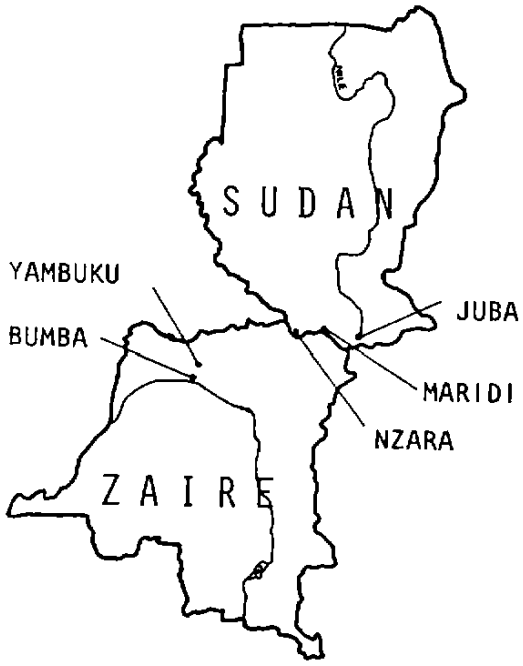

Figure 1-1 Map of Sudan and Zaire EBOV outbreaks. Map shows the main sites of the first two documented outbreaks of EBOV. Both outbreaks occurred during the fall of 1976 and were separated by only several hundred kilometers, yet the species of virus were genetically and serologically distinct.

Figure taken from: (1978) Ebola haemorrhagic fever in Sudan, 1976. Report of a WHO/International Study Team. Bull World Health Organ 56: 247-270. Reprinted with permission from the World Health Organization.

1.2 Outbreaks and natural reservoirs

The Ebola virus is not known to be endemic to any human population, but instead sporadically outbreaks. Since the first documented outbreaks in 1976, a total of 16 separate human outbreaks have occurred. Additionally, 5 additional human cases have been reported which did not result in a wider outbreak [7,8,9,10]. In total, 2,292 human cases of Ebola Hemorrhagic Fever (EHF) have been reported, resulting in 1,526 deaths. Furthermore, 13 human cases of asymptomatic EBOV infection have been reported in connection with outbreaks of the Reston subtype of EBOV in non-human primates or swine. These individuals seroconverted but showed no other symptoms of EHF [11,12,13].

Outbreaks of pathogenic EBOV in human populations have occurred exclusively in the sub-Saharan African countries of Zaire (DRC), Sudan, Côte d'Ivoire, Republic of Congo, Gabon and Uganda. Nonhuman primates, many species of which inhabit this region, are also acutely susceptible to EBOV. Serological studies and genetic detection in several central African primate species have revealed exposure to and infection with EBOV in Cameroon, Gabon and Republic of Congo [14,15]. Additionally, the Reston subtype of EBOV has caused disease outbreaks in the Philippines in nonhuman primates and swine [13,16].

Although humans can transmit the virus to one another, they are considered non-natural hosts for EBOV. There is no known insect vector that can transmit the virus. Index cases are thought to occur through zoonotic events, either from a natural animal reservoir or from an incidental animal host [17]. Human outbreaks in Gabon and the

Republic of Congo have been epidemiologically linked to such intermediate hosts, including chimpanzees, gorillas and forest duikers through the handling of infected carcasses by local hunters [18,19]. However, because EBOV is highly pathogenic in these animals, they are considered poor candidates for a natural reservoir for the virus. In the Philippines, where two documented outbreaks of the Reston subtype of EBOV have occurred, swine have been found to host the virus. Human exposure to this strain is thought to have occurred though contact by farmers with pigs or their products. However, it remains unknown whether swine are incidental hosts, or part of the natural replication cycle of the virus [13].

Recently, several species of fruit bats have been implicated as being a natural reservoir for EBOV [20,21,22]. The presence of EBOV-specific IgG or viral sequences have be detected in six species: *Micropteropus pusillus, Mops condylurus, Rousettus aegyptiacus, Hypsignathus monstrosus*, *Epomops franqueti,* and *Myonycteris torquata*, although live virus has yet to be isolated from a bat [21,22]. Interestingly, the natural habitat for several of these species encompasses the sub-Saharan region where EBOV outbreaks have occurred (Figure 1-2). Fruit bats have also been directly implicated as the source of a 2007 outbreak in the DRC [23]. EBOV may be non-pathogenic in these animals and may replicate at very low levels. Virus could be transmitted from bats to humans during hunting or from bats to forest animals through bodily fluids in droppings or partially eaten fruit. Taken together, these data- though not conclusive- strongly suggest that certain species of fruit bats may be a reservoir for EBOV.

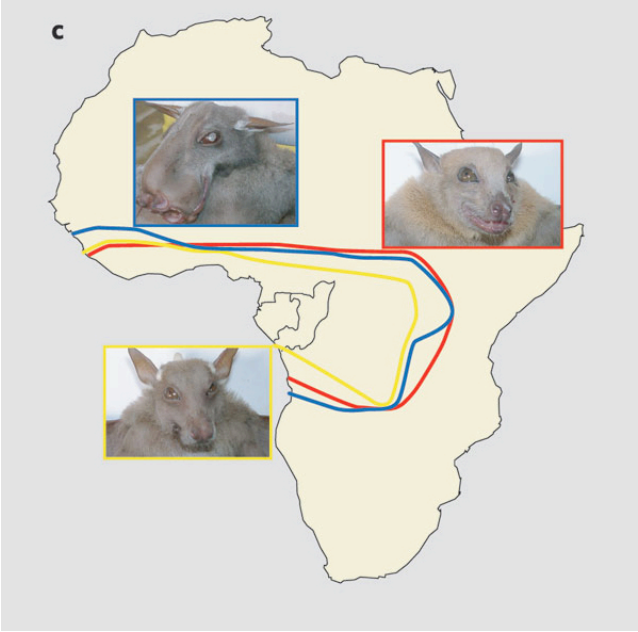

Figure 1-2 Habitat map of bats exposed to EBOV. Geographic distribution (inside coloured lines) of the fruit bats *Hypsignathus monstrosus* (blue), *Epomops franqueti* (red) and *Myonycteris torquata* (yellow).

Figure and legend taken from: Leroy EM, Kumulungui B, Pourrut X, Rouquet P, Hassanin A, et al. (2005) Fruit bats as reservoirs of Ebola virus. Nature 438: 575-576. Reprinted with permission from Nature Publishing Group.

1.3 Epidemiology and clinical syndrome

After an initial transmission event from animals to people, the spread of infection between individuals is dependent on close personal contact with infected bodily fluids. Nosocomial transmission is common and was observed in the first documented outbreak in Zaire, where poorly sterilized needles were used to give treatments to multiple patients at the Yambuku Mission Hospital, likely causing several infections [1]. During outbreaks, health care workers exposed to Ebola infected patients often became infected themselves, presumably through poor barrier-nursing practices [1,6,24,25,26,27]. Transmission can also occur when family members care for infected individuals at home, and also through contact with cadavers during certain burial practices [24,25,27].

EBOV infection in humans is acute and fulminant. To date, five subtypes of EBOV have been identified: Zaire, Sudan, Bundibugyo, Côte d'Ivoire, and Reston. Of these, Zaire, Sudan, and Bundibugyo cause EHF that is fatal in ~30 to 90% of cases (depending mostly on the subtype of virus in the outbreak) making EBOV a biosafety level (BSL) 4 agent [28,29]. Cote d'Ivoire was associated with one nonfatal human infection, and Reston is considered non-pathogenic in humans [7,11,12]. The average incubation period is approximately 6 days; however, incubation may range from 2 to 21 days [30,31]. The clinical syndrome of EHF may be divided into two phases. The first stage typically lasts about 1 week; during this time patients present with symptoms such as fever, myalgia, anorexia, nausea, vomiting, abdominal pain, arthralgia, asthenia, diarrhea, and back pain [1,31,32]. This first stage may also be characterized by conjunctivitis, sore throat and a maculopapular rash. About 7 days after the onset of

symptoms, patients often have the appearance of convalescence. Patients that will go on to survive continue convalescence for several weeks, while terminal patients encounter the latter stage, which last an average of 3 days [31]. This second stage of the disease may be characterized by bleeding at skin puncture sites, mucosal sites such as the gums, nose, eyes or in the stool; however, hemorrhaging is only observed in a subset of patients and there are conflicting reports as to the correlation of hemorrhaging and a fatal outcome [1,31,32]. Death often occurs with tachypnea and patients usually die in a state of shock or coma [31,33]. The cause of death is thought to be from septic shock and multi-system organ failure, though this has only been directly studied in nonhuman primate disease models [34,35].

1.4 Disease pathogenesis

Our understanding of the pathogenesis of EBOV is derived mostly from experimental infection of nonhuman primates, as in-depth human studies are difficult to perform in the rural setting of most human EBOV outbreaks. Two pathogenesis models, rhesus macaques and cynomolgus macaques are typically used [34,35,36]. Initially, EBOV is thought to replicate in monocytes and dendritic cells, which are aberrantly activated and show abnormal cytokine profiles [35,37,38,39]. From this early stage, two important pathogenic mechanisms may originate. First, coagulopathy may be initiated by the upregulation of tissue factor by infected monocytes and macrophages [40]. This may lead to disseminated intravascular coagulation (DIC), which is observed during infection and likely contributes to hemorrhage symptoms and multi-organ failure [1,40,41].

Second, adaptive immune responses appear to be disrupted. Cells of lymphocytic origin, which are not productively infected by EBOV, are nonetheless depleted during infection by an incompletely understood mechanism of bystander apoptosis [35,42,43,44,45]. The loss of T and B cells prevents an adaptive immune response against the virus and correlates with fatal outcomes [42,43]. Conversely, survivors of EHF are often distinguished by their ability to mount an adaptive response, as judged by the production of EBOV-specific IgG antibodies [42,43,46]. Left unchecked by aberrant or absent immune responses, EBOV replicates to high titers in the blood. Viremia has been reported above 10^6 PFU per mL blood and as high as 10^{10} viral RNA copies per mL [1,47]. Not surprisingly, higher viral titers correlate with a fatal outcome [46,47].

After initial replication in sentinel immune cells, the virus is then thought to traffic back to the regional lymph nodes, where the virus may disseminate through the blood to other tissues. EBOV can productively infect many organs, including the gastrointestinal tract, liver, and kidneys [35,38]. Endothelial and epithelial cells also become infected at later stages of disease [35,48].

Several viral proteins likely play a key role in EHF pathogenesis. EBOV encodes two proteins (VP35 and VP24, described later) that are specific inhibitors of the interferon response and have been shown be potent in dendritic cells [37,49,50,51]. A potential role for the viral glycoprotein in pathogenesis is the focus of this dissertation and will be discussed in detail in latter sections.

1.4 Treatment and Prevention

There are no licensed vaccines or antivirals for the treatment or prevention of EHF. During outbreaks in rural African settings, care is mostly supportive and includes pain management and fluid replacement. To contain ongoing outbreaks, international medial teams have found the education of local medical staff on barrier-nursing practices, and the institution of safe burial practices to be highly effective [24,25,26]. The administration of convalescent patient blood products has been used to treat EHF in an outbreak and an isolated case with reported success [9,33]. However, such passive immunotherapy is controversial, as other factors may have played a role in patient recovery and primate models have been unable to reproduce this efficacy [52,53,54].

Recently, several therapies for EHF have shown promise in experimental models. The administration of recombinant nematode anticoagulant protein c2 (rNAPc2) has been demonstrated to prolong and increase survival in rhesus macaques given a lethal EBOV challenge [55]. rNAPc2 presumably provides protection through its inhibition of the coagulation cascade, reducing the coagulopathy observed in this model. Other studies have shown initial therapeutic benefit from the administration of antisense phosphorodiamidate morpholino oligomers (PMOs) and small interfering RNAs (siRNA) against EBOV proteins, which presumably interfere with viral replication. PMOs directed against the polymerase, VP35 and VP24 have shown some prophylactic protection in rhesus macaques [56]. siRNAs directed against the viral polymerase were shown to protect guinea pigs and siRNAs directed against the polymerase, VP35 and VP24 were shown to protect macaques in pre- and post- exposure challenge models [57,58]. Post-exposure protection has also been achieved in primate models using recombinant

vesicular stomatitis virus (rVSV) encoding the EBOV glycoprotein [59]. Notably, rVSV was administered to an individual in the post-exposure setting of a laboratory needle stick. The patient did not develop EHF, though it has not been determined if they were productively infected [60].

Although only in the early stages of development, protein-based and small molecule inhibitors of EBOV entry and replication are currently being investigated for use as antivirals [61,62,63,64].

Although no approved vaccine exists for the prevention of EBOV infection, significant progress has been made using several vaccine platforms. Human parainfluenza virus type 3, rVSV, DNA and/or replication-defective adenoviral vectors, and virus like particles have all shown promise in protecting primates against a lethal EBOV challenge in a pre-exposure setting [65,66,67,68,69,70]. Efficacy trials of these candidate vaccines in humans will probably not be possible due to the sporadic nature and remote location of EBOV outbreaks. Thus, FDA licensure will be dependent on safety and efficacy demonstrations in two animal models, termed the 'animal rule' [71].

1.5 Genomic organization, viral proteins and virion structure

EBOV is a member of the family *Filoviridae* in the order *Mononegavirales*, and so encodes its genome in single-stranded linear RNA in the negative orientation. The genome is approximately 19 kb long, and encodes 7 open reading frames (ORFs) [29]. The different subtypes of EBOV are approximately 35-45% divergent at the nucleotide level but are considered highly genomically stable over time [28,72]. The EBOV genome

contains 3' and 5' (leader, trailer) extragenic sequences that can form secondary structures and serve to initiate transcription and genome replication [73,74]. Individual genes are separated by conserved transcriptional signals. Figure 1-3 (A) shows the organization of ORFs and intragenic features of the EBOV genome.

The EBOV genome encodes 8 major gene products, 7 of which are incorporated into viral particles. The viral genomic RNA is encapsulated in a ribonuclear protein (RNP) complex (nucleocapsid) consisting of the nucleoprotein (NP), minor nucleoprotein (VP30), VP35, and polymerase (L) protein [75]. This complex is then coated in a matrix layer consisting of the major matrix protein (VP40) and minor matrix protein (VP24). This is further enveloped by a lipid bilayer studded with the main viral glycoprotein (GP) (Figure 1-3 B). The eighth viral protein is the major product of the GP ORF, but is a smaller, secreted glycoprotein, sGP [76]. The full-length membrane-spanning form found in the viral envelope, GP, originates from the addition of an extra adenosine residue in the glycoprotein transcript by the polymerase during transcription [76]. During infection, the ratio between sGP and GP transcripts is approximately 80% / 20% [77]. The processing and function of the different glycoprotein forms are described in the following sections.

EBOV particles are filamentous in shape but are often branched or in circular confirmations; they have a diameter of approximately 80 nm and a variable length that can exceed 1000 nm [78,79].

A.

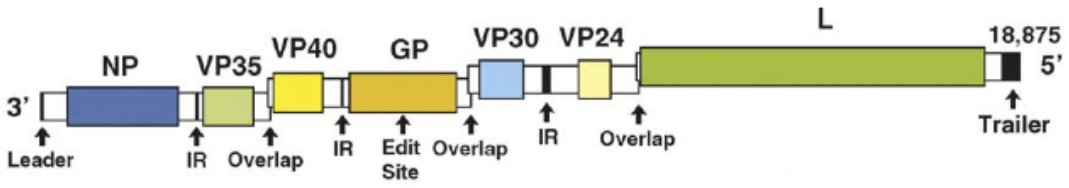

B.

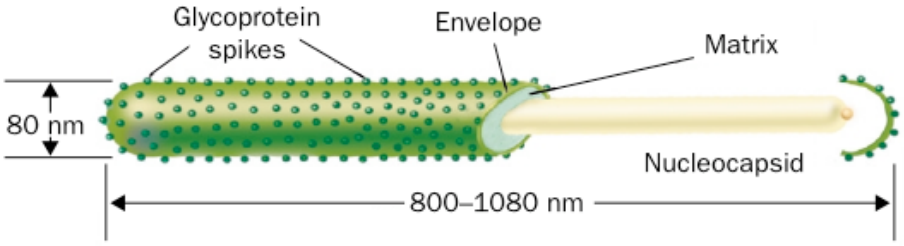

Figure 1-3 EBOV genome organization and virion structure. (A) Genomic organization of EBOV. Coding regions are shown in colored boxes. IR= intergenic region. NP= nucleoprotein. GP= glycoprotein. L= large polymerase subunit. (B) Structure of a filamentous EBOV particle. Genome is encapsulated by nucleocapsid complex (NP, L, VP30 and VP35), which is encased by the matrix (VP40 and VP24), which is surrounded by a lipid envelope studded with GP.

Figures taken from: (A) Sanchez A, Rollin PE (2005) Complete genome sequence of an Ebola virus (Sudan species) responsible for a 2000 outbreak of human disease in Uganda. Virus Res 113: 16-25. (B) Mahanty S, Bray M (2004) Pathogenesis of filoviral haemorrhagic fevers. The Lancet Infectious Diseases 4: 487-498. Reprinted with permission from Elsevier.

1.7 Glycoprotein processing, function and structure

Transcription and translation of the glycoprotein gene gives rise to several major and minor products during infection. The major product of transcription is the pre- sGP transcript. This is translated into pre- sGP protein, which is then cleaved by furin into sGP and a small C-terminal fragment, the Δ peptide [80]. However, during transcription the viral polymerase occasionally adds an extra adenosine residue while reading through an editing region of 7 uridine residues. The resulting -1 ORF reads through the remaining portion of the gene and encodes for the membrane-bound form of the EBOV glycoprotein, GP [76,77]. Similar editing by the polymerase into a -2 ORF produces a small secreted glycoprotein product (ssGP); however, this product has not been demonstrated in the context of EBOV infection [81].

The GP transcript is initially translated as a precursor (GP_0), which is then cleaved by furin in the Golgi into two subunits: a surface subunit, GP_1, and a membrane-spanning subunit, GP_2 [82]. These subunits remain covalently connected through a single intermolecular cysteine bond [83]. This heterodimer associates non-covalently with two other heterodimers in a higher-order trimeric complex to produce the GP spike that incorporates into budding virions [84]. Figure 1-4 (A) shows the domains and features of GP. In addition to anchoring the glycoprotein to the membrane, GP_2 houses the fusion machinery, which allows the RNP complex to be delivered to the cytosol [85]. Fusion is accomplished by the formation of a 6-helix bundle between the alpha-helical heptad repeat (HR) 1 and 2 regions after an internal fusion loop becomes anchored in the host

A.

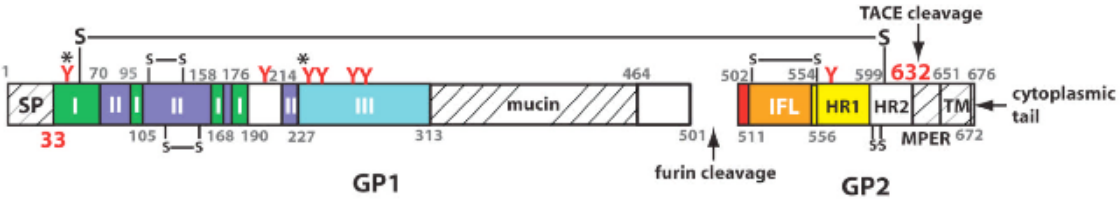

B.

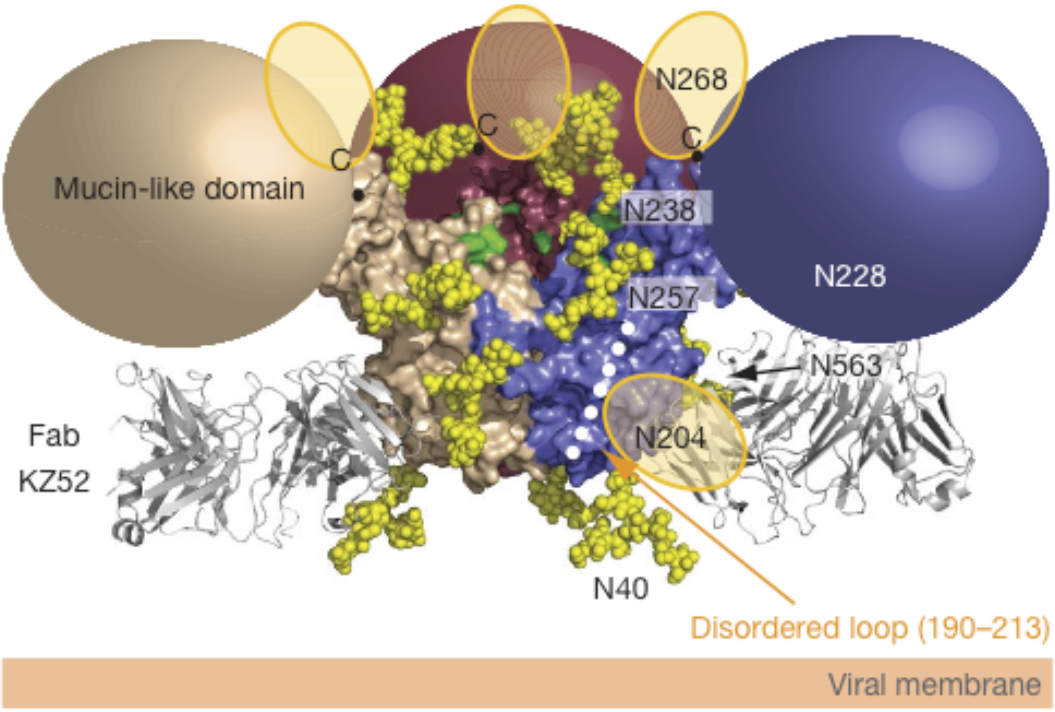

Figure 1-4 Feature map and structure of EBOV GP. (A) Domain schematic of GP. Domains observed in the crystal structure are coloured and numbered according to the description in the text. White and hash-marked regions designate crystallographically disordered and construct-deleted regions, respectively. SP, signal peptide; I, GP1 base; II, GP1 head; III, GP1 glycan cap; mucin, mucin-like domain; IFL, internal fusion loop; HR1, heptad repeat 1; HR2, heptad repeat 2; MPER, membrane-proximal external region; TM, transmembrane domain. Red Y-shaped symbols designate the predicted N-linked glycosylation sites; those sites marked with an asterisk were mutated. (B) Model of the fully glycosylated GP. N-linked bi-antennary complex-type glycans ($Gal_2Man_3GlcNAc_4$) were modelled onto the GP1 glycan-cap subdomain. Oligosaccharides are shown as yellow space-filling spheres and for clarity; only those glycans belonging to the purple monomer are labelled. Note that the glycans on N228 and N563 reside on the back of the

purple monomer and are partly obscured. The glycans at N204 and N268 are found in regions that are poorly ordered in the structure and as a result: their tentative locations are shown as orange ovals. The C termini of the last ordered residues of GP1, to which mucin-like domains are linked, are marked with 'C' (top of the chalice), and coloured spheres (beige, pink and purple) outline the predicted positions of the mucin-like domains attached in each of these regions. Surface residues previously identified to be critical for viral entry, recessed in the chalice bowl and RBS, are coloured green. Fab KZ52 (grey) recognizes a non-glycosylated, predominantly GP2-containing epitope at the base of the chalice.

Figures and legends taken from: Lee JE, Fusco ML, Hessell AJ, Oswald WB, Burton DR, et al. (2008) Structure of the Ebola virus glycoprotein bound to an antibody from a human survivor. Nature 454: 177-182. Reprinted with permission from Nature Publishing Group.

membrane [86,87,88]. The GP_1 subunit is responsible for mediating attachment and entry of the virus. This subunit houses a putative receptor-binding domain (RBD), which binds tightly to the surface of susceptible cells [89,90,91]. Interestingly, at the C-terminus of GP_1 there is a large, highly glycosylated domain, called the mucin domain. This domain plays a role in entry and GP-mediated cytopathology, both of which are described in the following sections.

Glycosylation is a prominent feature of GP and composes about half the mass of GP_1 [83,92]. The Zaire GP contains 17 predicted N-linked oligosaccharides, 8 of which are located in the mucin domain. The mucin domain may contain up to 80 O-linked sites, with at least 17 highly-predicted, clustered sites, which confer mucin-like properties to this domain. The level of N- and O- linked glycosylation in the mucin domain is maintained across the subtypes of EBOV, despite extremely low sequence conservation. The composition and structure of the glycans found on GP have been studied by mass spectrometry [93,94]. GP was found to contain bi-, tri-, and tetra-antennary branched N-linked glycans bearing reduced amounts of galactose, some high-mannose residues, and very low amounts of sialic acid compared to sGP. Although glycosylation is heterogeneous, these analyses indicate that, in general, glycans on sGP undergo more processing and modification than do those on GP. O-linked glycosylation in the mucin domain of GP was also examined and found to be composed of mostly core 2 glycosylation structures, with variable amounts of sialic acid.

The molecular structure of GP was solved to 3.4 Å resolution by Lee and colleagues (Figure 1-4 B) [95]. This crystallographic structure reveals that the three GP_1

subunits form a chalice-like globular structure. In the GP_2 subunit, the fusion loop and HR1 regions wrap around the outside of the globular GP_1 domains, and are thought to help stabilize the structure. The RBD sits on top of the base domain with residues critical for binding facing up. Positioned on top of and blocking access to the RBD is a small glycosylated domain, termed the glycan cap. The mucin domain, which was genetically deleted for crystallography, extends up and away from the viral membrane and globular GP domains. The entire trimeric complex is approximately 35 Å wide at the chalice base, 140 Å tall, and has a radius of approximately 125 Å from the center of the chalice to the distal end of the mucin domain (Lee, J. and Saphire, E.O., unpublished data)

1.8 Viral entry

EBOV, like all viruses, is an obligate intracellular pathogen, and so must enter a host cell to replicate. GP is the only viral protein found of the virion surface and so is responsible for mediating entry and fusion of the virus. The first step of entry is attachment. Because the mucin domain is the prominent feature on the virion surface, it seems likely that initial attachment steps occur through interactions of this domain with host cell surface factors. This hypothesis is supported by several studies, which have demonstrated that C-type lectins such as DC-SIGN or L-SIGN enhance GP-mediated entry through interactions with the mucin domain [96,97,98]. This is significant because residues in the RBD that mediate binding to the cell surface are not exposed on full-length GP, but buried under the glycan cap and mucin domains [95]. In the context of

virus-like particles, the mucin domain has also been shown to induce intracellular signaling in dendritic cells, which may aid in downstream entry or replication steps [99].

EBOV must traffic to a low pH compartment for fusion, however the mechanism of endocytosis is poorly understood [100,101]. Clathrin has been implicated in the endocytosis of EBOV, although the large size of EBOV particles would seem to exclude this pathway [102]. Several signaling molecules, such as phosphoinositide-3 kinase, Rho GTPases, and tyro3 family members have also been implicated in endocytic steps [103,104,105]. Recent, but as yet unpublished studies have also implicated macropinocytosis as an entry pathway [106,107].

The most well-characterized step in EBOV entry is the post-endocytic, pre-fusion stage. After endocytosis, an EBOV-containing endosome matures into a late endosome with a low pH, around 5.5. It is in this low pH compartment that resident endosomal cathepsin proteases process GP_1 into an activated form. Both cathepsin B and cathepsin L have been shown to endoproteolitically cleave GP_1, a process that is required for entry [108]. Cathepsin processing takes place at residues 201 and 222, both of which are located in a disordered and solution-exposed loop between the RBD and the glycan cap [91,95,109]. This cleavage serves to remove the glycan cap and mucin domain from its position over the RBD, potentially exposing the RBD for interactions with a receptor (Figure 1-5) [91,95,110,111]. Studies describing these processing steps are further supported by the fact that cathepsin processing of GP increases the binding and infectivity of GP-bearing pseudovirions [110,111]. Interestingly, this cleaved GP, termed primed GP, is still sensitive to inhibitors of cathepsins, suggesting that cathepsins are

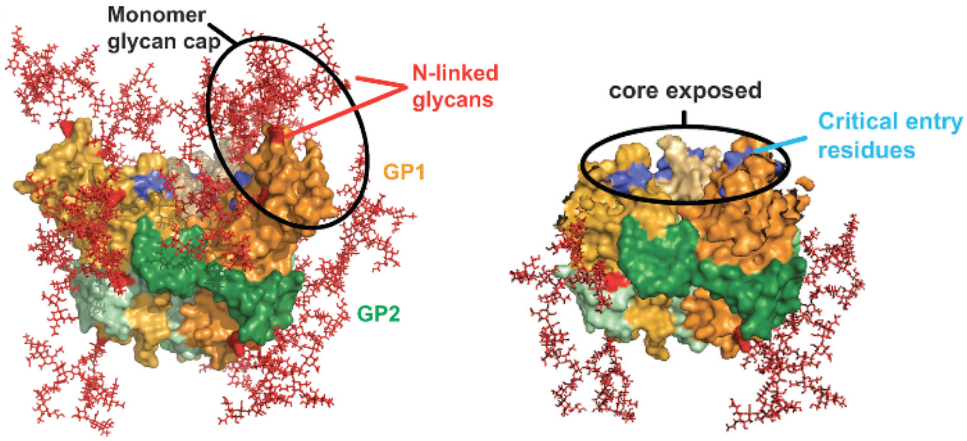

Figure 1-5 Structure of cathepsin processed GP. Receptor-binding residues modeled on CatL-cleaved EBOV GP trimer structure. Left: Surface representation of the ZEBOV-GP trimer structure (as reported in [95]) depicting N-glycan sites in the head region (red) and residues important for virus entry (blue). GP_1 is shown in shades of orange and GP_2 in shades of green. Right: The surface-modeled CatL-cleaved EBOV-GP trimer structure (based on [95]) reveals the complete removal of all N-linked glycans (red) from the head region surface and exposes the conserved core of the RBD and critical residues for virus entry (blue).

Figure and legend minimally modified from: Hood CL, Abraham J, Boyington JC, Leung K, Kwong PD, et al. Biochemical and structural characterization of cathepsin L-processed Ebola virus glycoprotein: implications for viral entry and immunogenicity. J Virol 84: 2972-2982. Reprinted with permission from the American Society for Microbiology. Structure based on: Lee JE, Fusco ML, Hessell AJ, Oswald WB, Burton DR, et al. (2008) Structure of the Ebola virus glycoprotein bound to an antibody from a human survivor. Nature 454: 177-182.

required for a second step during entry [108,110]. Cathepsins could be additionally required to act on a cellular receptor, or could further process GP after receptor-induced structural rearrangements are triggered. After cathepsin processing, fusion occurs and the contents of the viral particle are introduced into the cytoplasm.

1.9 Genome replication and viral budding

As with all RNA viruses with a negative sense genome, EBOV virus must package its own RNA-dependent RNA polymerase (RDRP) so that it can initiate transcription and replication. The L protein is the viral RDRP responsible for protein transcription and full-length genome and anti-genome transcripts [73]. Transcription and replication occurs in the cytoplasm where L works in complex with VP30, VP35 and NP [112]. After transcription of the negative sense viral genome from a positive sense intermediate, nacent genomes are packaged by nucleocapsid proteins.

Newly made RNP complexes must then associate with the matrix proteins for packaging into budding particles. VP40 is the main matrix protein, which drives budding at the plasma membrane and produces virus-like particles in the absence of other viral proteins [113,114]. EBOV VP40 contains two overlapping late domains, which recruit members of the endosomal sorting complexes required for transport (ESCRT) pathway [115,116,117]. ESCRT complexes contain members of the vacuolar protein sorting system, used by the cell to sort multivesicular body (MVB) cargo [118]. This same machinery is usurped by the virus to create the membrane envagination necessary to bud from the plasma membrane [117,119]. Lipid rafts at the plasma membrane may serve as

the site of viral assembly and budding, as VP40 has been shown to target to these microdomains [117,120]. Other potential sites of budding include MVBs and filopodia, as have been proposed for MARV [121,122].

1.10 Glycoprotein-mediated cytopathology

In the past few decades, the use of recombinant DNA technology became a common method to study individual viral gene products. The cloning of the EBOV GP gene allowed the independent expression of GP in cells for the study of processes related to this protein, such as viral entry. From these studies, a phenomenon was observed: GP appeared to induce toxicity in cells in which it was expressed. This observation is the focus of the studies described in this dissertation and is described in detail below.

EBOV GP expression, in the absence of other viral gene products, disrupts cell adhesion causing a loss of cell-cell contacts and of attachment to the culture substrate, resulting in rounded or floating cells [123,124,125]. This phenomenon is termed GP-mediated cytopathology and is displayed in Figure 1-6. Such cytopathology can be observed in a variety of cell lines, including human lines: 293T, 293H, HeLa, OV79, HT1080, U87, and PMA-pretreated U937 cell; other mammalian lines: Vero, CCC, BHK, and MC57 cells; and primary human cell types: umbilical vein endothelial, pulmonary artery endothelial, coronary artery smooth muscle, cardiac microvascular endothelial, and blood monocyte-derived macrophages (unpublished observations and [124,126]). Interestingly, transient GP expression in the transformed human embryonic kidney cell line, 293T, does not cause death, as these cells will regain their adhesive properties after

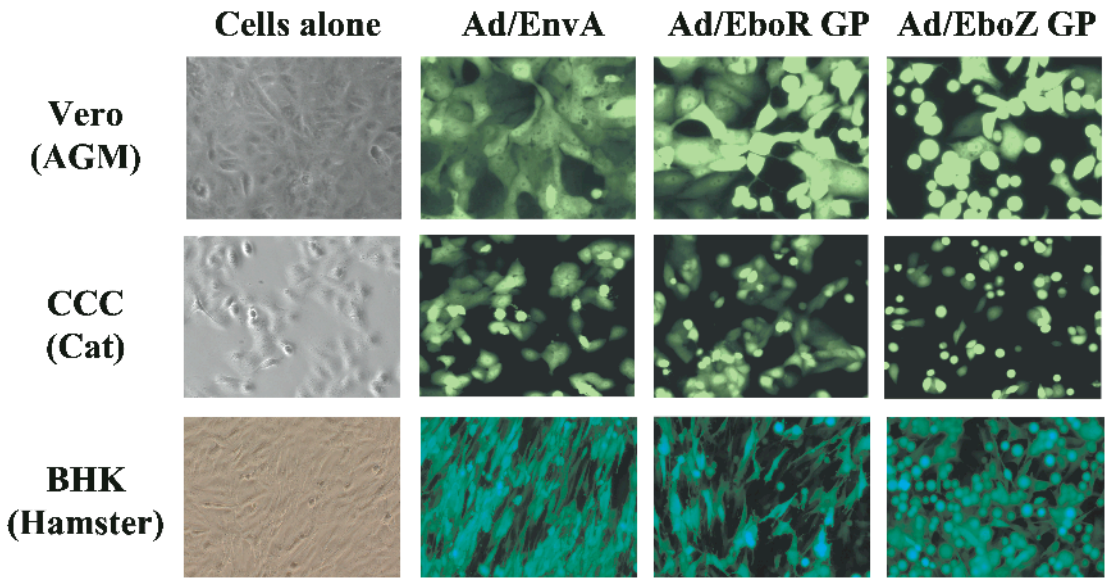

Figure 1-6 EBOV GP-mediated cytopathology. EBOV GP transduction of cell lines using adenovirus vectors. Adenovirus vectors (Ad) expressing avian sarcoma and leukosis virus type A evelop (EnvA), Reston EBOV GP (EboR), or Zaire EBOV GP (EboZ) were used to transduce a simian cell line, Vero (MOI, 10), a cat kidney cell line, CCC (MOI, 10), or baby hamster kidney cells (BHK; MOI, 50). Cells were monitored at regular intervals for evidence of cell rounding, and representative photographs were taken at 48 h posttransduction. AGM, African green monkey.

Figure and legend minimally modified from: Simmons G, Wool-Lewis RJ, Baribaud F, Netter RC, Bates P (2002) Ebola virus glycoproteins induce global surface protein down-modulation and loss of cell adherence. J Virol 76: 2518-2528. Reprinted with permission from the American Society for Microbiology.

GP expression wanes if maintained in culture [124]. In contrast, primary human cardiac microvascular endothelial cells have been reported to undergo anoikis, or detachment-mediated apoptosis, upon transduction of GP [126].

The loss of cell adhesion associated with GP expression does not occur in *trans*, meaning that in culture, non-expressing cells adjacent to a GP-expressing cell will not undergo detachment. Similarly, when sGP or soluble, full-length, trimeric GP is secreted from cells, neither these nor neighboring cells are affected [123]. This indicates that GP must be expressed in a particular cell to induce cytopathology.

Because cell adhesion was so dramatically affected by GP, the integrin family members were examined in several studies related to this topic. By flow cytometry, cells expressing GP display significantly reduced surface levels of β1, α1, α2, α3, α4, α5 and αV integrins [123,124,127]. Other surface proteins such as major histocompatibility complex class I (MHC1) and platelet endothelial cell adhesion molecule 1 (PECAM-1) are similarly effected; however, the exact complement of surface proteins affected by GP appears to differ by cell type [124]. This apparent down-modulation of surface proteins, in particular the various cell adhesion molecules (CAMs), provided an initial explanation for the cell rounding phenotype.

The GPs from 4 of the 5 subtypes of EBOV (Zaire, Sudan, Côte d'Ivoire, and Reston) have been examined for their ability to cause cytopathology. All 4 subtypes are able to induce some degree of cell rounding, although Reston GP seems less able to do so. Additionally, Reston GP induces only a modest down-modulation of surface integrins

by flow cytometry [124]. Interestingly, MARV GP also contains a mucin domain, which does not appear to cause cytopathology [128].

EBOV GP-mediated cytopathology is known to be dependent on the highly glycosylated mucin domain within GP_1. Constructs expressing GP with a genetic deletion of this domain, GPΔmuc, do not cause cell rounding or detachment and do not show down-modulation of surface proteins by flow cytometry [124,125,127]. Indeed, sequential deletions of the mucin domain result in a progressive loss of cell detachment, indicating the overall size or level of glycosylation of the domain is important for the disruption of cell adhesion [124].

The role that GP-mediated cytopathology plays during viral pathogenesis is largely unknown. It is important to note that EBOV infection of 293T cells was observed to cause similar disruption of adhesion and a reduction of β1 and αV integrin and MHC1 staining by flow cytometry by 48 hours post infection, suggesting that observations from transient GP expression are not simply artifacts of overexpression [129]. However, it has been suggested that the balance between sGP and GP transcription, which produces approximately 80% sGP and 20% GP, is a deliberate mechanism used by the virus to limit GP cytopathology. To directly address this hypothesis, Volchkov and colleagues used a reverse genetics system to rescue EBOV bearing an extra adenosine residue in the GP gene RNA edit site [77]. This mutant virus produced significantly more GP and less sGP and caused more cytopathic effects (CPE) in infected 293T cells than wt EBOV, for which the authors report minimal CPE [77]. Because the extent of cytopathology may differ between cell types, its effect on viral pathogenesis is difficult to gauge. In an initial

study of GP-mediated cytopathology, the authors proposed that GP-induced loss of cell-cell contacts could help explain the loss of vascular barrier integrity and resulting leakage often seen during infection, though this remains controversial [48,125]. The disruption of integrins and other CAMs such as PECAM-1 suggests that trafficking and diapedesis of antigen presenting cells (APCs) could be disrupted upon infection [124]. Additionally, the apparent down-modulation of β1 integrin was suggested to be indicative of its role in viral entry, as viruses are known to down-modulate their receptors to aid in egress and prevent superinfection; however, integrins have not been directly implicated as receptors for the virus [123,130,131]. Additional mechanisms by which GP-mediated cytopathology may contribute to pathogenesis are proposed in this dissertation and discussed below.

1.11 Hypotheses addressed in this dissertation

The goal of this dissertation is to utilize cell biological and biochemical techniques to explore the mechanism and consequences of GP-mediated cytopathology. The domain requirements for GP had initially been investigated by our group and others. As previously detailed, the mucin domain is a known requirement for the disruption of adhesion and surface staining. However, it was not known whether the mucin domain was also sufficient to induce cytopathology. This hypothesis is addressed in Chapter 2, wherein we provide evidence that this domain is fully sufficient cause cytopathology. Of critical focus in this dissertation is the cellular and molecular mechanism by which GP-mediated cytopathology occurs. Before the present study was undertaken, there had been

very few investigations into the mechanism by which Ebola GP disrupts adhesion and causes surface protein down-modulation. Sullivan and colleagues had reported that this process requires the cellular GTPase dynamin, which is an active regulator of several endocytic pathways [127]. Additionally, it had also been reported that the extracellular signal-regulated kinases (ERK 1/2) play a role in down-modulation, suggesting that active signaling helped to drive these effects [132]. Therefore, we first undertook studies to examine the role of dynamin in the process of cytopathology (also described in Chapter 2) but found results that contrasted with Sullivan's previous report. We then developed a hypothesis based on the structure of GP and queried whether the heavily-glycosylated mucin domain of GP might be causing cytopathology by sterically inhibiting the function of cell surface proteins. Chapter 3 details this study, which supports a model of steric occlusion as the explanation for both the disruption of adhesion and the appearance of surface protein down-modulation by flow cytometry. Interestingly, we also found that GP could sterically shield its own epitopes from antibody recognition at the cell surface, including a well-studied neutralizing epitope, bound by the KZ52 antibody.

We next wanted to address the potential consequences that GP-mediated cytopathology might have on the immune response during virus infection. First, we hypothesized that the occlusion of surface MHC1 molecules would have the functional consequence of blocking antigen presentation to CD8 T cells, thereby preventing their activation. We have found this to be the case, and have described these experiments in Chapter 3. In Chapter 4, we explore the possibility that the heavily glycosylated domains

within GP sterically affect access to virus. We hypothesize that steric occlusion of the neutralizing epitope bound by the KZ52 antibody, occurs on viral particles and that this may aid in the escape of neutralization. We have undertaken studies to identify the domain in GP that occludes the KZ52 antibody. Furthermore, our experiments indicate that steric occlusion does occur on viral particles; however, it remains unclear whether this effect impacts virus neutralization.

1.12 Experimental approach

The following dissertation takes a reductionist approach to the study of the EBOV by examining the interactions between GP and host cells. Such an approach has both advantages and disadvantages. The justification for this approach is two-fold. First, the low frequency and geographic seclusion of EBOV outbreaks make in-depth studies of infected patients a near-impossibility. This has led to the characterization of several animal models for studying EHF disease pathogenesis. Nevertheless, EBOV is a BSL 4 agent, adding significant cost and feasibility burdens to any live virus study. Therefore, much of our understanding of the biology and biochemistry of the virus is accomplished outside the context of viral infection for the sake of safety and feasibility. Second, it is well appreciated that viruses are complex pathogens that interact with their hosts through many pathways simultaneously. Viruses often encode functional redundancy, meaning that more than one viral protein may function to accomplish a given task. One could think of virus-cell interplay as a dense web of signals and interactions. Therefore, a reductionist approach helps to simplify and focus the study of a single phenomenon in question.

However, a reductionist approach also contains inherent caveats and drawbacks. Functional redundancy could mean that important contributions to a certain phenomenon from a supporting viral protein may be overlooked. Additionally, viruses also encode functional ambiguity in their proteins, meaning that one viral protein may accomplish multiple tasks. The latter is particularly well acknowledged for EBOV, whose genome is relatively small and so whose proteins often interact with the cell in multiple ways. This could introduce additional complexity into a given system; for example, GP may mediate several functions within the cell through separate or intersecting pathways. These limitations are well acknowledged, but it is judged here that the potential disadvantages are outweighed by the opportunities presented by a reductionist approach.

1.13 References

1. (1978) Ebola haemorrhagic fever in Zaire, 1976. Bull World Health Organ 56: 271-293.
2. Bres P (1978) [The epidemic of Ebola haemorrhagic fever in Sudan and Zaire, 1976: introductory note.]. Bull World Health Organ 56: 245.
3. Johnson KM, Lange JV, Webb PA, Murphy FA (1977) Isolation and partial characterisation of a new virus causing acute haemorrhagic fever in Zaire. Lancet 1: 569-571.
4. Bowen ET, Lloyd G, Harris WJ, Platt GS, Baskerville A, et al. (1977) Viral haemorrhagic fever in southern Sudan and northern Zaire. Preliminary studies on the aetiological agent. Lancet 1: 571-573.
5. Pattyn S, van der Groen G, Courteille G, Jacob W, Piot P (1977) Isolation of Marburg-like virus from a case of haemorrhagic fever in Zaire. Lancet 1: 573-574.
6. (1978) Ebola haemorrhagic fever in Sudan, 1976. Report of a WHO/International Study Team. Bull World Health Organ 56: 247-270.
7. Le Guenno B, Formenty P, Wyers M, Gounon P, Walker F, et al. (1995) Isolation and partial characterisation of a new strain of Ebola virus. Lancet 345: 1271-1274.
8. Heymann DL, Weisfeld JS, Webb PA, Johnson KM, Cairns T, et al. (1980) Ebola hemorrhagic fever: Tandala, Zaire, 1977-1978. J Infect Dis 142: 372-376.
9. Emond RT, Evans B, Bowen ET, Lloyd G (1977) A case of Ebola virus infection. Br Med J 2: 541-544.
10. (1996) Ebola haemorrhagic fever. Wkly Epidemiol Rec 71: 359.
11. (1990) Update: filovirus infection in animal handlers. MMWR Morb Mortal Wkly Rep 39: 221.
12. Miranda ME, White ME, Dayrit MM, Hayes CG, Ksiazek TG, et al. (1991) Seroepidemiological study of filovirus related to Ebola in the Philippines. Lancet 337: 425-426.
13. Barrette RW, Metwally SA, Rowland JM, Xu L, Zaki SR, et al. (2009) Discovery of swine as a host for the Reston ebolavirus. Science 325: 204-206.
14. Leroy EM, Telfer P, Kumulungui B, Yaba P, Rouquet P, et al. (2004) A serological survey of Ebola virus infection in central African nonhuman primates. J Infect Dis 190: 1895-1899.
15. Rouquet P, Froment JM, Bermejo M, Kilbourn A, Karesh W, et al. (2005) Wild animal mortality monitoring and human Ebola outbreaks, Gabon and Republic of Congo, 2001-2003. Emerg Infect Dis 11: 283-290.
16. Miranda ME, Ksiazek TG, Retuya TJ, Khan AS, Sanchez A, et al. (1999) Epidemiology of Ebola (subtype Reston) virus in the Philippines, 1996. J Infect Dis 179 Suppl 1: S115-119.
17. Groseth A, Feldmann H, Strong JE (2007) The ecology of Ebola virus. Trends Microbiol 15: 408-416.
18. Gonzalez JP, Pourrut X, Leroy E (2007) Ebolavirus and other filoviruses. Curr Top Microbiol Immunol 315: 363-387.

19. Leroy EM, Rouquet P, Formenty P, Souquiere S, Kilbourne A, et al. (2004) Multiple Ebola virus transmission events and rapid decline of central African wildlife. Science 303: 387-390.
20. Pourrut X, Delicat A, Rollin PE, Ksiazek TG, Gonzalez JP, et al. (2007) Spatial and temporal patterns of Zaire ebolavirus antibody prevalence in the possible reservoir bat species. J Infect Dis 196 Suppl 2: S176-183.
21. Leroy EM, Kumulungui B, Pourrut X, Rouquet P, Hassanin A, et al. (2005) Fruit bats as reservoirs of Ebola virus. Nature 438: 575-576.
22. Pourrut X, Souris M, Towner JS, Rollin PE, Nichol ST, et al. (2009) Large serological survey showing cocirculation of Ebola and Marburg viruses in Gabonese bat populations, and a high seroprevalence of both viruses in Rousettus aegyptiacus. BMC Infect Dis 9: 159.
23. Leroy EM, Epelboin A, Mondonge V, Pourrut X, Gonzalez JP, et al. (2009) Human Ebola outbreak resulting from direct exposure to fruit bats in Luebo, Democratic Republic of Congo, 2007. Vector Borne Zoonotic Dis 9: 723-728.
24. Khan AS, Tshioko FK, Heymann DL, Le Guenno B, Nabeth P, et al. (1999) The reemergence of Ebola hemorrhagic fever, Democratic Republic of the Congo, 1995. Commission de Lutte contre les Epidemies a Kikwit. J Infect Dis 179 Suppl 1: S76-86.
25. Georges AJ, Leroy EM, Renaut AA, Benissan CT, Nabias RJ, et al. (1999) Ebola hemorrhagic fever outbreaks in Gabon, 1994-1997: epidemiologic and health control issues. J Infect Dis 179 Suppl 1: S65-75.
26. Okware SI, Omaswa FG, Zaramba S, Opio A, Lutwama JJ, et al. (2002) An outbreak of Ebola in Uganda. Trop Med Int Health 7: 1068-1075.
27. Baron RC, McCormick JB, Zubeir OA (1983) Ebola virus disease in southern Sudan: hospital dissemination and intrafamilial spread. Bull World Health Organ 61: 997-1003.
28. Towner JS, Sealy TK, Khristova ML, Albarino CG, Conlan S, et al. (2008) Newly discovered ebola virus associated with hemorrhagic fever outbreak in Uganda. PLoS Pathog 4: e1000212.
29. Sanchez A, Khan AS, Zaki SR, Nabel GJ, Ksiazek TG, et al. (2001) Filoviridae: Marburg and Eboila Viruses. In: Knipe DM, Howley PM, Griggen DE, Lamb RA, Martin MA et al., editors. Fields Virology: Lippincott, Williams & Wilkins. pp. 1279-1304.
30. Casillas AM, Nyamathi AM, Sosa A, Wilder CL, Sands H (2003) A current review of Ebola virus: pathogenesis, clinical presentation, and diagnostic assessment. Biol Res Nurs 4: 268-275.
31. Bwaka MA, Bonnet MJ, Calain P, Colebunders R, De Roo A, et al. (1999) Ebola hemorrhagic fever in Kikwit, Democratic Republic of the Congo: clinical observations in 103 patients. J Infect Dis 179 Suppl 1: S1-7.
32. Sureau PH (1989) Firsthand clinical observations of hemorrhagic manifestations in Ebola hemorrhagic fever in Zaire. Rev Infect Dis 11 Suppl 4: S790-793.
33. Mupapa K, Massamba M, Kibadi K, Kuvula K, Bwaka A, et al. (1999) Treatment of Ebola hemorrhagic fever with blood transfusions from convalescent patients.

International Scientific and Technical Committee. J Infect Dis 179 Suppl 1: S18-23.
34. Jaax NK, Davis KJ, Geisbert TJ, Vogel P, Jaax GP, et al. (1996) Lethal experimental infection of rhesus monkeys with Ebola-Zaire (Mayinga) virus by the oral and conjunctival route of exposure. Arch Pathol Lab Med 120: 140-155.
35. Geisbert TW, Hensley LE, Larsen T, Young HA, Reed DS, et al. (2003) Pathogenesis of Ebola hemorrhagic fever in cynomolgus macaques: evidence that dendritic cells are early and sustained targets of infection. Am J Pathol 163: 2347-2370.
36. Geisbert TW, Pushko P, Anderson K, Smith J, Davis KJ, et al. (2002) Evaluation in nonhuman primates of vaccines against Ebola virus. Emerg Infect Dis 8: 503-507.
37. Bosio CM, Aman MJ, Grogan C, Hogan R, Ruthel G, et al. (2003) Ebola and Marburg viruses replicate in monocyte-derived dendritic cells without inducing the production of cytokines and full maturation. J Infect Dis 188: 1630-1638.
38. Ryabchikova EI, Kolesnikova LV, Luchko SV (1999) An analysis of features of pathogenesis in two animal models of Ebola virus infection. J Infect Dis 179 Suppl 1: S199-202.
39. Mahanty S, Hutchinson K, Agarwal S, McRae M, Rollin PE, et al. (2003) Cutting edge: impairment of dendritic cells and adaptive immunity by Ebola and Lassa viruses. J Immunol 170: 2797-2801.
40. Geisbert TW, Young HA, Jahrling PB, Davis KJ, Kagan E, et al. (2003) Mechanisms underlying coagulation abnormalities in ebola hemorrhagic fever: overexpression of tissue factor in primate monocytes/macrophages is a key event. J Infect Dis 188: 1618-1629.
41. Zampieri CA, Sullivan NJ, Nabel GJ (2007) Immunopathology of highly virulent pathogens: insights from Ebola virus. Nat Immunol 8: 1159-1164.
42. Sanchez A, Lukwiya M, Bausch D, Mahanty S, Sanchez AJ, et al. (2004) Analysis of human peripheral blood samples from fatal and nonfatal cases of Ebola (Sudan) hemorrhagic fever: cellular responses, virus load, and nitric oxide levels. J Virol 78: 10370-10377.
43. Baize S, Leroy EM, Georges-Courbot MC, Capron M, Lansoud-Soukate J, et al. (1999) Defective humoral responses and extensive intravascular apoptosis are associated with fatal outcome in Ebola virus-infected patients. Nat Med 5: 423-426.
44. Wool-Lewis RJ, Bates P (1998) Characterization of Ebola virus entry by using pseudotyped viruses: identification of receptor-deficient cell lines. J Virol 72: 3155-3160.
45. Reed DS, Hensley LE, Geisbert JB, Jahrling PB, Geisbert TW (2004) Depletion of peripheral blood T lymphocytes and NK cells during the course of ebola hemorrhagic Fever in cynomolgus macaques. Viral Immunol 17: 390-400.
46. Ksiazek TG, Rollin PE, Williams AJ, Bressler DS, Martin ML, et al. (1999) Clinical virology of Ebola hemorrhagic fever (EHF): virus, virus antigen, and IgG and IgM antibody findings among EHF patients in Kikwit, Democratic Republic of the Congo, 1995. J Infect Dis 179 Suppl 1: S177-187.

47. Towner JS, Rollin PE, Bausch DG, Sanchez A, Crary SM, et al. (2004) Rapid diagnosis of Ebola hemorrhagic fever by reverse transcription-PCR in an outbreak setting and assessment of patient viral load as a predictor of outcome. J Virol 78: 4330-4341.
48. Geisbert TW, Young HA, Jahrling PB, Davis KJ, Larsen T, et al. (2003) Pathogenesis of Ebola Hemorrhagic Fever in Primate Models: Evidence that Hemorrhage Is Not a Direct Effect of Virus-Induced Cytolysis of Endothelial Cells. Am J Pathol 163: 2371-2382.
49. Reid SP, Leung LW, Hartman AL, Martinez O, Shaw ML, et al. (2006) Ebola virus VP24 binds karyopherin alpha1 and blocks STAT1 nuclear accumulation. J Virol 80: 5156-5167.
50. Basler CF, Mikulasova A, Martinez-Sobrido L, Paragas J, Muhlberger E, et al. (2003) The Ebola virus VP35 protein inhibits activation of interferon regulatory factor 3. J Virol 77: 7945-7956.
51. Basler CF, Wang X, Muhlberger E, Volchkov V, Paragas J, et al. (2000) The Ebola virus VP35 protein functions as a type I IFN antagonist. Proc Natl Acad Sci U S A 97: 12289-12294.
52. Jahrling PB, Geisbert JB, Swearengen JR, Larsen T, Geisbert TW (2007) Ebola hemorrhagic fever: evaluation of passive immunotherapy in nonhuman primates. J Infect Dis 196 Suppl 2: S400-403.
53. Oswald WB, Geisbert TW, Davis KJ, Geisbert JB, Sullivan NJ, et al. (2007) Neutralizing antibody fails to impact the course of Ebola virus infection in monkeys. PLoS Pathog 3: e9.
54. Jahrling PB, Geisbert TW, Geisbert JB, Swearengen JR, Bray M, et al. (1999) Evaluation of immune globulin and recombinant interferon-alpha2b for treatment of experimental Ebola virus infections. J Infect Dis 179 Suppl 1: S224-234.
55. Geisbert TW, Hensley LE, Jahrling PB, Larsen T, Geisbert JB, et al. (2003) Treatment of Ebola virus infection with a recombinant inhibitor of factor VIIa/tissue factor: a study in rhesus monkeys. Lancet 362: 1953-1958.
56. Warfield KL, Swenson DL, Olinger GG, Nichols DK, Pratt WD, et al. (2006) Gene-specific countermeasures against Ebola virus based on antisense phosphorodiamidate morpholino oligomers. PLoS Pathog 2: e1.
57. Geisbert TW, Hensley LE, Kagan E, Yu EZ, Geisbert JB, et al. (2006) Postexposure protection of guinea pigs against a lethal ebola virus challenge is conferred by RNA interference. J Infect Dis 193: 1650-1657.
58. Geisbert TW, Lee AC, Robbins M, Geisbert JB, Honko AN, et al. Postexposure protection of non-human primates against a lethal Ebola virus challenge with RNA interference: a proof-of-concept study. Lancet 375: 1896-1905.
59. Feldmann H, Jones SM, Daddario-DiCaprio KM, Geisbert JB, Stroher U, et al. (2007) Effective post-exposure treatment of Ebola infection. PLoS Pathog 3: e2.
60. Gunther S, Schmiedel S. Management of needle stick injury in BSL4 laboratory, Hamburg, Germany; 2010; Tokyo, Japan.
61. Kinch MS, Yunus AS, Lear C, Mao H, Chen H, et al. (2009) FGI-104: a broad-spectrum small molecule inhibitor of viral infection. Am J Transl Res 1: 87-98.

62. Michelow IC, Dong M, Mungall BA, Yantosca LM, Lear C, et al. A novel L-ficolin/mannose-binding lectin chimeric molecule with enhanced activity against Ebola virus. J Biol Chem.
63. Shah PP, Wang T, Kaletsky RL, Myers M, Puvis JE, et al. A small molecule oxocarbazate inhibitor of human cathepsin L blocks SARS and Ebola pseudotype virus infection into HEK 293T cells. Mol Pharmacol.
64. Wolf MC, Freiberg AN, Zhang T, Akyol-Ataman Z, Grock A, et al. A broad-spectrum antiviral targeting entry of enveloped viruses. Proc Natl Acad Sci U S A 107: 3157-3162.
65. Sullivan NJ, Geisbert TW, Geisbert JB, Xu L, Yang ZY, et al. (2003) Accelerated vaccination for Ebola virus haemorrhagic fever in non-human primates. Nature 424: 681-684.
66. Bukreyev A, Rollin PE, Tate MK, Yang L, Zaki SR, et al. (2007) Successful topical respiratory tract immunization of primates against Ebola virus. J Virol 81: 6379-6388.
67. Geisbert TW, Daddario-Dicaprio KM, Geisbert JB, Reed DS, Feldmann F, et al. (2008) Vesicular stomatitis virus-based vaccines protect nonhuman primates against aerosol challenge with Ebola and Marburg viruses. Vaccine 26: 6894-6900.
68. Jones SM, Feldmann H, Stroher U, Geisbert JB, Fernando L, et al. (2005) Live attenuated recombinant vaccine protects nonhuman primates against Ebola and Marburg viruses. Nat Med 11: 786-790.
69. Sullivan NJ, Geisbert TW, Geisbert JB, Shedlock DJ, Xu L, et al. (2006) Immune protection of nonhuman primates against Ebola virus with single low-dose adenovirus vectors encoding modified GPs. PLoS Med 3: e177.
70. Warfield KL, Swenson DL, Olinger GG, Kalina WV, Aman MJ, et al. (2007) Ebola virus-like particle-based vaccine protects nonhuman primates against lethal Ebola virus challenge. J Infect Dis 196 Suppl 2: S430-437.
71. Sullivan NJ, Martin JE, Graham BS, Nabel GJ (2009) Correlates of protective immunity for Ebola vaccines: implications for regulatory approval by the animal rule. Nat Rev Microbiol 7: 393-400.
72. Rodriguez LL, De Roo A, Guimard Y, Trappier SG, Sanchez A, et al. (1999) Persistence and genetic stability of Ebola virus during the outbreak in Kikwit, Democratic Republic of the Congo, 1995. J Infect Dis 179 Suppl 1: S170-176.
73. Volchkov VE, Volchkova VA, Chepurnov AA, Blinov VM, Dolnik O, et al. (1999) Characterization of the L gene and 5' trailer region of Ebola virus. J Gen Virol 80 (Pt 2): 355-362.
74. Weik M, Enterlein S, Schlenz K, Muhlberger E (2005) The Ebola virus genomic replication promoter is bipartite and follows the rule of six. J Virol 79: 10660-10671.
75. Elliott LH, Kiley MP, McCormick JB (1985) Descriptive analysis of Ebola virus proteins. Virology 147: 169-176.
76. Sanchez A, Trappier SG, Mahy BW, Peters CJ, Nichol ST (1996) The virion glycoproteins of Ebola viruses are encoded in two reading frames and are

expressed through transcriptional editing. Proceedings of the National Academy of Sciences of the United States of America 93: 3602-3607.
77. Volchkov VE, Volchkova VA, Muhlberger E, Kolesnikova LV, Weik M, et al. (2001) Recovery of infectious Ebola virus from complementary DNA: RNA editing of the GP gene and viral cytotoxicity. Science 291: 1965-1969.
78. Ellis DS, Stamford S, Lloyd G, Bowen ET, Platt GS, et al. (1979) Ebola and Marburg viruses: I. Some ultrastructural differences between strains when grown in Vero cells. J Med Virol 4: 201-211.
79. Geisbert TW, Jahrling PB (1995) Differentiation of filoviruses by electron microscopy. Virus Res 39: 129-150.
80. Volchkova VA, Klenk HD, Volchkov VE (1999) Delta-peptide is the carboxy-terminal cleavage fragment of the nonstructural small glycoprotein sGP of Ebola virus. Virology 265: 164-171.
81. Volchkov VE, Becker S, Volchkova VA, Ternovoj VA, Kotov AN, et al. (1995) GP mRNA of Ebola virus is edited by the Ebola virus polymerase and by T7 and vaccinia virus polymerases. Virology 214: 421-430.
82. Volchkov VE, Feldmann H, Volchkova VA, Klenk HD (1998) Processing of the Ebola virus glycoprotein by the proprotein convertase furin. Proc Natl Acad Sci U S A 95: 5762-5767.
83. Jeffers SA, Sanders DA, Sanchez A (2002) Covalent modifications of the ebola virus glycoprotein. J Virol 76: 12463-12472.
84. Sanchez A, Yang ZY, Xu L, Nabel GJ, Crews T, et al. (1998) Biochemical analysis of the secreted and virion glycoproteins of Ebola virus. J Virol 72: 6442-6447.
85. Weissenhorn W, Calder LJ, Wharton SA, Skehel JJ, Wiley DC (1998) The central structural feature of the membrane fusion protein subunit from the Ebola virus glycoprotein is a long triple-stranded coiled coil. Proc Natl Acad Sci U S A 95: 6032-6036.
86. Malashkevich VN, Schneider BJ, McNally ML, Milhollen MA, Pang JX, et al. (1999) Core structure of the envelope glycoprotein GP2 from Ebola virus at 1.9-A resolution. Proc Natl Acad Sci U S A 96: 2662-2667.
87. Weissenhorn W, Carfi A, Lee KH, Skehel JJ, Wiley DC (1998) Crystal structure of the Ebola virus membrane fusion subunit, GP2, from the envelope glycoprotein ectodomain. Mol Cell 2: 605-616.
88. Ruiz-Arguello MB, Goni FM, Pereira FB, Nieva JL (1998) Phosphatidylinositol-dependent membrane fusion induced by a putative fusogenic sequence of Ebola virus. J Virol 72: 1775-1781.
89. Brindley MA, Hughes L, Ruiz A, McCray PB, Jr., Sanchez A, et al. (2007) Ebola virus glycoprotein 1: identification of residues important for binding and postbinding events. J Virol 81: 7702-7709.
90. Manicassamy B, Wang J, Jiang H, Rong L (2005) Comprehensive analysis of ebola virus GP1 in viral entry. J Virol 79: 4793-4805.
91. Dube D, Brecher MB, Delos SE, Rose SC, Park EW, et al. (2009) The primed ebolavirus glycoprotein (19-kilodalton GP1,2): sequence and residues critical for host cell binding. J Virol 83: 2883-2891.

92. Feldmann H, Nichol ST, Klenk HD, Peters CJ, Sanchez A (1994) Characterization of filoviruses based on differences in structure and antigenicity of the virion glycoprotein. Virology 199: 469-473.
93. Ritchie G, Harvey DJ, Stroeher U, Feldmann F, Feldmann H, et al. Identification of N-glycans from Ebola virus glycoproteins by matrix-assisted laser desorption/ionisation time-of-flight and negative ion electrospray tandem mass spectrometry. Rapid Commun Mass Spectrom 24: 571-585.
94. Powlesland AS, Fisch T, Taylor ME, Smith DF, Tissot B, et al. (2008) A novel mechanism for LSECtin binding to Ebola virus surface glycoprotein through truncated glycans. J Biol Chem 283: 593-602.
95. Lee JE, Fusco ML, Hessell AJ, Oswald WB, Burton DR, et al. (2008) Structure of the Ebola virus glycoprotein bound to an antibody from a human survivor. Nature 454: 177-182.
96. Alvarez CP, Lasala F, Carrillo J, Muniz O, Corbi AL, et al. (2002) C-type lectins DC-SIGN and L-SIGN mediate cellular entry by Ebola virus in cis and in trans. J Virol 76: 6841-6844.
97. Takada A, Fujioka K, Tsuiji M, Morikawa A, Higashi N, et al. (2004) Human macrophage C-type lectin specific for galactose and N-acetylgalactosamine promotes filovirus entry. J Virol 78: 2943-2947.
98. Simmons G, Reeves JD, Grogan CC, Vandenberghe LH, Baribaud F, et al. (2003) DC-SIGN and DC-SIGNR bind ebola glycoproteins and enhance infection of macrophages and endothelial cells. Virology 305: 115-123.
99. Martinez O, Valmas C, Basler CF (2007) Ebola virus-like particle-induced activation of NF-kappaB and Erk signaling in human dendritic cells requires the glycoprotein mucin domain. Virology 364: 342-354.
100. Chan SY, Speck RF, Ma MC, Goldsmith MA (2000) Distinct mechanisms of entry by envelope glycoproteins of Marburg and Ebola (Zaire) viruses. J Virol 74: 4933-4937.
101. Takada A, Robison C, Goto H, Sanchez A, Murti KG, et al. (1997) A system for functional analysis of Ebola virus glycoprotein. Proc Natl Acad Sci U S A 94: 14764-14769.
102. Bhattacharyya S, Warfield KL, Ruthel G, Bavari S, Aman MJ, et al. Ebola virus uses clathrin-mediated endocytosis as an entry pathway. Virology 401: 18-28.
103. Shimojima M, Ikeda Y, Kawaoka Y (2007) The mechanism of Axl-mediated Ebola virus infection. J Infect Dis 196 Suppl 2: S259-263.
104. Saeed MF, Kolokoltsov AA, Freiberg AN, Holbrook MR, Davey RA (2008) Phosphoinositide-3 kinase-Akt pathway controls cellular entry of Ebola virus. PLoS Pathog 4: e1000141.
105. Quinn K, Brindley MA, Weller ML, Kaludov N, Kondratowicz A, et al. (2009) Rho GTPases modulate entry of Ebola virus and vesicular stomatitis virus pseudotyped vectors. J Virol 83: 10176-10186.
106. Nanbo A, Imai M, Watanabe S, Neumann G, Halfmann P, et al. Ebolavirus is internalized into host cells via macropinocytosis in a viral glycoprotein-dependent manner; 2010; Tokyo, Japan.

107. Saeed MF, albrecht T, Davey RA. Ebola virus uses macropinocytosis and is trafficked to the golgi complex before nucleocapsid release into the cell cytoplasm; 2010; Tokyo, Japan.
108. Chandran K, Sullivan NJ, Felbor U, Whelan SP, Cunningham JM (2005) Endosomal proteolysis of the Ebola virus glycoprotein is necessary for infection. Science 308: 1643-1645.
109. Hood CL, Abraham J, Boyington JC, Leung K, Kwong PD, et al. Biochemical and structural characterization of cathepsin L-processed Ebola virus glycoprotein: implications for viral entry and immunogenicity. J Virol 84: 2972-2982.
110. Schornberg K, Matsuyama S, Kabsch K, Delos S, Bouton A, et al. (2006) Role of endosomal cathepsins in entry mediated by the Ebola virus glycoprotein. J Virol 80: 4174-4178.
111. Kaletsky RL, Simmons G, Bates P (2007) Proteolysis of the Ebola virus glycoproteins enhances virus binding and infectivity. J Virol 81: 13378-13384.
112. Muhlberger E, Weik M, Volchkov VE, Klenk HD, Becker S (1999) Comparison of the transcription and replication strategies of marburg virus and Ebola virus by using artificial replication systems. J Virol 73: 2333-2342.
113. Noda T, Sagara H, Suzuki E, Takada A, Kida H, et al. (2002) Ebola virus VP40 drives the formation of virus-like filamentous particles along with GP. J Virol 76: 4855-4865.
114. Jasenosky LD, Neumann G, Lukashevich I, Kawaoka Y (2001) Ebola virus VP40-induced particle formation and association with the lipid bilayer. J Virol 75: 5205-5214.
115. Harty RN, Brown ME, Wang G, Huibregtse J, Hayes FP (2000) A PPxY motif within the VP40 protein of Ebola virus interacts physically and functionally with a ubiquitin ligase: implications for filovirus budding. Proc Natl Acad Sci U S A 97: 13871-13876.
116. Martin-Serrano J, Zang T, Bieniasz PD (2001) HIV-1 and Ebola virus encode small peptide motifs that recruit Tsg101 to sites of particle assembly to facilitate egress. Nat Med 7: 1313-1319.
117. Licata JM, Simpson-Holley M, Wright NT, Han Z, Paragas J, et al. (2003) Overlapping motifs (PTAP and PPEY) within the Ebola virus VP40 protein function independently as late budding domains: involvement of host proteins TSG101 and VPS-4. J Virol 77: 1812-1819.
118. Hurley JH, Emr SD (2006) The ESCRT complexes: structure and mechanism of a membrane-trafficking network. Annu Rev Biophys Biomol Struct 35: 277-298.
119. Welsch S, Muller B, Krausslich HG (2007) More than one door - Budding of enveloped viruses through cellular membranes. FEBS Lett 581: 2089-2097.
120. Bavari S, Bosio CM, Wiegand E, Ruthel G, Will AB, et al. (2002) Lipid raft microdomains: a gateway for compartmentalized trafficking of Ebola and Marburg viruses. J Exp Med 195: 593-602.
121. Kolesnikova L, Bohil AB, Cheney RE, Becker S (2007) Budding of Marburgvirus is associated with filopodia. Cell Microbiol 9: 939-951.

122. Kolesnikova L, Bugany H, Klenk HD, Becker S (2002) VP40, the matrix protein of Marburg virus, is associated with membranes of the late endosomal compartment. J Virol 76: 1825-1838.
123. Takada A, Watanabe S, Ito H, Okazaki K, Kida H, et al. (2000) Downregulation of beta1 integrins by Ebola virus glycoprotein: implication for virus entry. Virology 278: 20-26.
124. Simmons G, Wool-Lewis RJ, Baribaud F, Netter RC, Bates P (2002) Ebola virus glycoproteins induce global surface protein down-modulation and loss of cell adherence. J Virol 76: 2518-2528.
125. Yang ZY, Duckers HJ, Sullivan NJ, Sanchez A, Nabel EG, et al. (2000) Identification of the Ebola virus glycoprotein as the main viral determinant of vascular cell cytotoxicity and injury. Nat Med 6: 886-889.
126. Ray RB, Basu A, Steele R, Beyene A, McHowat J, et al. (2004) Ebola virus glycoprotein-mediated anoikis of primary human cardiac microvascular endothelial cells. Virology 321: 181-188.
127. Sullivan NJ, Peterson M, Yang ZY, Kong WP, Duckers H, et al. (2005) Ebola virus glycoprotein toxicity is mediated by a dynamin-dependent protein-trafficking pathway. J Virol 79: 547-553.
128. Chan SY, Ma MC, Goldsmith MA (2000) Differential induction of cellular detachment by envelope glycoproteins of Marburg and Ebola (Zaire) viruses. J Gen Virol 81: 2155-2159.
129. Alazard-Dany N, Volchkova V, Reynard O, Carbonnelle C, Dolnik O, et al. (2006) Ebola virus glycoprotein GP is not cytotoxic when expressed constitutively at a moderate level. J Gen Virol 87: 1247-1257.
130. Nethe M, Berkhout B, van der Kuyl AC (2005) Retroviral superinfection resistance. Retrovirology 2: 52.
131. Martin RA, Nayak DP (1996) Membrane anchorage of gp160 is necessary and sufficient to prevent CD4 transport to the cell surface. Virology 220: 473-479.
132. Zampieri CA, Fortin JF, Nolan GP, Nabel GJ (2007) The ERK mitogen-activated protein kinase pathway contributes to Ebola virus glycoprotein-induced cytotoxicity. J Virol 81: 1230-1240.

CHAPTER 2 – REQUIREMENTS FOR CELL ROUNDING AND SURFACE PROTEIN DOWN-REGULATION BY EBOLA VIRUS GLYCOPROTEIN

Joseph R. Francica[1], Meghan K. Matukonis[1], and Paul Bates[1]

[1] Department of Microbiology, University of Pennsylvania School of Medicine
225 Johnson Pavilion 3610 Hamilton Walk, Philadelphia, PA 19104-6076

Virology. 2009 Jan 20;383(2):237-47. Reprinted with permission from Elsevier.

2.1 Abstract

The Ebola virus (EBOV) causes an acute hemorrhagic fever that is associated with high morbidity and mortality. The viral glycoprotein is thought to play a significant role in the pathogenesis of disease, though precise mechanisms are unknown. Cellular pathogenesis can be modeled *in vitro* by the expression of the glycoprotein (GP) in cells, which causes dramatic morphological changes, including cell rounding and surface protein down-regulation. These effects are known to be dependent on the presence of a highly glycosylated region of the glycoprotein, the mucin domain. Here we show that the mucin domain from the highly pathogenic Zaire subtype of EBOV is sufficient to cause characteristic cytopathology when expressed in the context of a foreign glycoprotein. Similarly to full length Ebola GP, expression of the mucin domain causes rounding, detachment from the extracellular matrix, and the down-regulation of cell surface levels of β1 integrin and major histocompatibility complex class 1. These effects were not seen when the mucin domain was expressed in the context of a glycophosphatidylinositol- (GPI-) anchored isoform of the foreign glycoprotein. Moreover, cytopathology associated with Ebola glycoprotein expression does not occur when GP expression is

restricted to the endoplasmic reticulum. We also report that GP-induced surface protein down-regulation is not mediated through a dynamin-dependent pathway, in contrast to a previously published report.

2.2 Introduction

The Ebola virus (EBOV) is a member of the family *Filoviridae*, and causes a severe hemorrhagic fever in humans and non-human primates [1]. In cell culture, EBOV infection causes pathogenic effects that result in destruction of the monolayer [2,3]. The specific determinants of viral pathogenicity *in vivo* are still unknown; however, the viral glycoproteins are thought to play a large role in cellular pathogenesis [4,5,6]. EBOV encodes two forms of its glycoprotein, a dimeric secreted form (sGP) [7] and a trimeric membrane-spanning form, GP, which originates from RNA editing of the glycoprotein ORF [8]. No toxicity has been associated with sGP; however, because it is the predominant form that is transcribed and translated, it is thought that the balance between sGP and GP may be necessary to control the cytopathic effects attributed to GP [4,6]. When expressed *in vitro* and *in vivo*, GP causes cell rounding, detachment, and down-regulation of many surface proteins, though cells are not immediately killed [4,9,10]. Among the surface proteins down-modulated by GP are β1 integrin (CD 29), α5 integrin, αV integrin, and major histocompatibility complex class 1 (MHC1) in 293T cells [10]. However, the exact profile of protein down-regulation seems to differ by cell type. In HUVEC cells, GP reduces surface expression of MHC1 and PECAM-1 but not β1 integrin [10].

Analysis of Ebola GP deletion mutants demonstrated that these morphological changes, along with the down-regulation of surface proteins, are dependent on a highly O- and N- glycosylated domain within GP, termed the mucin domain [4,9,10,11]. The mucin domain is approximately 150 amino acids in length and is a conserved feature of

filoviruses, though the primary sequence is highly variable among subtypes and strains. The domain is thought to have little secondary or tertiary structure because of its high level of glycosylation. Biochemical analysis has shown that after cleavage of the glycoprotein precursor by furin [12] into GP_1 (receptor-recognizing) and GP_2 (membrane-spanning) fragments, the N-terminus of GP_1 remains associated with GP_2, leaving the mucin domain exposed at the C-terminus of GP_1 [13]. The mucin domain is not necessary for GP surface expression or formation of infectious pseudotyped virions [4,14,15]. There is no single region of the domain that contributes disproportionately to the rounding phenotype, indicating that the phenotype may be dependent on the overall size of the domain or level of its glycosylation [10].

Other viruses, such as the Bunyavirus, Crimean Congo Hemorrhagic Fever Virus (CCHV) and the polydnavirus, *Microplitis demolitor* bracovirus (MdBV), encode proteins with mucin-like domains. While no rounding or other cytopathology has been reported for the CCHV mucin-like protein, the MdBV protein Glc1.8 causes rounding when transfected into insect cells in a manner dependent on membrane association [16]. In addition, the cellular mucin protein MUC1 (episialin) has been shown to play a direct role in the disruption of attachment factors such as β1 integrin when expressed in melanoma and epithelial cell lines [17]. MUC1 is known to be highly and aberrantly expressed in many adenocarcinomas and its expression correlates with increased metastasis and poor prognosis [18,19,20]. MUC1 is thought to interfere with adhesion through steric hindrance of necessary adhesion molecules [17]. In addition, it has been shown that the size of the glycosylated region of MUC1 positively contributes to its

ability to interfere with E-cadherin-based cell-cell interactions [21]. These data agree with our previously-published study, which correlated the rounding phenotype to the size of the EBOV GP mucin domain [10].

Although it has been well documented that the presence of the mucin domain is necessary for GP-mediated cytopathology, it has yet to be shown that the mucin domain is fully sufficient to induce the effects discussed above. One report found that murine leukemia virus amphotropic envelope containing the mucin domain caused an increase in floating cells in culture [4]. Here we analyzed the requirements for Ebola GP-mediated cytopathology. We show that the mucin domain from the Zaire subtype of the EBOV glycoprotein is sufficient to cause morphological alterations characteristic of GP expression by placing it in the context of a heterologous, monomeric glycoprotein. Using isoforms of this heterologous protein, we further demonstrate that a membrane-bound form induces cytopathology, whereas a lipid- (GPI) anchored isoform does not. In addition, very little is known about the mechanism of GP-induced cytopathology. Here we show that cytopathology associated with the expression of GP does not occur when GP is restricted to the endoplasmic reticulum (ER). It has also been reported that the down-regulation of surface proteins by Ebola GP is likely mediated through a dynamin-dependent pathway [11]. However, data reported here support the alternative hypothesis that this process occurs independently of dynamin.

2.3 Materials and Methods

Plasmids, cell culture and transfections

Tva constructs were created by using two isoforms of the quail Tva ORF, Tva950 and Tva800 [22]. The transmembrane (Tva950) and GPI-anchored (Tva800) isoforms of Tva used here have the accession numbers L22753 and L22752, respectively. For each isoform, the mucin domain from the Zaire subtype (Mayinga strain) of the EBOV glycoprotein (amino acids 312-462) or Reston subtype (amino acids 317-478) was cloned between residues 77 and 78 of Tva. At the C-terminal end of the mucin domain, a flexible three amino acid linker, AAV, or PAV was added just before Tva amino acid 78 for the Zaire and Reston subtypes, respectively. To create an ER-retained version of Ebola GP, cDNA encoding the membrane-anchored form of Ebola GP (Mayinga strain, accession number U23187) was used. The four amino acid tag, KKMP, was appended to the C-terminus of the GP ORF. Constructs were cloned into the pCAGGS expression vector, except where indicated. Amino acid positions stated here are counted from the initial methionine. The dominant negative version of dynamin I (Dyn K44A) was a gift from Sandra Schmid [23]. The coding region for Dyn K44A was removed from its original vector by EcoRI and XbaI digest and cloned into a pcDNA3.1+ backbone to create a mammalian expression vector.

All cells were cultured in DMEM (Gibco) with 10% bovine cosmic-calf serum (HyClone) and penicillin/streptomycin (Gibco) at 37 ºC with 5% CO_2. For flow cytometry, fluorescence microscopy, and western blotting, 293T cells were plated at ~8 x 10^5 cells per well in 6-well plates one day prior to transfection. Cells were transiently

transfected by calcium-phosphate precipitation with 6 µg DNA per well unless otherwise stated. Cells to be visualized with GFP were co-transfected with an additional 2 µg cDNA encoding eGFP. For enumeration of floating cells, 10 cm plates were plated with 4.5 x 10^6 293T cells one day prior to transfection; cells were transiently transfected with 30 µg DNA encoding GP or Tva constructs and 10 µg DNA encoding eCFP. Immunofluorescence was performed using HeLa cells that were plated on glass coverslips at 6 x 10^4 cells per coverslip in 24-well plates one day prior to transfection. HeLa cells were transiently transfected by calcium-phosphate precipitation with 1.5 µg DNA per coverslip. For all transfections, media was replaced 5 hours post-transfection.

Floating cell assay

24 hours after transfection, supernatants were removed and combined with 2 ml PBS that had been used to gently wash the monolayer. An aliquot of the sample was employed to determine cell concentration and total sample volume was measured. Only CFP positive cells were counted using an improved Neubauer hemocytometer (Reichert) on an Nikon TE300 inverted fluorescent microscope. Percent non-adherent cells were calculated as: non-adherent cells / (adherent + non-adherent cells) x 100%. All experiments were performed in triplicate.

Cell lysates and western blotting

Transfected cells were removed by resuspension in the culturing media. Cells were pelleted at 4 ºC for 5 min at 1300 x g. Pellets were resuspended in RIPA buffer with

complete protease inhibitor cocktail (Roche) for 5 minutes on ice or at room temperature. Lysates were cleared by centrifugation at 4 ºC for 5 minutes at 20,800 x g. 30 µl samples were mixed with reducing SDS buffer, boiled for 5 minutes, and separated on a 4-15% Criterion PAGE gel (Bio-Rad). Proteins were transferred to PVDF (Millipore) at a 400 mA constant current. Membranes were blocked in 5% milk in TBS or 3% BSA in TBST for 45 minutes or overnight. Membranes were probed with rabbit polyclonal anti-GP sera [24], rabbit polyclonal anti-Tva sera [22], or mouse anti-dynamin I MAb (clone 41, BD Transduction Labs) in blocking buffer. Protein was detected with stabilized goat anti-rabbit or anti-mouse HRP conjugated antibodies (Pierce) in blocking buffer for 45 minutes. Membranes were visualized with SuperSignal Femto substrate (Pierce).

Endoglycosidase assay

30 µl of each 293T cell lysate was incubated with denaturing buffer (NEB) for 10 minutes at 60 ºC. Samples were then incubated with buffer alone (G7 and NP40, NEB), PNGase F, or Endo H_f plus appropriate buffers (NEB) for 4 to 6 hours at 37 ºC. Samples were then separated by SDS-PAGE and blotted as described above.

Transferrin uptake assay

HeLa cells were plated at 1 x 10^5 cells per coverslip in a 24-well plate format. Cells were transfected with Lipofectamine 2000 (Invitrogen) according to manufacturer's instructions with 1.5 µg per well of Dyn K44A or empty pcDNA3.1 vector. At 22 hrs post transfection, media was removed and replaced with DMEM lacking serum. At 24 hrs

post transfection, cells were placed on ice for 10 min. Human transferrin conjugated to Alexa Fluor 594 (Invitrogen) was added to a final concentration of 100 μg/ml and incubated on ice for 30 min. Cells were then washed 3 times with ice-cold PBS and either immediately fixed (T=0) or incubated with DMEM + 10% serum at 37 ºC for 15, 30, or 60 min, then fixed. Cells were then stained for dynamin I as described later.

Flow cytometry

293T cells were detached from the TC plate 24 hours post transfection with PBS -/-, 0.5 mM EDTA and combined with well media. Cells were pelleted at 4 ºC for 5 min at 250 x g, then resuspended in wash buffer (PBS with 1% bovine calf serum and 0.05% NaAzide) and aliquoted for staining. For detection of Ebola GP, cells were stained with the human MAb, KZ52 [25] and detected with FITC anti-human IgG (PharMingen). For detection of Tva proteins, cells were stained with rabbit polyclonal anti-Tva sera [22] and detected with FITC goat anti-rabbit IgG (Rockland). For detection of β1-integrin, cells were co-stained with anti-human CD29 PE-Cy5 conjugate (eBioscience); for detection of MHC-1, cells were co-stained with anti- HLA-ABC PE-Cy5 conjugate (eBioscience). For intracellular dynamin I staining, cells were permeabilized using Cytofix/Cytoperm (BD Biosciences) for 20 min, followed by washing with Permwash (BD Biosciences). For detection of dynamin I, cells were stained with mouse anti-dynamin Mab (clone 41, BD Transduction Labs) and detected with anti-mouse Alexa Fluor 488 antibodies (Invitrogen) in Permwash buffer. All staining was performed on ice for 1 hour, followed by washing. Live cell gates were drawn based on forward and side scatter. For each

sample, 10,000 events in the live cell gate were analyzed. Data were collected on a Becton Dickinson FACSCalibur and analyzed using FlowJo software (Tree Star, Inc.).

Immunofluorescence microscopy

At 48 hours post-transfection, media was removed, cells were washed with PBS, and fixed with 3% PFA in PBS for 20 minutes. Cells were then washed with PBS, then permeabilized with 0.2% saponin, 1% goat serum in PBS for 5 minutes, then washed with PBS. Cells were blocked with 10% goat serum, 0.1% Tween-20 in PBS for 2 hours. For GP and ER staining, coverslips were incubated with mouse anti-Ebola GP MAb (gift from Yoshihiro Kawaoka) and rabbit anti-calnexin (StressGen) and detected with goat anti- mouse or rabbit Alexa Fluor 594 or 488 antibodies, respectively (Invitrogen). For Golgi staining, cells were re-blocked with 10% mouse sera, then probed with mouse MAb FITC anti-GM 130 (BD Transduction Labs). For Tva staining, coverslips were incubated with rabbit polyclonal anti-Tva sera and detected with anti-rabbit Alexa Fluor 594 antibodies (Invitrogen). For dynamin I staining, coverslips were incubated with mouse anti-dynamin I MAb (clone 41, BD Transduction Labs) and detected with anti-mouse Alexa Fluor 488 antibodies (Invitrogen). Cells were washed with PBS after each staining step. For non-permeabilizing conditions, cells were fixed with 1% PFA in PBS for 20 minutes, washed, then blocked with 10% goat serum in PBS and stained as described above. All coverslips were mounted on glass slides with mounting medium containing DAPI (Vectasheild). Z-section images were collected on a Leica DMRE fluorescence microscope using Open Lab software (Improvision). Thirty z-sections per

image were collected at 0.2 μm intervals. Z-section data were deconvoluted using Velocity software (Improvision) to a 98% confidence level or 15 iterations. Images shown are single, deconvoluted, z-sections except where indicated.

2.4 Results

Characterization of Tva-mucin chimeric constructs

To investigate whether the mucin domain of Ebola GP was sufficient to cause cell rounding and protein down-regulation, we created constructs in which the mucin domain was placed into the heterologous, small monomeric glycoprotein, Tva. Tva is an avian glycoprotein and is the cellular receptor for subgroup A avian sarcoma and leukosis virus (ASLV) [22]. The quail Tva locus also produces a naturally-occurring splice variant that associates with membranes through a GPI anchor instead of a transmembrane domain (P. Bates, unpublished data), termed here, GPI Tva. The mucin domain from the Zaire subtype of Ebola GP was cloned into vectors expressing both isoforms of Tva to create expression plasmids for the proteins designated here as Tva-muc and GPI Tva-muc (Figure 2-1 A). Analysis of lysates produced from 293T cells transfected with these constructs demonstrated processing differences among the proteins (Figure 2-1 B). The multiple bands within each lane represent glycosylation variants of the proteins while differences between lanes reflect the transmembrane- verses GPI- anchored forms and the added mucin domain. To investigate the cellular localization of these proteins, immunofluorescence microscopy was performed on HeLa cells transfected with each construct (Figure 2-1 C). Staining with a polyclonal antibody to a Tva peptide showed both plasma membrane and cytoplasmic staining of each of the proteins. Expression of the transmembrane-bound isoforms, Tva and Tva-muc exhibits a punctuate or vesicular cytoplasmic staining, whereas GPI Tva and GPI Tva-muc show more of a reticular cytoplasmic staining pattern. Addition of the mucin domain to either of the Tva isoforms

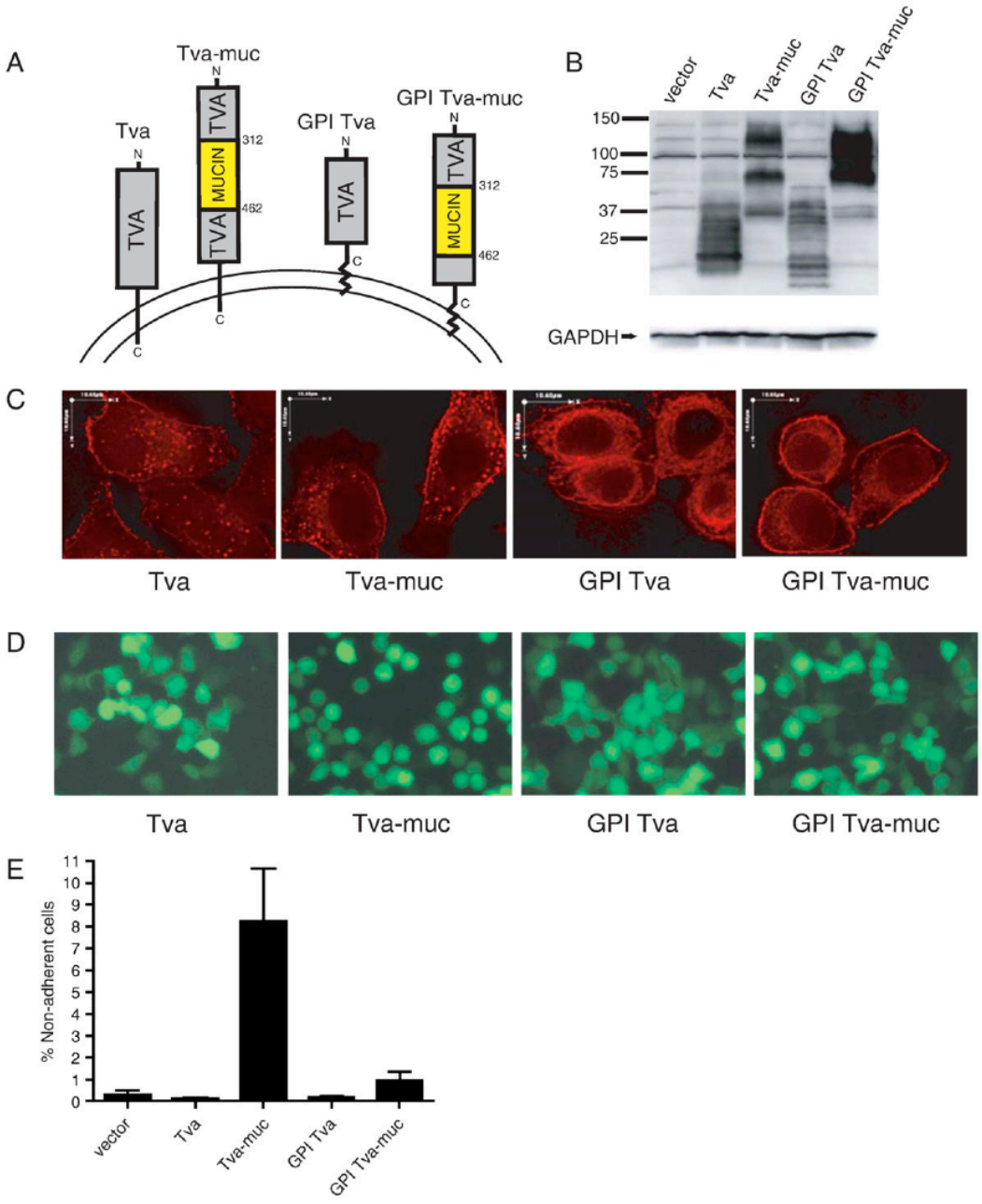

Figure 2-1 EBOV GP-mucin domain is sufficient to induce cell rounding and detachment. (A) Diagram of Tva constructs used to express Ebola Zaire GP-mucin domain. Numbers indicate amino acid position starting from the initial methionine. (B) 239T cells were transfected with pCAGGS alone (vector) or pCAGGS encoding the Tva constructs described in (A). Lysates were harvested in RIPA buffer after 24 h and subjected to SDS-4 to 15% PAGE, transferred to PVDF, and immunoblotted with polyclonal rabbit anti-Tva sera or GAPDH-specific monoclonal antibodies on blots run in parallel. (C) HeLa cells were transfected with Tva constructs. 48 h posttransfection,

cells were fixed, permeabilized, and stained for Tva with polyclonal rabbit anti-Tva sera followed by Alexa 594 conjugated antibodies. Z-sections were captured on a fluorescence microscope and deconvolved with software. Images shown are single, deconvolved Z-sections. Scale bars are 10.6 μm. (D) 293T cells were co-transfected with Tva constructs and a vector encoding eGFP in a 3:1 ratio. After 24 h fluorescent images were captured on an inverted microscope using a GFP filter. Fields represent findings from multiple experiments. (E) 239T cells were transfected with pCB6 vector alone or pCB6 encoding the Tva constructs described in (A) and co-transfected with a vector encoding eCFP in a 3:1 ratio. 24 h post-transfection, adherent and non-adherent cells were removed. CFP positive cells were counted; data is shown as % non-adherent cells. Graph shows mean of 3 replicates; error bars indicate SD. Results are representative of 2 independent experiments.

did not cause any significant change in the observed staining patterns (Figure 2-1 C).

GP mucin domain is sufficient to cause GP-characteristic cytopathology

To address whether the expression of the chimeric mucin domain proteins could induce similar morphological changes to those seen upon expression of EBOV GP, each of the Tva constructs described above was mixed with an eGFP encoding vector and used to transfect 293T cells. 24 hours after transfection, fluorescence microscopy was performed to visualize transfected cells (Figure 2-1 D). While transfection of Tva or GPI Tva did not induce any change in cell morphology, cells transfected with Tva-muc were rounded and many had lost their ability to adhere to the extracellular matrix. In contrast, the transfection of GPI Tva-muc had no effect on cell morphology. To quantify the mucin domain-induced loss of adhesion to the extracellular matrix, 293T cells were co-transfected with the Tva constructs and an eCFP-encoding vector. Floating and adherent cells were removed 24 hours post-transfection; only transfected (CFP positive) cells were counted. Expression of Tva-muc caused cell detachment that was over ten-fold higher than background levels (Figure 2-1 E). Transfection with Tva, GPI Tva, or GPI Tva-muc did not result in cellular detachment significantly above background levels.

To further characterize the effects of the Ebola mucin domain on cellular physiology, we used flow cytometry to measure surface levels of β1 integrin and MHC1 in transfected cells. Both of these proteins are known to be down-regulated from the surface of cells expressing high levels of EBOV GP [9,10]. Cells that were transfected with Tva showed no change in levels of β1 integrin or MHC1 after 24 hours; however,

cells transfected with Tva-muc showed a roughly one log decrease in fluorescence of both proteins (Figure 2-2). Close inspection of the FACS plots reveals that cells with low expression of Tva-muc have intact levels of β1 integrin and MHC1; however, there seems to be a threshold of Tva-muc expression, above which β1 integrin and MHC1 levels drop precipitously. By contrast, this threshold effect is not seen with GPI Tva-muc. The GPI Tva-muc sample has expression levels of the chimeric protein that would be predicted to cause down-regulation of β1 integrin and MHC1, yet this is not observed. From these results we conclude that the mucin domain of Ebola GP, when expressed within the context of a transmembrane-bound form of Tva, is sufficient to cause cytopathology characteristic of full-length GP expression.

To address whether mucin domains of different subtypes of EBOV differ in their ability to cause cytopathology, we compared the mucin regions from Ebola Zaire to Ebola Reston. Reston is considered to be the least pathogenic subtype of Ebola, while Zaire is the most pathogenic [26]. The mucin domain of Ebola Reston was expressed within the transmembrane-bound form of Tva. Interestingly, 293T cells that were transfected with Tva-muc of the Reston and Zaire subtypes both showed equal reduction of β1 integrin and MHC1 surface staining after 24 hours by flow cytometry (data not shown).

Characterization of GP-kk

To address whether GP could exert its effects from the endoplasmic reticulum or if transport to the cell surface is required, we created a version of the Ebola

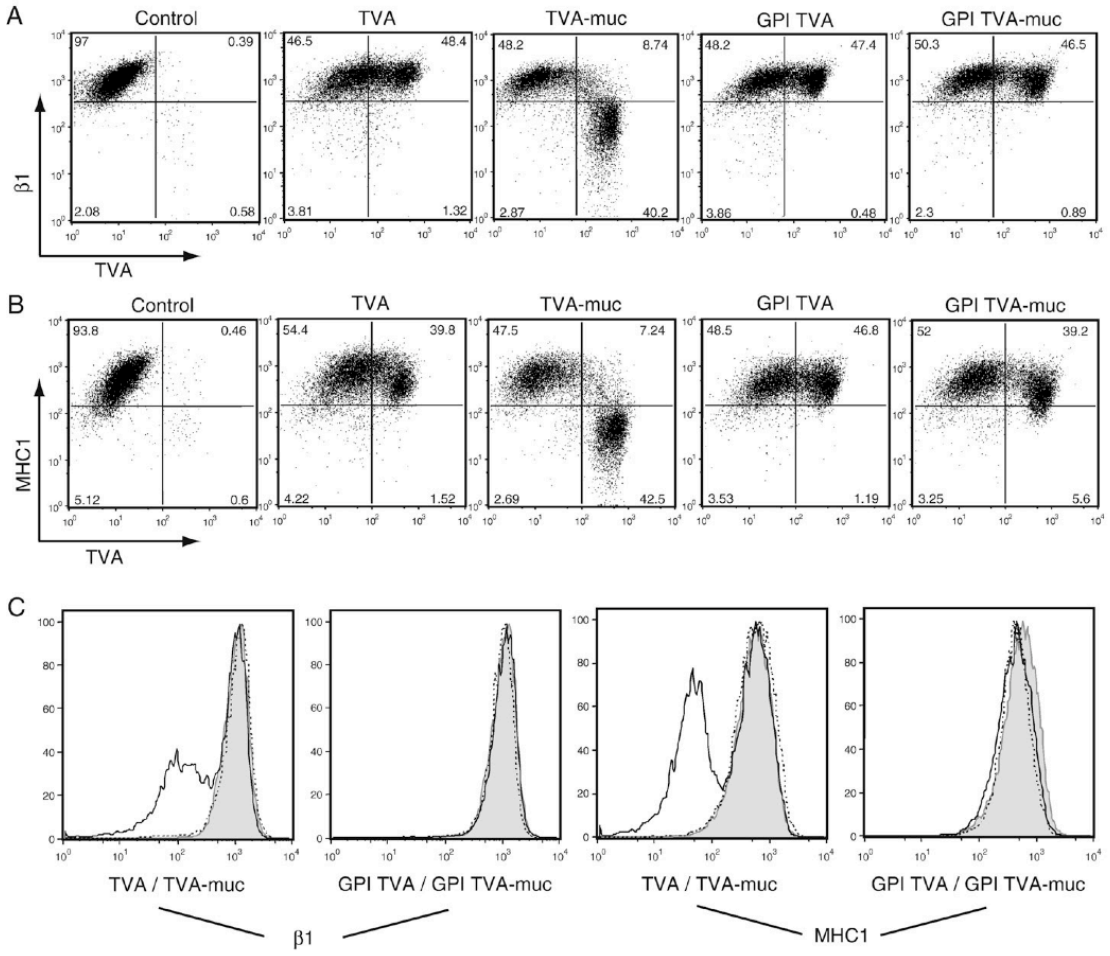

Figure 2-2 Surface protein down-regulation by EBOV GP mucin domain. 239T cells were transfected with vector alone or vector encoding the Tva constructs described in Figure 2-1 A. Floating and adherent cells were harvested 24 h after transfection, pooled, and stained with polyclonal rabbit anti-Tva sera and FITC-labeled secondary antibodies, co-stained for β1 integrin or MHC1 with PE-Cy5 conjugated monoclonal antibodies and assayed by flow cytometry. Analysis is shown for events in the live cell gate. (A) β1 integrin vs. Tva surface expression. (B) MHC1 vs. Tva surface expression. (C) Histogram representation of β1 integrin surface expression (left panels) and MHC1 surface expression (right panels). Control samples are shown shaded; Tva or GPI Tva is shown as a dashed line; Tva-muc or GPI Tva-muc is shown as a solid line. Data is representative of multiple independent experiments.

GP with an ER retention signal, KKMP, appended to the cytoplasmic tail of the protein (GP-kk). Analysis of lysates made from 293T cells transfected with GP and GP-kk demonstrated that the constructs were expressed to a similar level (Figure 2-3 A). To characterize the glycosylation state of GP-kk, lysates from GP or GP-kk transfected cells were incubated with PNGase F, which removes all N-linked glycans, and Endo H_f, which removes high-mannose glycans, characteristic of proteins that have not matured through the Golgi (Figure 2-3 B). When incubated with Endo H_f, the majority of GP-kk protein co-migrates with PNGase F digested protein on SDS-PAGE. This Endo H_f sensitivity suggests that GP-kk is not transported to the Golgi and remains in the ER. By comparison, the majority of GP is resistant to Endo H_f digestion, as would be expected of protein that has matured through the Golgi.

GP cellular localization

To further examine the localization of GP-kk, immunofluorescence microscopy was performed on HeLa cells transfected with GP and GP-kk (Figure 2-3 C). Permeabilized and non-permeabilized cells were stained with a monoclonal antibody to Ebola GP and co-stained with an antibody to GM-130, a *cis*-Golgi localized scaffold protein, to test the integrity of the plasma membrane during staining (Figure 2-3 C, top and middle panels). GP-transfected cells displayed intense plasma membrane staining in both permeabilized and non-permeabilized cells. Some internal vesicular staining was noted for GP, however this showed no significant colocalization with GM-130 (Figure 2-

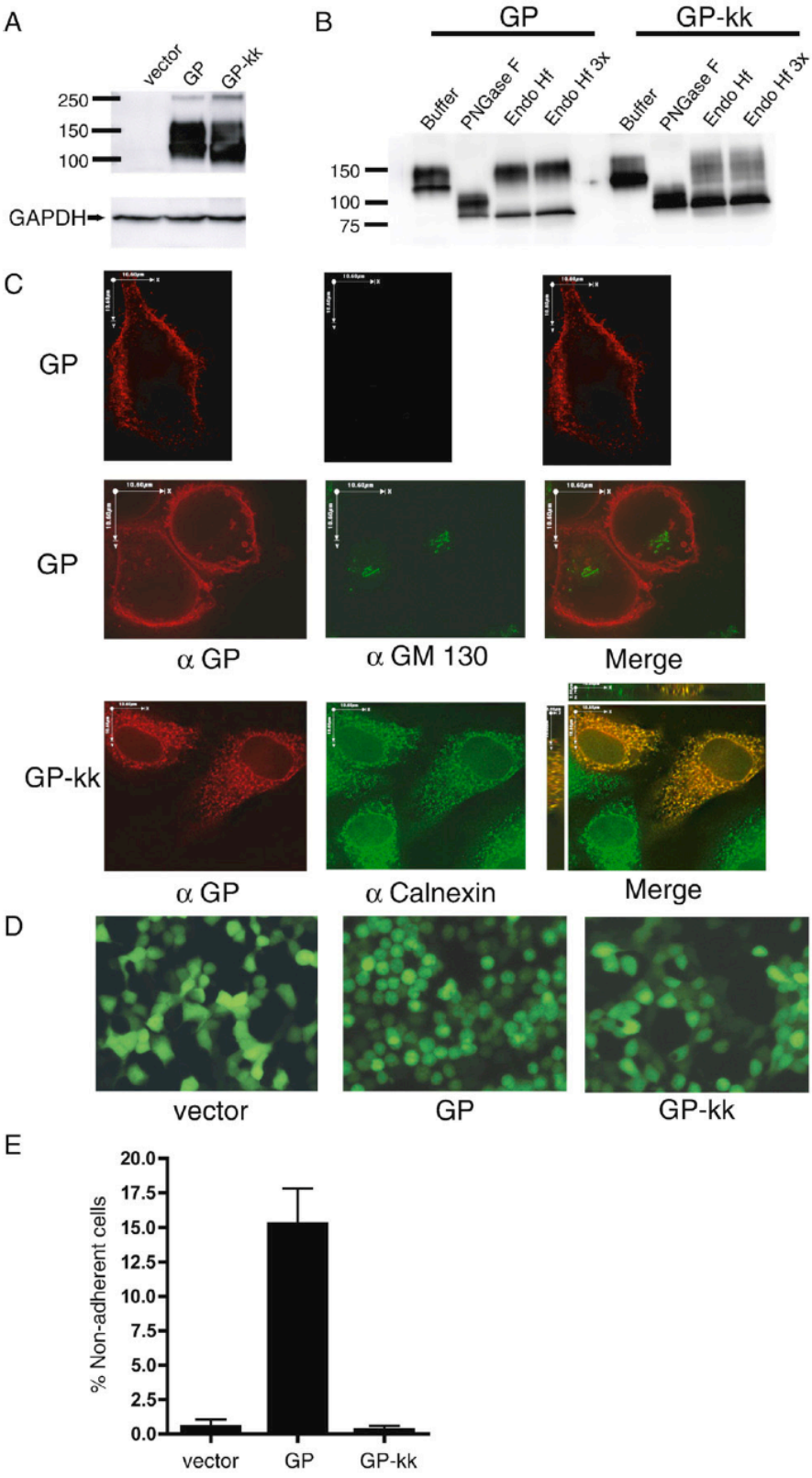
A
vector
GP
GP-kk
250
150
100
GAPDH
B
GP
GP-kk
Buffer
PNGase F
Endo Hf
Endo Hf 3x
Buffer
PNGase F
Endo Hf
Endo Hf 3x
150
100
75
C
GP
GP
α GP
α GM 130
Merge
GP-kk
α GP
α Calnexin
Merge
D
vector
GP
GP-kk
E
% Non-adherent cells
20.0
17.5
15.0
12.5
10.0
7.5
5.0
2.5
0.0
vector
GP
GP-kk

Figure 2-3 EBOV GP does not round cells when restricted to the ER. (A) 293T cells were transfected with vector alone, vector encoding for GP, or GP-kk (ER-restricted). Lysates were harvested in RIPA buffer after 24 h and subjected to SDS-4 to 15% PAGE, transferred to PVDF, and immunoblotted with polyclonal rabbit anti-GP sera and GAPDH-specific monoclonal antibodies. (B) GP and GP-kk lysates were denatured and incubated with enzyme buffer alone or buffer with PNGase F or Endoglycosidase H_f (at normal or 3x concentration), then subjected to SDS-PAGE and immunoblotting as described in (A). (C) HeLa cells were transfected with GP or GP-kk. 48 h posttransfection, cells were fixed, either not permeabilized (top row) or permeabilized (middle and bottom rows) and stained for GP with mouse monoclonal antibodies, followed by Alexa 594 conjugated antibodies (red). Cells were also co-stained with FITC-conjugated monoclonal antibodies to GM 130 (green) or with rabbit polyclonal antibodies to calnexin, followed by Alexa 488 antibodies (green). Z-sections were captured on a fluorescence microscope and deconvoluted. Images shown in top and middle rows are composite, deconvoluted Z-sections. Images in the bottom row are single, deconvoluted Z-sections; the merge panel also shows views in the XZ and YZ planes. Scale bars are 10.6 μm. (D) 293T cells were transfected with vector alone, or vector encoding GP, or GP-kk and co-transfected with eGFP in a 3:1 ratio. After 24 h fluorescent images were captured on an inverted microscope using a GFP filter. Fields represent findings from multiple experiments. (E) 293T cells were transfected with vector alone or vector encoding for GP or GP-kk and co-transfected with a vector encoding eCFP in a 3:1 ratio. 24 h post-transfection, adherent and non-adherent cells were removed. CFP positive cells were counted; data is shown as % non-adherent cells. Graph shows mean of 3 replicates; error bars indicate SD. Results are representative of 2 independent experiments.

3 C, middle panels). By contrast, only very few non-permeabilized cells transfected with GP-kk showed any surface staining (data not shown). For the majority of GP-kk expressing cells, GP staining could only be seen upon permeablization (Figure 2-3 C, bottom panels). Staining of these cells revealed a cytoplasmic, reticular pattern. GP-kk appeared to co-localize with staining of the ER-resident protein, calnexin, but did not demonstrate detectable colocalization with GM-130 (data not shown). Thus, we conclude that GP-kk is actively retained in the ER through its retention signal.

GP-kk does not cause cytopathology

We then asked whether retaining Ebola GP in the ER had any effect on cell rounding and protein down-regulation. 293T cells were transfected with GP, GP-kk, or the empty vector and co-transfected with eGFP as above. 24 hours after transfection, microscopy was performed using a GFP filter so that only transfected cells were visualized (Figure 2-3 D). Cells transfected with the vector were flat and adherent, whereas GP transfected cells were rounded and floating. Cells that had been transfected with GP-kk were morphologically indistinguishable from the vector control. To quantify this result, floating and adherent cells in culture dishes were counted 24 hours after co-transfection of the GP constructs with an eCFP-encoding vector (Figure 2-3 E). The addition of the ER retention signal to GP resulted in a reduction the number of floating cells by approximately 98%, to background levels. 293T cells transfected with GP or GP-kk were stained with antibodies to Ebola GP and β1 integrin or MHC1 and analyzed by flow cytometry. Whereas GP strongly down-regulated β1 integrin and MHC1, GP-kk

did not (Figure 2-4). Flow cytometric analysis of GP-kk transfected cells, surfaced stained for Ebola GP, reveals that a small percentage of transfected cells express GP-kk on the surface, despite the ER retention signal (Figure 2-4). This observation is supported by immunofluorescence microscopy studies, where some surface-stained cells are observed, and also endoglycosidase assay data (Figure 2-3 B), in which a small amount of Endo Hf-resistant protein in the GP-kk sample is visible. Interestingly, in the small amount of cells that show some surface staining for GP-kk, levels of β1 integrin and MHC1 do not appear altered. It should also be noted that GP-transfected cells show down-regulation of GP from the surface resulting in comma-shaped FACS plots (Figure 2-4 A, B). However, this comma-shaped profile was not observed with the Tva constructs (Figure 2-2 A, B). These data allow us to conclude that the Ebola GP does not cause morphological changes and protein down-regulation when retained in the ER.

Surface protein down-regulation is not mediated through a dynamin-dependent pathway

To address whether surface protein down-regulation was affected by the expression of a dominant-negative version of dynamin as previously reported [11], we employed a construct expressing human dynamin I with a K44A mutation (Dyn K44A). This mutation is known to disrupt coated vesicle formation and trafficking by exerting a dominant negative effect on dynamin's role in vesicle formation [23]. Analysis of lysates made from 293T cells transfected with Dyn K44A demonstrated that the construct was expressed and that the dynamin I antibody specifically recognized the transfected dynamin I protein, not endogenous dynamin II (Figure 2-5 A). To examine the ability of

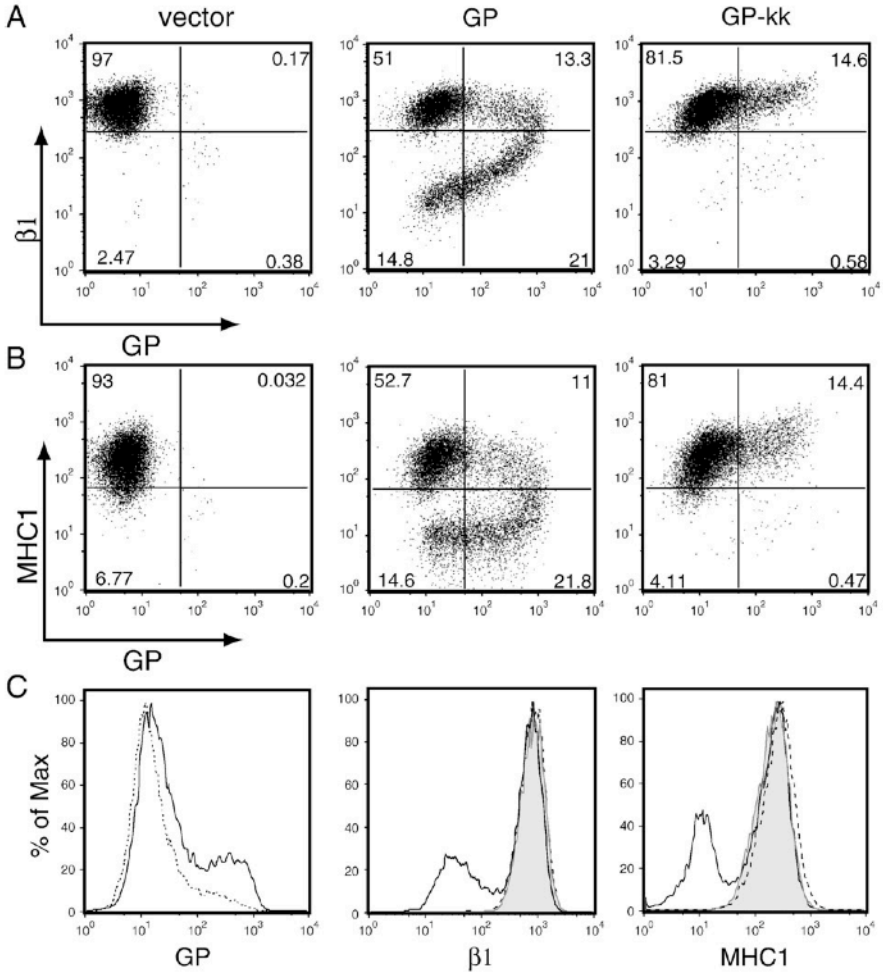

Figure 2-4 EBOV GP does not induce surface protein down-regulation when restricted to ER. 293T cells were transfected with vector alone or vector encoding GP or GP-kk. Floating and adherent cells were harvested 24 h after transfection, pooled, and stained with antibodies to GP using human monoclonal antibodies and FITC-labeled secondary antibodies, co-stained for β1 integrin or MHC1 with PE-Cy5 conjugated monoclonal antibodies and assayed by flow cytometry. Analysis is shown for events in the live cell gate. (A) β1 integrin vs. GP surface expression. (B) MHC1 vs. GP surface expression. (C) Histogram representation of GP surface expression (left panel), β1 surface expression (middle panel), and MHC1 surface expression (right panel). Control samples are shown shaded; GP is shown as a solid line, and GP-kk is shown as a dashed line. Data are representative of multiple independent experiments.

Dyn K44A to block vesicle trafficking, a transferrin uptake assay was performed. As shown in Figure 2-5 B, labeled transferrin bound the surface of HeLa cells at 4 ºC. When incubated at 37 ºC for 15 min., cells internalized the transferrin; however, transferrin remained at the surface of cells transfected with Dyn K44A. This effect was also seen after incubation for 30 min.; after 60 min. the transferrin was mostly degraded (data not shown). Thus, our Dyn K44A behaves as a functional dominant negative of dynamin-dependent pathways.

We then addressed whether the expression of Dyn K44A would alter the level of surface protein down-regulation in GP-transfected cells. Transfection of Dyn K44A alone did not alter the surface levels of β1 integrin or MHC1 (data not shown). However, Sullivan *et. al* reported that transfection of dominant negative dynamin reduced nearly half of the down-regulation of αV integrin and a significant portion of the down-regulation of MHC1 by GP [11]. In contrast, we found that after co-transfection of DNA encoding Dyn K44A and GP in a ratio of 3:1, no change in the down-regulation of MHC1 or β1 integrin could be observed (Figure 2-5 C). It should be noted that the transfection efficiency of GP in these experiments varied by less than 2% between samples (Figure 2-5 C, upper left-hand quadrants). We also examined the effect of Dyn K44A on the down-regulation of β1 integrin and MHC1 by Tva-muc. Transfections were performed as with GP. Our data indicate that Dyn K44A does not reduce the number of cells in Tva-muc transfected cultures that have down-regulated levels of β1 integrin and MHC1 (Figure 2-5 D).

We have previously reported that in cultures transfected with GP, floating cells are 90% positive for GP expression and 95% viable [10]. Here we demonstrate that floating cells also exhibited the most dramatic phenotype of surface protein down-regulation (Figure 2-5 E). To ensure that cells co-transfected with GP and Dyn K44A expressed Dyn K44A, floating cells were also analyzed by intracellular staining for dynamin I. Flow cytometry revealed that 95% of floating cells stained positive for dynamin I (Figure 2-5 F).

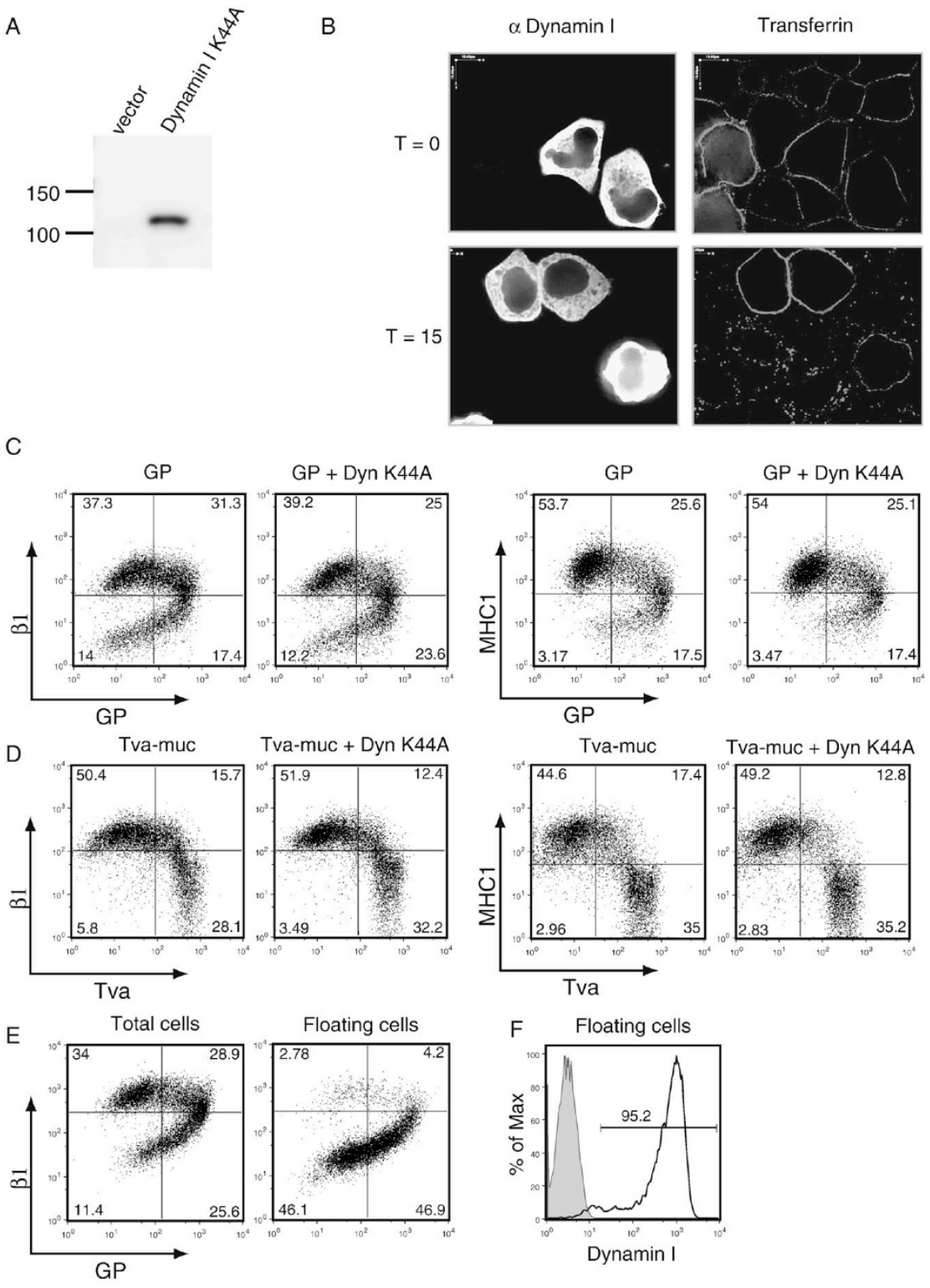
A
vector
Dynamin I K44A
150
100
B
α Dynamin I
Transferrin
T = 0
T = 15
C
GP
GP + Dyn K44A
GP
GP + Dyn K44A
37.3
31.3
14
17.4
39.2
25
12.2
23.6
53.7
25.6
3.17
17.5
54
25.1
3.47
17.4
β1
GP
MHC1
GP
D
Tva-muc
Tva-muc + Dyn K44A
Tva-muc
Tva-muc + Dyn K44A
50.4
15.7
5.8
28.1
51.9
12.4
3.49
32.2
44.6
17.4
2.96
35
49.2
12.8
2.83
35.2
β1
Tva
MHC1
Tva
E
Total cells
Floating cells
34
28.9
11.4
25.6
2.78
4.2
46.1
46.9
β1
GP
F
Floating cells
% of Max
95.2
Dynamin I

Figure 2-5 GP-mediated surface protein down-regulation is not mediated by dynamin I. (A) 293T cells were transfected with vector alone or vector encoding dynamin I K44A (Dyn K44A). Lysates were harvested in RIPA buffer after 24 h and subjected to SDS-4 to 15% PAGE, transferred to PVDF, and immunoblotted with anti-dynamin I mouse MAb. (B) HeLa cells were transfected with Dyn K44A. After 22 hours, cells were serum starved for 2 hours. Cells were then iced and incubated with Alexa 594-conjugated human transferrin. Cells were either immediately fixed (T=0), or incubated at 37ºC for 15 minutes (T=15). Cells were fixed, permeabilized, and stained for dynamin I as described in Materials and Methods, then analyzed by fluorescent microscopy. (C, D) 293T cells were co-transfected (in a 1:3 ratio) with GP and vector or GP and Dyn K44A (C), Tva-muc and vector or Tva-muc and Dyn K44A (D). Floating and adherent cells were harvested 24 h after transfection, pooled, and stained with antibodies to GP using human monoclonal antibodies and antibodies to Tva using a polyclonal rabbit anti-Tva sera followed by FITC-labeled secondary antibodies, co-stained for β1 integrin or MHC1 with PE-Cy5 conjugated monoclonal antibodies, and assayed by flow cytometry. (E) 239T cells were transfected with GP. After 24 hours, floating cells were either pooled with adherent cells (left plot) or separated from adherent cells (right plot) and stained for GP and β1 integrin as described previously. (F) 293T cells were co-transfected with GP and Dyn K44A (black line) in a 1:3 ratio. Floating cells were harvested after 24 hours, permeabilized, and stained for intracellular dynamin I. Shaded peak represents GP + vector-transfected cells stained for dynamin I. Analyses are shown for events in the live cell gate. Data are representative of multiple independent experiments.

2.5 Discussion

The mucin domain of Ebola GP seems to have no critical function in entry or fusion of Ebola pseudotypes, but instead decreases the efficiency of *in vitro* pseudotype infection [14,15]. However, selective pressure to maintain this domain and conserve its length and glycosylation suggests that this portion of the viral glycoprotein plays an important role in other aspects of the viral infection cycle *in vivo*. Because of its placement within the glycoprotein trimer, the mucin domain is in a position to interact with other cellular surface proteins or protect the rest of GP from immune recognition. In fact, Takada and colleagues have shown that the mucin domain is important for interactions with certain C-type lectins and suggest that these interactions may play a role in virus entry [27]. Such interactions may also be the basis for the cytopathic effects discussed here.

A recent report by Alazard-Dany *et al*. demonstrated that moderate to low levels of GP expression do not induce cell rounding [2]; this is in agreement with our data, which indicates that 293T cells down-regulate surface proteins after reaching a threshold of surface GP expression (Figure 2-4 A, B). Data from Alazard-Dany *et al*. also demonstrate that cell rounding, detachment, and the down-regulation of β1 integrin and MHC1 can be observed by 48 hours post-infection with EBOV, suggesting that this effect is not an artifact of over-expressing GP *in vitro*.

The data presented here demonstrate that the mucin domain of Ebola Zaire is sufficient to cause cytopathic effects that are comparable with those caused by full-length Ebola GP. Tva-muc induces cell rounding and detachment in 293T cells and significant

surface down-regulation of both β1 integrin and MHC1. The extent to which this cellular phenomenon contributes to viral pathogenesis remains to be tested; however, cytopathology may have several effects. Non-human primate studies have revealed that the innate immune response and resulting communication of antigen-presenting cells (APCs) to the adaptive arm of the immune system is disrupted during Ebola infection (reviewed in [28]). Therefore, effects of GP-mediated cytopathology on APCs could contribute to immune dysregulation. Because integrins are known to play a critical role in the homing of leukocytes to sites of infection [29], loss of adhesion may disrupt the function of macrophages or dendritic cells; we have shown GP expression to cause rounding in macrophages [10]. The down-regulation of MHC1 in other cell types could be a mechanism of escape from $CD8^+$ T-cell surveillance. Additionally, loss of adhesion by GP transduction in cultured saphenous veins is thought to be a model for hemorrhagic symptoms seen during Ebola infection [4,11]. Finally, loss of adhesion by Ebola GP has been shown to cause anoikis in primary endothelial cells [30]. GP-induced loss of adhesion and resulting anoikis could provide one mechanism for necrosis seen during infection, specifically in organs such as the liver where immune infiltration is limited; other cellular factors such as tumor necrosis factor-related apoptosis-inducing ligand have also been implicated [31,32].

If the effects of the mucin domain contribute to the pathogenesis of the Zaire subtype of EBOV, one might expect cytopathology caused by the less-pathogenic Reston subtype to be measurably less. Indeed, our previous report comparing Ebola GP Zaire and Reston found that GP Reston caused fewer floating cells in culture and less loss of

surface staining of integrins and MHC1 by flow cytometry [10]. Interestingly, our comparison of the mucin domains from the Ebola subtypes Reston and Zaire indicate that both are equal in their ability to cause cytopathology from the Tva platform. This suggests that the presentation of the mucin domain the context of the full glycoprotein may affect the ability of the domain to cause cytopathology. It is also interesting that, while the mucin domain normally induces the rounding phenotype from within the GP trimer, we have demonstrated that it is able to exert these effects from within the monomeric protein, Tva.

When the mucin domain of GP is expressed in the context of the GPI-anchored isoform of Tva, the rounding phenotype is abolished and protein down-regulation of MHC1 and β1 integrin is not observed. It is possible that the mucin domain in GPI Tva-muc is physically positioned or becomes differentially glycosylated in such a way that prevents rounding. A more appealing alternative is that GPI Tva traffics or is localized at the plasma membrane differently than Tva. Immunofluorescence microscopy analysis of these constructs in HeLa cells shows possible differences in internal staining, but does not reveal any discernable difference in plasma membrane staining (Figure 2-1 C). However, it has been reported that GPI Tva localizes to detergent-resistant membranes, while Tva does not, and that GPI Tva traffics to an acidic compartment through a different endocytic pathway than Tva upon binding of ASLV [33]. These characteristics could explain the differences between Tva-muc and GPI Tva-muc. It is also probable that the addition of the Ebola mucin domain further affects the membrane localization or trafficking pathways used by Tva.

The mechanism by which Ebola GP causes cytopathology is also unknown. A recent report provides evidence that GP utilizes a dynamin-dependent pathway to cause surface protein down-regulation [11]. Dynamin has been implicated in vesicle fission for several pathways, including clathrin- dependent and independent endocytosis, as well as *trans*-Golgi budding [34,35,36]. Therefore, it is possible that GP alters surface protein levels by affecting endocytosis. We addressed the function of dynamin in the process of GP- and Tva-muc- mediated surface protein down-regulation. As demonstrated in Figure 2-5, a dominant negative version of dynamin I was able to block the endocytosis of the transferrin receptor, but could not block the down-regulation of β1 integrin or MHC1 by GP or Tva-muc. Thus, we propose a model of down-regulation that is independent of dynamin-regulated pathways.

The two surface proteins studied here, β1 integrin and MHC1, both undergo constant endocytosis and recycling back to the plasma membrane [37,38,39,40]. Many viruses encode proteins that modulate MHC1 levels at the cell surface. For example, the K3 and K5 proteins from Kaposi's sarcoma-associated herpesvirus increase the rate of MHC1 endocytosis [41]. Other viruses block MHC1 expression by interfering in the ER. The US11 gene encoded by the human cytomegalovirus retro-translocates newly synthesized MHC1 molecules out of the ER where they are degraded by the proteosome [42]. Furthermore, some viral proteins are able to modulate MHC1 levels by influencing multiple pathways. The Nef protein from HIV has been reported to increase endocytosis of MHC1 and also to redirect newly-sythesized MHC1 from the *trans*-Golgi network (TGN) to the lysosome [43,44,45]. Therefore, it seemed prudent to ask whether Ebola

GP could cause rounding and protein down-regulation when restricted to the ER. As shown in Figures 2-3 and 2-4, our findings reject a model of down-regulation of β1 integrin and MHC1 by interference in the ER. These data suggest a mechanism of regulation at the plasma membrane or TGN.

GP directs the down-regulation of surface proteins, but also appears to down-regulate its own surface expression in a manner that seems concurrent with that of β1 integrin and MHC1 (Figure 2-4 A, B). Because the mechanism of action is unknown, it is not clear if GP plays a direct role in guiding the down-regulation of other surface molecules. It has, however, been reported that GP and αV integrin, which is also down-regulated in 293T cells, can be co-immunoprecipitated [11]. If GP directly binds to proteins to facilitate down-regulation, this could explain the observation that cells showing down-modulation of β1 integrin or MHC1 have reduced surface levels of GP (Figure 2-4). Interestingly, Tva-muc is able to down-regulate β1 integrin and MHC1 without a reduction in surface expression of Tva-muc (Figure 2-2 A, B). This could indicate that the mechanism of down-regulation is indirect, such as through a signaling cascade which affects endocytosis and/or recycling. Alternatively, it is possible that Tva-muc interacts directly with β1 integrin and MHC1, but simply recycles back to the plasma membrane more efficiently than GP.

When GP-kk is expressed in 293T and HeLa cells, a portion of cells show some expression on the surface despite the ER retention motif (Figure 2-4 C). It is unclear whether this is the result of cleavage of the KK signal off of the C-terminus, or overwhelming of the ER retention machinery due to over-expression. Interestingly, cells

that do express GP-kk on the surface do not round or detach and show no down-regulation of β1 integrin or MHC1. FACS analysis (Figure 2-4 C, left panel) shows that surface-localized GP-kk is expressed at a much lower level than GP. In addition, analysis of GP down-regulation seems to indicate that GP reaches a critical density on the surface before down-regulation occurs (Figure 2-4 A, B). Thus, it is possible that in the cells where GP-kk is expressed on the surface, the glycoprotein does not reach the required density and therefore does not induce protein down-regulation. Although the precise mechanism of GP-mediated cytopathology remains unknown, the mucin domain of GP has the ability to play an important role in the pathogenesis of EBOV. Cellular loss of adhesion by the mucin domain of GP may contribute to hemorrhagic symptoms, and in combination with reduction in levels of immune regulatory proteins such as MHC1, is likely a critical part of the strategy for immune evasion by EBOV. In this regard it will be interesting to analyze the effects of the mucin domain in cells derived from the natural hosts for Ebola.

2.6 Acknowledgements

The authors would like to thank Andrew Piefer for assistance with fluorescence microscopy and manuscript comments, Rachel Kaletsky for manuscript comments, Dennis Burton for providing the KZ52 antibody, Sandra Schmid for the dynamin I K44A construct, and Yoshihiro Kawaoka for providing anti-GP monoclonal antibodies for IF. This work was funded by Public Health Service grants T32-GM07229 (JF), T32-AI07324 (MM), and R01-AI43455 (PB).

2.7 References

1. Sanchez A, Khan AS, Zaki SR, Nabel GJ, Ksiazek TG, et al. (2001) Filoviridae: Marburg and Eboila Viruses. In: Knipe DM, Howley PM, Griggen DE, Lamb RA, Martin MA et al., editors. Fields Virology: Lippincott, Williams & Wilkins. pp. 1279-1304.
2. Alazard-Dany N, Volchkova V, Reynard O, Carbonnelle C, Dolnik O, et al. (2006) Ebola virus glycoprotein GP is not cytotoxic when expressed constitutively at a moderate level. J Gen Virol 87: 1247-1257.
3. Barrientos LG, Rollin PE (2006) Release of cellular proteases into the acidic extracellular milieu exacerbates Ebola virus-induced cell damage. Virology.
4. Yang ZY, Duckers HJ, Sullivan NJ, Sanchez A, Nabel EG, et al. (2000) Identification of the Ebola virus glycoprotein as the main viral determinant of vascular cell cytotoxicity and injury. Nat Med 6: 886-889.
5. Chan SY, Ma MC, Goldsmith MA (2000) Differential induction of cellular detachment by envelope glycoproteins of Marburg and Ebola (Zaire) viruses. J Gen Virol 81: 2155-2159.
6. Volchkov VE, Volchkova VA, Muhlberger E, Kolesnikova LV, Weik M, et al. (2001) Recovery of infectious Ebola virus from complementary DNA: RNA editing of the GP gene and viral cytotoxicity. Science 291: 1965-1969.
7. Volchkova VA, Feldmann H, Klenk HD, Volchkov VE (1998) The nonstructural small glycoprotein sGP of Ebola virus is secreted as an antiparallel-orientated homodimer. Virology 250: 408-414.
8. Sanchez A, Trappier SG, Mahy BW, Peters CJ, Nichol ST (1996) The virion glycoproteins of Ebola viruses are encoded in two reading frames and are expressed through transcriptional editing. Proceedings of the National Academy of Sciences of the United States of America 93: 3602-3607.
9. Takada A, Watanabe S, Ito H, Okazaki K, Kida H, et al. (2000) Downregulation of beta1 integrins by Ebola virus glycoprotein: implication for virus entry. Virology 278: 20-26.
10. Simmons G, Wool-Lewis RJ, Baribaud F, Netter RC, Bates P (2002) Ebola virus glycoproteins induce global surface protein down-modulation and loss of cell adherence. J Virol 76: 2518-2528.
11. Sullivan NJ, Peterson M, Yang ZY, Kong WP, Duckers H, et al. (2005) Ebola virus glycoprotein toxicity is mediated by a dynamin-dependent protein-trafficking pathway. J Virol 79: 547-553.
12. Volchkov VE, Feldmann H, Volchkova VA, Klenk HD (1998) Processing of the Ebola virus glycoprotein by the proprotein convertase furin. Proc Natl Acad Sci U S A 95: 5762-5767.
13. Sanchez A, Yang ZY, Xu L, Nabel GJ, Crews T, et al. (1998) Biochemical analysis of the secreted and virion glycoproteins of Ebola virus. J Virol 72: 6442-6447.
14. Manicassamy B, Wang J, Jiang H, Rong L (2005) Comprehensive analysis of ebola virus GP1 in viral entry. J Virol 79: 4793-4805.

15. Medina MF, Kobinger GP, Rux J, Gasmi M, Looney DJ, et al. (2003) Lentiviral vectors pseudotyped with minimal filovirus envelopes increased gene transfer in murine lung. Mol Ther 8: 777-789.
16. Beck M, Strand MR (2005) Glc1.8 from Microplitis demolitor bracovirus induces a loss of adhesion and phagocytosis in insect high five and S2 cells. J Virol 79: 1861-1870.
17. Wesseling J, van der Valk SW, Vos HL, Sonnenberg A, Hilkens J (1995) Episialin (MUC1) overexpression inhibits integrin-mediated cell adhesion to extracellular matrix components. J Cell Biol 129: 255-265.
18. Osako M, Yonezawa S, Siddiki B, Huang J, Ho JJ, et al. (1993) Immunohistochemical study of mucin carbohydrates and core proteins in human pancreatic tumors. Cancer 71: 2191-2199.
19. Yamashita K, Yonezawa S, Tanaka S, Shirahama H, Sakoda K, et al. (1993) Immunohistochemical study of mucin carbohydrates and core proteins in hepatolithiasis and cholangiocarcinoma. Int J Cancer 55: 82-91.
20. McGuckin MA, Walsh MD, Hohn BG, Ward BG, Wright RG (1995) Prognostic significance of MUC1 epithelial mucin expression in breast cancer. Hum Pathol 26: 432-439.
21. Wesseling J, van der Valk SW, Hilkens J (1996) A mechanism for inhibition of E-cadherin-mediated cell-cell adhesion by the membrane-associated mucin episialin/MUC1. Mol Biol Cell 7: 565-577.
22. Bates P, Young JA, Varmus HE (1993) A receptor for subgroup A Rous sarcoma virus is related to the low density lipoprotein receptor. Cell 74: 1043-1051.
23. Damke H, Baba T, Warnock DE, Schmid SL (1994) Induction of mutant dynamin specifically blocks endocytic coated vesicle formation. J Cell Biol 127: 915-934.
24. Lin G, Simmons G, Pohlmann S, Baribaud F, Ni H, et al. (2003) Differential N-linked glycosylation of human immunodeficiency virus and Ebola virus envelope glycoproteins modulates interactions with DC-SIGN and DC-SIGNR. J Virol 77: 1337-1346.
25. Maruyama T, Rodriguez LL, Jahrling PB, Sanchez A, Khan AS, et al. (1999) Ebola virus can be effectively neutralized by antibody produced in natural human infection. J Virol 73: 6024-6030.
26. Fisher-Hoch SP, Brammer TL, Trappier SG, Hutwagner LC, Farrar BB, et al. (1992) Pathogenic potential of filoviruses: role of geographic origin of primate host and virus strain. Journal of Infectious Diseases 166: 753-763.
27. Takada A, Fujioka K, Tsuiji M, Morikawa A, Higashi N, et al. (2004) Human macrophage C-type lectin specific for galactose and N-acetylgalactosamine promotes filovirus entry. J Virol 78: 2943-2947.
28. Mahanty S, Bray M (2004) Pathogenesis of filoviral haemorrhagic fevers. The Lancet Infectious Diseases 4: 487-498.
29. Butcher EC (1991) Leukocyte-endothelial cell recognition: three (or more) steps to specificity and diversity. Cell 67: 1033-1036.

30. Ray RB, Basu A, Steele R, Beyene A, McHowat J, et al. (2004) Ebola virus glycoprotein-mediated anoikis of primary human cardiac microvascular endothelial cells. Virology 321: 181-188.
31. Geisbert TW, Hensley LE, Larsen T, Young HA, Reed DS, et al. (2003) Pathogenesis of Ebola Hemorrhagic Fever in Cynomolgus Macaques: Evidence that Dendritic Cells Are Early and Sustained Targets of Infection. Am J Pathol 163: 2347-2370.
32. Geisbert TW, Young HA, Jahrling PB, Davis KJ, Larsen T, et al. (2003) Pathogenesis of Ebola Hemorrhagic Fever in Primate Models: Evidence that Hemorrhage Is Not a Direct Effect of Virus-Induced Cytolysis of Endothelial Cells. Am J Pathol 163: 2371-2382.
33. Narayan S, Barnard RJ, Young JA (2003) Two retroviral entry pathways distinguished by lipid raft association of the viral receptor and differences in viral infectivity. J Virol 77: 1977-1983.
34. Jones SM, Howell KE, Henley JR, Cao H, McNiven MA (1998) Role of dynamin in the formation of transport vesicles from the trans-Golgi network. Science 279: 573-577.
35. Oh P, McIntosh DP, Schnitzer JE (1998) Dynamin at the neck of caveolae mediates their budding to form transport vesicles by GTP-driven fission from the plasma membrane of endothelium. J Cell Biol 141: 101-114.
36. van der Bliek AM, Redelmeier TE, Damke H, Tisdale EJ, Meyerowitz EM, et al. (1993) Mutations in human dynamin block an intermediate stage in coated vesicle formation. J Cell Biol 122: 553-563.
37. Bretscher MS (1992) Circulating integrins: alpha 5 beta 1, alpha 6 beta 4 and Mac-1, but not alpha 3 beta 1, alpha 4 beta 1 or LFA-1. Embo J 11: 405-410.
38. Bretscher MS (1989) Endocytosis and recycling of the fibronectin receptor in CHO cells. Embo J 8: 1341-1348.
39. Mahmutefendic H, Blagojevic G, Kucic N, Lucin P (2006) Constitutive internalization of murine MHC class I molecules. J Cell Physiol.
40. Reid PA, Watts C (1990) Cycling of cell-surface MHC glycoproteins through primaquine-sensitive intracellular compartments. Nature 346: 655-657.
41. Coscoy L, Ganem D (2000) Kaposi's sarcoma-associated herpesvirus encodes two proteins that block cell surface display of MHC class I chains by enhancing their endocytosis. Proc Natl Acad Sci U S A 97: 8051-8056.
42. Wiertz EJ, Jones TR, Sun L, Bogyo M, Geuze HJ, et al. (1996) The human cytomegalovirus US11 gene product dislocates MHC class I heavy chains from the endoplasmic reticulum to the cytosol. Cell 84: 769-779.
43. Schwartz O, Marechal V, Le Gall S, Lemonnier F, Heard JM (1996) Endocytosis of major histocompatibility complex class I molecules is induced by the HIV-1 Nef protein. Nat Med 2: 338-342.
44. Kasper MR, Collins KL (2003) Nef-mediated disruption of HLA-A2 transport to the cell surface in T cells. J Virol 77: 3041-3049.
45. Roeth JF, Williams M, Kasper MR, Filzen TM, Collins KL (2004) HIV-1 Nef disrupts MHC-I trafficking by recruiting AP-1 to the MHC-I cytoplasmic tail. J Cell Biol 167: 903-913.

CHAPTER 3 – STERIC SHIELDING OF SURFACE EPITOPES AND IMPAIRED IMMUNE RECOGNITION INDUCED BY THE EBOLA VIRUS GLYCOPROTEIN

Joseph R. Francica[1], Angel Varela-Rohena[2], Andrew Medvec[2], Gabriela Plesa[2], James L. Riley[2] and Paul Bates[1]

Departments of Microbiology[1], Pathology and Lab Medicine[2] and Abramson Family Cancer Research Institute[2], University of Pennsylvania School of Medicine
225 Johnson Pavilion 3610 Hamilton Walk Philadelphia, PA 19104-6076

3.1 Abstract

Many viruses alter expression of proteins on the surface of infected cells including molecules important for immune recognition, such as the major histocompatibility complex (MHC) class I and II molecules. Virus induced down-regulation of surface proteins has been observed to occur by a variety of mechanisms including impaired transcription, blocks to synthesis, and increased turnover. Viral infection or transient expression of the Ebola viral glycoprotein (GP) was previously shown to result in loss of staining of various host cell surface proteins including MHC1 and β1 integrin, however the mechanism responsible for this effect has not been delineated. In the present study we demonstrate that Ebola GP does not decrease surface levels of β1 integrin or MHC1, but rather impedes recognition by steric occlusion of these proteins on the cell surface. Furthermore, steric occlusion also occurs for epitopes on the Ebola glycoprotein itself. The occluded epitopes in host proteins and Ebola GP can be revealed by removal of the surface subunit of GP or by removal of surface N- and O- linked glycans, resulting in increased surface staining by flow cytometry. Importantly, expression of Ebola GP impairs CD8 T cell recognition of MHC1 on antigen presenting

cells. Glycan-mediated steric shielding of surface proteins by Ebola GP represents a novel mechanism for a virus to affect host cell function and escape immune detection.

3.2 Introduction

The Ebola virus (EBOV) is an enveloped, negative-stranded RNA virus, a member of the family *Filoviridae*, and the causative agent of Ebola hemorrhagic fever. To date, five subtypes of EBOV have been identified: Zaire, Sudan, Côte d'Ivoire, Reston and Bundibugyo. Zaire is the most pathogenic subtype in humans, with mortality rates reaching 90% [1]. The basis for the high pathogenicity of EBOV is unclear, however immune dysregulation has been hypothesized to play a role [2]. Similarly to many other viral systems, EBOV infection appears to down-modulate the expression of host surface proteins involved in cellular recognition, most notably major histocompatibility complex (MHC) molecules and integrins [3].

EBOV encodes two forms of its glycoprotein. One is a dimeric, secreted form (sGP), which is transcribed directly from the viral RNA [4,5] and whose function remains unclear. A second glycoprotein species results from transcriptional editing of the glycoprotein ORF and encodes a trimeric, membrane-bound form (GP). This form is expressed at the cell surface and is incorporated into the virion [4] and drives viral attachment and membrane fusion. GP is initially translated as a precursor (GP_0), which is then cleaved by furin in the Golgi into two subunits, a surface subunit, GP_1 and a membrane-spanning subunit, GP_2 [6]. These subunits remain covalently connected through a single intermolecular cysteine bond [7]. Expression of the main viral glycoprotein, GP, has been shown to cause effects in cell culture on host surface proteins similar to those observed during viral infection, and so is proposed to be an important determinant of viral pathogenesis [8,9,10,11]. Because sGP is the predominant form

transcribed, it has been postulated that the balance between sGP and GP serves to regulate the effects of GP [11].

EBOV GP expression in cultured cells disrupts cell adhesion resulting in loss of cell-cell contacts as well as cell rounding and loss of attachment to the culture substrate [8,10,12]. This can be observed in a variety of cell lines and primary cell types [12]. Interestingly, while transient GP expression does not cause death in human embryonic kidney 293T cells, primary human cardiac microvascular endothelial cells have been reported to undergo anoikis, or detachment-mediated apoptosis, upon transduction of GP [12,13]. By flow cytometry, cells expressing GP display dramatically lowered levels of various surface proteins, including several members of the integrin family and MHC class I (MHC1); however, the exact complement of surface proteins affected by GP appears to differ by cell type [10,12,14]. Importantly, EBOV infection of 293T cells was observed to cause similar reduction of β1 integrin and MHC1 staining by flow cytometry, suggesting that observations from transient GP expression are not simply artifacts of overexpression [3]. The effects of EBOV GP are known to be caused by a highly glycosylated region in GP_1, the mucin domain [8,12,14]. This domain encompasses approximately 150 amino acids, contains numerous N- and O- linked glycosylation sites, and is a unique feature of Filovirus GPs. The mucin domain is not only necessary, but also sufficient for the observed EBOV GP-mediated effects upon surface protein expression and cellular adhesion [8,15].

Few studies have been undertaken to investigate the mechanism by which EBOV GP disrupts adhesion and causes surface protein down-modulation. Our recent analysis

concluded the cellular endocytic factor dynamin does not play a role in surface protein down-modulation, suggesting the process may not involve cycling of proteins from the cell surface [15]. In contrast, Sullivan and colleagues have reported that this process requires dynamin [14]. Additionally, it has been reported that the extracellular signal-regulated kinases (ERK 1/2) play a role in down-modulation [16] suggesting an active process. In the present study, we provide direct evidence that EBOV GP-mediated loss of surface protein recognition occurs via steric shielding of surface epitopes, not by protein removal from the cell surface. Moreover, we demonstrate that EBOV GP expression blocks MHC1-mediated stimulation of T cells. Based upon these findings, we present a model in which the heavily glycosylated EBOV glycoprotein acts as a "glycan shield" to physically occlude access to host proteins, and GP itself, thereby impairing host protein function. EBOV GP-mediated steric occlusion represents a unique viral mechanism to interfere with the function of host proteins.

3.3 Materials and Methods

Plasmids, cell culture and transfections

For GP studies, cDNA encoding the membrane-anchored form of Zaire EBOV GP (Mayinga strain, accession number U23187) was used. For AU1 tagged GPs, the amino acids, DTYRYI were added using linker insertion into GP that had been engineered to have a unique XhoI site at position 312 encoding the amino acids LE (NmucAU1) and a unique NotI site replacing amino acid 463 with the amino acids KRPL (CmucAU1). EBOV GP harboring mutations in the endoproteolytic site, GP cl(-), has been previously described [17]. All constructs were cloned into the pCAGGS expression vector.

293T and HeLa cells were cultured in DMEM (Gibco) with 10% fetal bovine serum (HyClone) and penicillin/streptomycin (Gibco) at 37 ºC with 5% CO_2. For flow cytometry and western blotting, 293T cells were plated in 10 cm or 6-well plates one day prior to transfection. Cells were transiently transfected by Lipofectamine 2000 according to manufacturer's directions with 30 µg or 4 µg DNA per 10 cm plate or 6-well, respectively. Immunofluorescence was performed using HeLa cells that were plated on glass coverslips in 24-well plates and transfected with 1.5 µg DNA as above.

Antigen-presenting and primary cells

Purified CD8 T cells from normal donors were obtained from the University of Pennsylvania Center for AIDS Research Immunology Core under a University of Pennsylvania IRB approved protocol. The human ovarian adenocarcinoma line OV79

has been described previously [18]. To create the OV79-SL9 antigen-presentig cells, OV79 cells were sequentially transduced to express HLA-A*02 [19] and a construct of GFP fused to a codon-optimized sequence of HIV-1 p17 Gag50–102. High titer lentiviral vectors were produced as described previously [20].

Generation of SL9-specific CD8 T cells

Primary human CD8 T cells were cultured in X-Vivo 15 (Lonza) supplemented with 5% HABS (Valley Biomedical, Winchester, VA), 2 mM GlutaMax and 25 mM HEPES (Invitrogen). CD8 T cells were transduced to express the SL9-specific HLA-A2 restricted 869TCR as described previously [21]. Transduction efficiencies were assessed by flow cytometric analysis of TRBV5-6 staining (anti-Vbeta5a, Thermo-Fisher) or HLA-A*02- SL9 tetramer stain (Beckman Coulter Immunomics).

Stimulation and analysis of SL9-specific CD8 T cells

OV79-SL9 cells were plated at 16,000 cells/well on 48 well plates. After an overnight incubation cells were transduced with adenovirus expressing GFP (Ad GFP) or GFP and the EBOV Zaire glycoprotein (Ad GP) as described previously [12]. Briefly, adenoviruses were diluted in media and applied to cells at an MOI of 300. Media alone was used as a control. 48 h after transduction, target cells were analyzed for GFP and HLA expression. Floating and adherent cells, lifted by incubation with versene, were combined and stained for HLA-ABC or isotype control with APC-conjugated antibodies (BD-Biosciences). Alternatively, cells were stained for different MHC1 epitopes with

W6/32 (eBiosciences), YTH862.2 (Santa Cruz Biotechnology), BB7.2 (BD Pharmingen), or GJ14 (Chemicon) primary antibodies, flowed by Alexa Fluor 647 (Invitrogen) secondary antibodies. 10,000 viable (forward scatter versus side scatter) events were collected on an LSR-II flow cytometer running BD FACSDiva-6 (BD-Biosciences), and analyzed in FlowJo (Tree Star Inc.).

SL9-specific TCR–transduced CD8 T cells were mixed with unmodified or adenovirally transduced OV79-SL9 target cells at a 2:1 ratio for 1 h, followed by 4 h in the presence of brefeldin-A (Golgiplug, BD Biosciences). Stimulation with TPA (3 mg/ml, Sigma-Aldrich) and ionomycin (1 mg/ml; Calbiochem) with brefeldin-A was used as positive control. Cells were washed in PBS and surface-stained using CD8 conjugated to APC-H7, and then fixed and permeabilized with the Caltag Fix & Perm kit (Invitrogen) and stained using anti-TRBV5-6 FITC and macrophage inflammatory protein-1b (MIP-1b, CCL4)-PE. Sequential gates of 10,000 viable (forward scatter versus side scatter), CD8 positive events were acquired for all conditions on an LSR-II flow cytometer running BD FACSDiva-6 (BD-Biosciences). Data were analyzed for cytokine production in FlowJo (Tree Star Inc.).

Cell lysates and western blotting

Transfected cells were removed by resuspension in the culturing media. Cells were pelleted at 4 ºC for 3 min at 1300 x g. Pellets were resuspended in 1% Triton X-100 or RIPA buffer with complete protease inhibitor cocktail (Roche) for 5 minutes. Lysates were cleared by centrifugation at 4 ºC at 20,800 x g. 30 µl samples were mixed with

reducing SDS buffer, boiled for 5 minutes, and separated on a 4-15% Criterion PAGE gel (Bio-Rad). Proteins were transferred to PVDF (Millipore) at a 400 mA constant current. Membranes were blocked in 5% milk in TBS. Membranes were probed with rabbit polyclonal anti-GP sera which recognizes the GP_1 subunit [22], rabbit anti-AU1 antibodies (Bethyl labs), or anti-GAPDH monoclonal antibodies (Calbiochem) in blocking buffer. Protein was detected with stabilized goat anti- rabbit or mouse HRP conjugated antibodies (Pierce) in blocking buffer. Membranes were visualized with SuperSignal Femto substrate (Pierce).

Flow cytometry

293T cells were detached from the plate 24 hours post transfection with PBS -/-, 0.5 mM EDTA and combined with floating cells in culture media. Alternatively, floating cells in cluture media were removed and used exclusively (where indicated). Cells were pelleted at 4 ºC at 250 x g, then resuspended in flow wash buffer (PBS -/- with 1% bovine calf serum and 0.05% NaAzide) and aliquoted for staining. For detection of EBOV GP, cells were stained with the human MAb, KZ52 [23] and detected with FITC anti-human IgG (PharMingen). For detection of AU1 epitopes, cells were stained with rabbit polyclonal anti-AU1 antibodies (Bethyl labs) and detected with FITC goat anti-rabbit IgG (Rockland). For detection of β1 integrin, cells were stained with anti-human CD29 PE-Cy5 conjugate (eBioscience); for detection of MHC1, cells were stained with anti- HLA-ABC PE-Cy5 conjugate (eBioscience). For intracellular staining, cells were permeabilized using Cytofix/Cytoperm (BD Biosciences) for 20 min on ice, followed by

washing with Permwash (BD Biosciences). Antibodies where then diluted in Permwash buffer. For detection of GM130 and calnexin, mouse monoclonal FITC-conjugated antibodies were used (BD Transduction Labs). All staining was performed on ice, followed by washing. Live cell gates were drawn based on forward and side scatter. For each sample, 10,000 or 20,000 events in the live cell gate were collected and analyzed. Data were collected on a Becton Dickinson FACSCalibur and analyzed using FlowJo software (Tree Star, Inc.).

Immunofluorescence microscopy

For HeLa cells, media was removed at 24 hours post-transfection, cells were washed with PBS and fixed with 3% PFA in PBS for 20 minutes. For non-adherent 293T cells, media containing floating cells was removed from plate, then centrifuged onto poly-D-lysine coated coverslips (BD Biosciences), then fixed. All samples were then washed with PBS, then permeabilized with 0.2% saponin, 1% goat serum in PBS for 5 minutes, then washed with PBS. Cells were blocked with 10% goat serum, 0.1% Tween-20 in PBS for 2 hours. For GP staining, coverslips were incubated with mouse anti-EBOV GP MAb 42/3.7 (gift from Yoshihiro Kawaoka) and detected with goat anti-rabbit Alexa Fluor 594 antibodies (Invitrogen). For AU1 staining, coverslips were incubated with rabbit anti-AU1 antibodies (Bethyl labs) and detected with anti-rabbit Alexa Fluor 488 antibodies (Invitrogen). Cells were washed with PBS after each staining step. Coverslips were mounted on glass slides with mounting medium containing DAPI (Vectasheild). Z-section images were collected on a Leica DMRE fluorescence

microscope using Open Lab software (Improvision). Thirty z-sections per image were collected at 0.2 μm intervals. Z-section data were deconvoluted using Velocity software (Improvision) to a 98% confidence level or 15 iterations. Images shown are single, deconvoluted, z-sections.

DTT treatment

At 24 hours post-transfection, sodium azide was added to 0.1% and 2-deoxy glucose was added to 10 mM. Cells were incubated an additional 30 min. Cells were then harvested and resuspended in flow wash buffer supplemented with 0.1% azide and 10 mM 2-deoxy glucose. DTT was then added to 150 mM and cells were incubated at 37 ºC for 20 minutes. Cells were then pelleted at room temperature and the supernatant was removed and blotted for GP as described above. Cells were then washed twice in flow wash and stained for flow cytometry as described above.

Glycosidase treatment

At 24 hours post-transfection, floating cells were harvested and resuspended in 100 μl flow wash buffer. 100 U of neuraminidase (NEB) and/or 1000 U of PNGaseF (NEB) was then added. Cells were then incubated at 37 ºC for 20 minutes. Cells were then washed twice and aliquoted for flow cytometry or western blotting as described above. Alternatively, cells were incubated with 2 mM benzyl-α-GalNAc (Sigma) or DMSO at 31 ºC for 48 hours. Cells were then given fresh media with 2 mM benzyl-α-GalNAc or DMSO and cultured at 37 ºC for 1 hour. Cells were then transfected as

described above. At 24 hours post-transfection, floating and adherent cells were harvested and resuspended in 100 µl flow wash buffer. 1000 U of PNGaseF (NEB) or 2.5 mU of O-glycosidase (Sigma) was then added. Cells were then incubated and analyzed as above. For PNGaseF treatment of cell lysates, 30 µl of lysate was incubated with glycoprotein denaturing buffer (NEB) for 10 minutes at 60 ºC. Samples were then incubated with G7 buffer, NP40, and 500 U PNGase F (NEB) for 2 hours at 37 ºC, then blotted for GP as described above.

3.4 Results

EBOV GP expression blocks surface protein staining

EBOV GP expression can dramatically reduce the levels of numerous host cell surface proteins including factors involved in immune recognition and cellular adhesion [10,12,14]. This effect can be seen by analysis of MHC1 or β1 integrin by flow cytometry in HEK293T cells transiently expressing Zaire EBOV GP (Figure 3-1 A). Overall, a 10- to 50-fold reduction in surface levels of these host markers is observed in cells transfected with an EBOV GP cDNA. Additionally, there appears to be a critical threshold of EBOV GP expression required to induce surface protein down-modulation [15]. In parallel with the decrease in staining for host proteins, EBOV GP expression also appears to be reduced, resulting in a distinctive comma-shaped FACS profile (Figure 3-1 A and [14,15,16]). Despite this apparent decrease in surface protein levels observed by flow cytometry, there were no consistent, significant changes in total protein levels for the EBOV glycoprotein upon analysis by western blot in either adherent or non-adherent EBOV GP transfected cells (data not shown). To look directly at host protein expression in cells expressing GP, nonadherent, GP-transfected 293T cells were collected and analyzed by flow cytometry for expression of β1 integrin ([15] and Figure 3-1 B, left panel). As previously described [15], these nonadherent cells represent the lower two quadrants of the "comma" and appear to have reduced levels of both β1 integrin and EBOV GP. In contrast to the FACS results, analysis of EBOV GP in these cells by immunofluorescence microscopy after fixation and permeabilization reveals extensive staining at the plasma membrane (Figure 3-1 B, right panel).

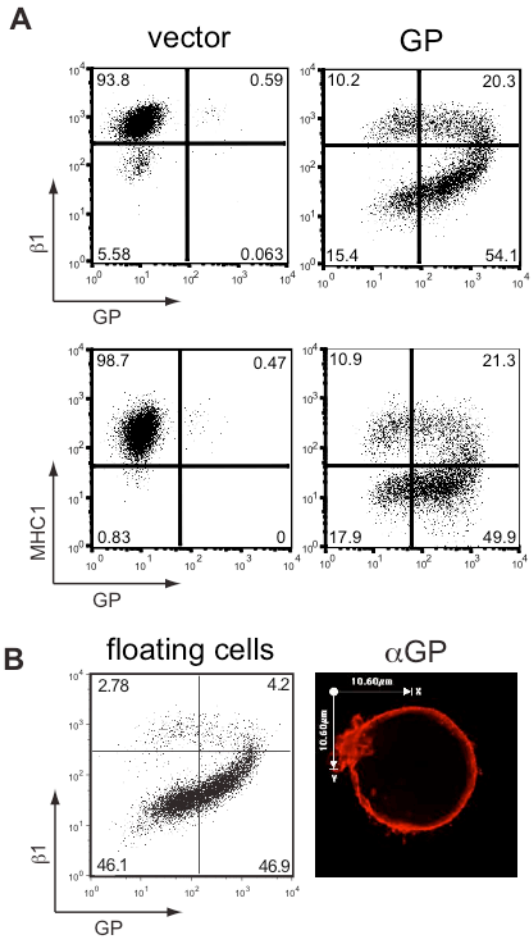

Figure 3-1 Transient expression of the EBOV glycoprotein results in loss of surface staining of β1 integrin and MHC1. (A) 293T cells were transfected with empty pCAGGS (vector) or vector encoding GP. Floating and adherent cells were harvested 24 h after transfection, pooled, and stained for GP using the KZ52 antibody, followed by FITC-labeled secondary antibodies, and co-stained for β1 integrin or MHC1 with PE-Cy5 conjugated monoclonal antibodies and assayed by flow cytometry. (B) Following transfection with vector encoding GP, floating 293T cells were removed from adherent cells, stained for β1 integrin and assayed by flow cytometry (left panel). Similarly treated cells were mounted on coverslips, fixed, permeabilized and stained for GP with mouse monoclonal antibodies, followed by Alexa 594 conjugated antibodies and assayed by immunofluorescence microscopy. A representative cell is shown (right panel).

Similar to these results, previously published microscopic analysis of cells expressing EBOV GP also shows extensive plasma membrane staining with little evidence of significant accumulation of GP in internal vesicles [15,24].

To evaluate steady state levels of host proteins and EBOV GP in cells transiently expressing the EBOV glycoprotein, the transfected cells were fixed, permeabilized and analyzed by flow cytometry. In vector-transfected cells, the permeabilization treatment had little effect upon staining for β1 integrin or MHC1 (Figure 3-2 A). However, in cells transiently expressing EBOV GP, which displayed dramatically reduced levels of β1 integrin and MHC1 by surface staining (Figure 3-2 B, left column), fixation and permeabilization reveals no decrease in either of these host proteins (Figure 3-2 B, right column). Similarly, the apparent loss of EBOV GP staining is reversed by this treatment. These effects are best illustrated by comparison of the lower two panels in Figure 3-2 B where without treatment, 9.3% of the cells displayed low MHC1 and EBOV GP levels, however after fixation and permeabilization the number of double negative cells was reduced to background levels and these now appear as MHC^+, GP^+ cells in the upper right quadrant. As expected, the untransfected cell population of 32-34% remains unaltered by this treatment (Figure 3-2 B, upper left quadrants). Overall, this analysis suggests that the apparent down-modulation observed is not due to reduced steady-state levels of protein. Rather these transfected cells express unaltered levels of EBOV GP and MHC1, however these proteins are inaccessible for surface staining.

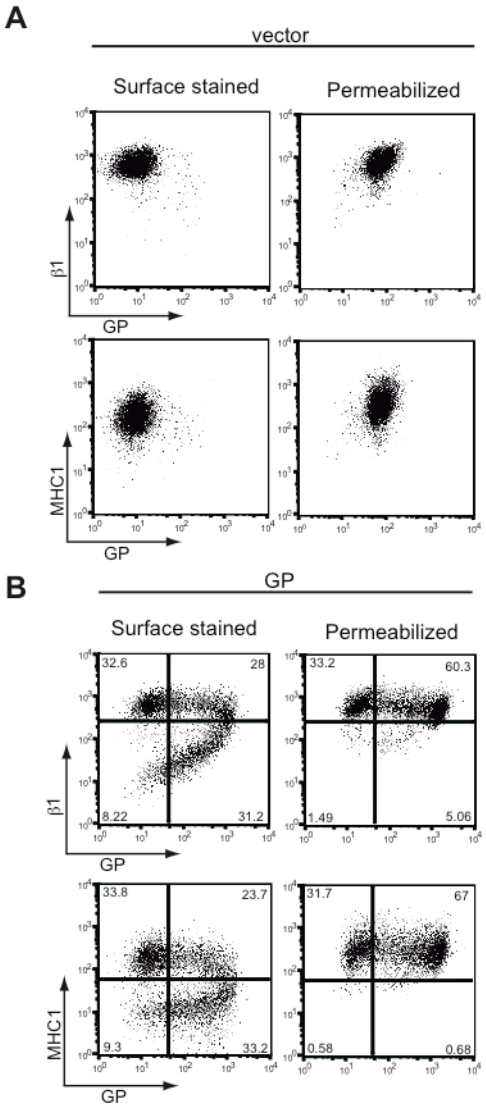

Figure 3-2 Steady-state levels of β1 integrin and MHC1 are unchanged in GP-expressing cells. 293T cells were transfected with empty vector (A) or vector encoding wt GP (B). Floating and adherent cells were harvested 24 h after transfection, pooled, and stained for GP, β1 integrin, and MHC1 as described earlier and assayed by flow cytometry. Prior to staining, a portion of cells were fixed and permeabilized to expose occluded surface and internal epitopes.

EBOV GP shields its own epitopes at the cell surface

Recent structural analysis of EBOV GP suggests that the recognition site for the monoclonal antibody, KZ52, employed in the FACS analysis resides near the base of the protein [25] below the globular GP_1 and heavily glycosylated mucin domains in GP. This finding, coupled with our results suggesting that down-modulation in these cells was not accompanied by a reduction in steady-state levels of β1 integrin or MHC1, or a significant re-localization of EBOV GP, prompted us to consider the hypothesis that EBOV GP mediates its effects by blocking access to surface epitopes. Additionally, this hypothesis is consistent with the apparent threshold of GP expression required for down-modulation as well as the lack of a dynamin requirement [15].

To test this hypothesis, we engineered epitopes within EBOV GP at locations which, based on their position relative to the mucin domain and the globular region of GP, are predicted to be more accessible than the KZ52 epitope. Two constructs were created with an AU1 antibody epitope tag at the N or C terminus of the mucin domain, termed NmucAU1 GP and CmucAU1 GP, respectively. Cartoon depictions of each construct are shown in Figure 3-3 C and D. These constructs were well expressed, as judged by western blot analysis for EBOV GP and the AU1 tag (Figure 3-3 A). The sub-cellular localization of these constructs was also evaluated in HeLa cells by immunofluorescence microscopy and was found to be indistinguishable from wt GP (Figure 3-3 B).

Although the structure of the mucin domain is unknown, its mucin-like O glycosylation may force the domain into an extended conformation as has been

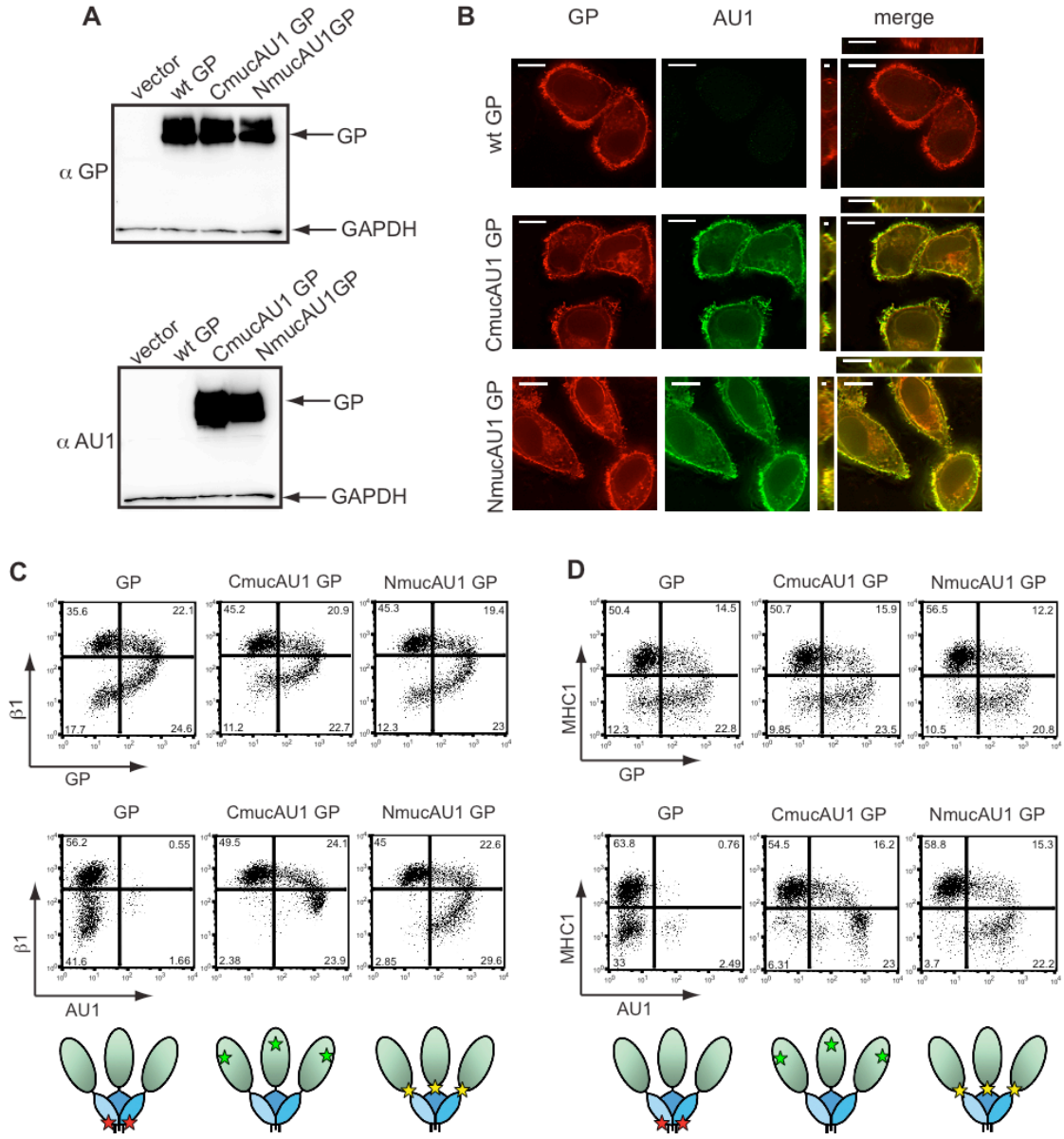

Figure 3-3 The mucin and globular domains of the EBOV glycoprotein mask the KZ52 epitope on the cell surface. (A) 293T cells were transfected with empty vector or vector encoding wt GP, CmucAU1 GP, or NmucAU1 GP. Lysates were harvested in RIPA buffer after 24 h and subjected to SDS-4 to 15% PAGE, transferred to PVDF, and immunoblotted with anti-GP polyclonal rabbit antibodies (top blot) or anti-AU1 antibodies (bottom blot) and anti-GAPDH antibodies. (B) HeLa cells were transfected with vector encoding wt GP, CmucAU1 GP, or NmucAU1 GP. 24 h after transfection, cells were fixed, permeabilized, and stained for GP with mouse monoclonal antibodies,

and the AU1 epitope with anti-AU1 antibodies, followed by Alexa 594 and Alexa 488 conjugated antibodies, respectively and assayed by immunofluorescence microscopy. Scale bars are 10.6 μm. (C, D) 293T cells were transfected with vector encoding wt GP, CmucAU1 GP, or NmucAU1 GP. Floating and adherent cells were harvested 24 h after transfection, pooled, and stained for GP using the KZ52 antibody or the AU1 tag, β1 integrin, and MHC1, as described earlier and assayed by flow cytometry. (C) β1 integrin vs. GP or AU1 surface staining. (D) MHC1 vs. GP or AU1 surface staining. Cartoon depictions of the KZ52 epitope (red star), CmucAU1 epitope (green star) or NmucAU1 epitope (yellow star) are shown below their respective flow cytometry plots. The globular region of GP is shown shaded blue; the mucin domain is shown shaded green.

suggested for cellular mucin proteins [26]. This would place C terminus of the mucin domain distal from the rest of the domain and the other globular GP domains (Figure 3-3 C and D). Based upon the proposed steric occlusion model, we hypothesized that the AU1 epitope of CmucAU1 would be most accessible to antibody staining. In contrast, the AU1 epitope in NmucAU1 might be less accessible than the epitope in CmucAU1 because of its location at the base of the mucin domain. Cells expressing wt GP, CmucAU1 GP, and NmucAU1 GP were analyzed by flow cytometry. When stained with the GP-specific KZ52 antibody, the epitope-tagged mutants displayed the characteristic comma-shaped FACS plot seen with wt GP (Figure 3-3 C and D; top rows). In contrast to the reduced KZ52 staining observed, the AU1 epitope in CmucAU1 was highly visible by flow cytometry (Figure 3-3 C and D; bottom middle panels). Staining of the AU1 epitope on NmucAU1 GP was intermediate relative to CmucAU1 GP and wt GP KZ52 staining (Figure 3-3 C and D; bottom right panels). In support of the shielding model, these data demonstrate that cells exhibiting reduced levels of β1 integrin and MHC1 have high surface levels of GP as indicated by AU1 staining, not reduced levels as indicated by KZ52 staining. Furthermore, these data suggest that antibody accessibility to epitopes in GP differs based on the epitope position relative to the mucin domain and the globular regions of GP_1.

Removal of the EBOV GP_1 subunit reveals shielded host surface proteins

The data presented above are consistent with EBOV GP affecting recognition of epitopes within GP by shielding, however we wished to address if a similar mechanism

was responsible for the apparent down-modulation of host surface proteins. To directly address whether EBOV GP sterically occludes host surface protein epitopes, we sought to unmask MHC1 and β1 integrin staining. We hypothesized that dissociation of the GP_1 subunit, which includes the mucin domain and globular "head" region of EBOV GP, from GP_2 at the cell surface should relieve the shielding of previously occluded epitopes. The GP_1 subunit is covalently linked to GP_2 via a single sulfahydryl bridge between residues C53 and C609 [7]. We have previously demonstrated that this bond can be reduced by incubation with DTT, allowing for dissociation of the EBOV GP_1 subunit from the surface of virions [17]. To confirm that DTT is able to effectively remove GP_1 from the cell surface, cells expressing GP were incubated with DTT then the supernatant was analyzed for GP by western blot. Figure 3-4 A reveals that GP_1 was readily detected in the supernatant of cells incubated with DTT compared to mock treated cells. Control experiments also demonstrated that the DTT treatment did not significantly alter surface expression of β1 integrin or MHC1 in mock-transfected cells (Figure 3-4 B). Additionally, this treatment did not result in permeabilization of the cells (Figure 3-4 C) which, as shown above (Figure 3-2), could also rescue β1 integrin and MHC1 staining. In addition, these and the following experiments were carried out in the presence of azide and 2-deoxy glucose to ensure that the trafficking of nascent or recycled protein did not complicate the interpretation of this assay.

We next examined the effect of DTT treatment on surface staining of β1 integrin and MHC1 in cells expressing EBOV GP. FACS analysis of the DTT-treated, GP-

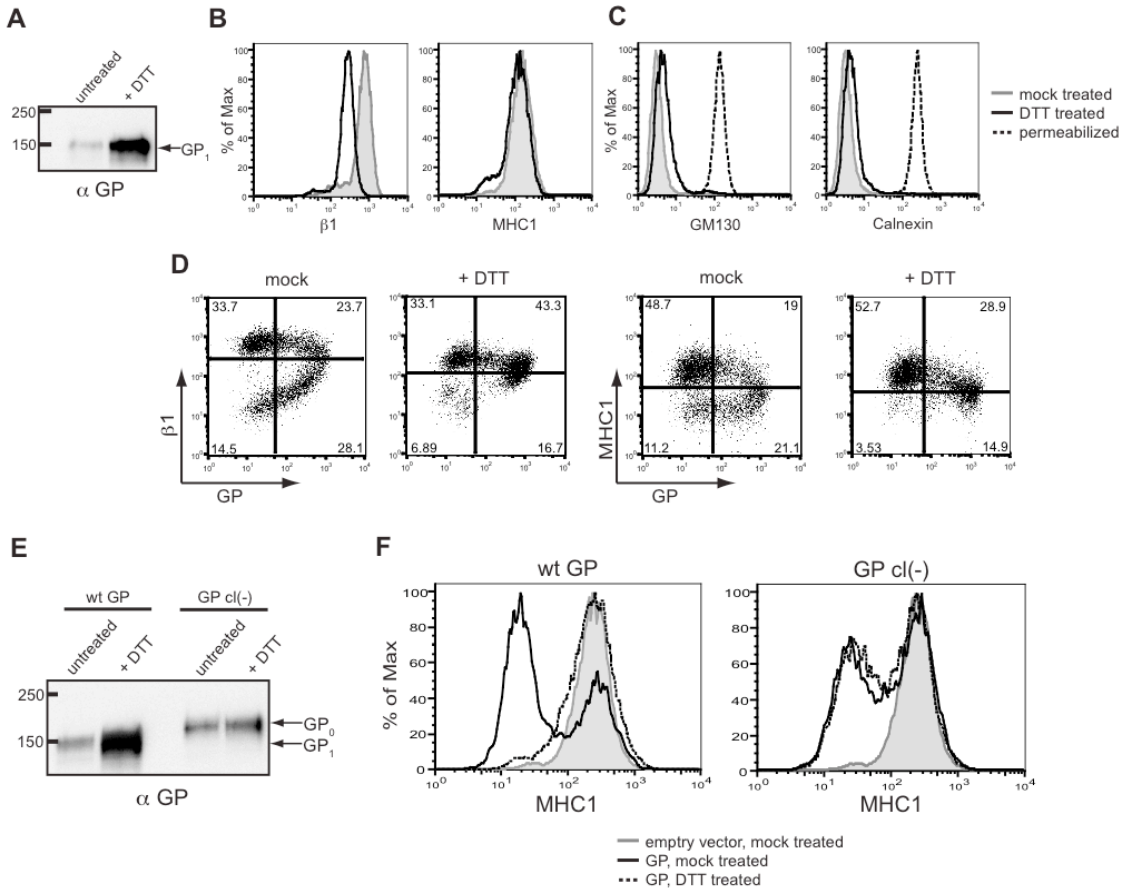

Figure 3-4 Removal of the GP_1 subunit from the cell surface results in exposure of previously occluded surface epitopes. (A-C) 293T cells were transfected with empty vector or vector encoding wt GP. Floating and adherent cells were harvested 24 h after transfection, pooled, and either left untreated, or incubated at 37 ºC for 20 minutes in 150 mM DTT. (A) Western blot analysis of the GP_1 subunit shed into the supernatant of untreated or DTT-treated cells. (B) Cells were transfected with empty vector and assayed by flow cytometry to show baseline differences in surface staining for β1 integrin and MHC1 between untreated cells (grey shading) and DTT-treated cells (black trace). (C) Cells were transfected with vector encoding wt GP and assayed by flow cytometry for the internal proteins GM130 and calnexin to show the effect of DTT on cell permeabilization. Untreated cells are shown in the grey shading; DTT-treated cells are shown in the black trace, and, as a positive control, fixed/permeabilized cells are shown in the dashed trace. (D) Cells were transfected with vector encoding wt GP, were mock- or DTT-treated, stained for GP and β1 integrin or MHC1 as described above, and assayed by flow cytometry. (E, F) 293T cells were transfected with empty vector or vector encoding wt GP or GP cl(-). Cells were harvested and treated as above. (E) Western blot analysis using rabbit polyclonal antibodies of GP_1 or GP_0 shed into the supernatant of untreated or DTT-treated cells. (F) Transfected and treated cells were surface stained for

MHC1 and assayed by flow cytometry. Empty vector-transfected, untreated cells are shown in the grey shading; GP-expressing cells are shown after mock treatment (black trace) or DTT treatment (dashed trace).

expressing cells indicates that GP-induced loss of staining of β1 integrin and MHC1 is reversed by DTT treatment and subsequent dissociation of GP_1 from the cells: upon DTT treatment, staining of β1 integrin and MHC1 is restored to nearly control levels (Figure 3-4 D). Interestingly, staining for GP was also rescued, resulting in cells that stained positively for both GP and β1 integrin or MHC1. This is somewhat counter-intuitive, as KZ52 makes critical contacts with residues on GP_1 [25], which is removed from the cell surface by DTT. These data suggest that DTT treatment removes a significant amount of GP_1 from the cell surface – enough to reverse the steric occlusion of β1 integrin and MHC1 epitopes, as well as the KZ52 epitope. However, sufficient GP_1 remains on the cell surface to allow for staining of GP by flow cytometry. This finding agrees with our previously published study that suggests a threshold level of EBOV GP is needed to downmodulate β1 integrin, MHC1 or GP [15].

Removal of surface GP_1 by DTT reverses the apparent down-modulation of surface proteins induced by EBOV GP. To ensure this effect could be directly attributed to the EBOV glycoprotein we tested the effect of DTT on cells expressing a mutant form of GP lacking the endoproteolytic site required for processing GP_0 into GP_1 and GP_2 subunits. Previous analysis demonstrated that this mutant EBOV glycoprotein, GP cl(-), retains normal viral entry function [17,27] and is therefore likely folded similarly to wt EBOV GP. As shown in Figure 3-4 F, GP cl(-) also downmodulates MHC1 similarly to wt EBOV GP. However in contrast to wt GP, DTT treatment of cells expressing this uncleaved form of GP does not relieve the observed down-modulation of MHC1 (Figure 3-4 F). As anticipated, DTT treatment of cells expressing GP cl(-) produced no increase

in GP release compared to untreated cells (Figure 3-4 E). The EBOV glycoprotein found in the supernatant from the GP cl(-) expressing cells likely represents trimeric GP released by the cellular enzyme TACE [28]. Overall, these data strongly support the model proposed for EBOV GP mediated occlusion of host surface proteins.

Carbohydrate modification of GP is important for steric shielding

GP is a heavily glycosylated protein, and we have previously shown the mucin domain to be sufficient to induce loss of staining of host surface proteins by flow cytometry [15]. Therefore, we directly addressed whether GP glycosylation plays a role in the shielding of surface epitopes. GP-expressing cells were treated with several glycosidases or pre-treated with a small molecule inhibitor of mucin synthesis, benzyl-α-GalNAc, then assayed for β1 integrin staining by flow cytometry. Importantly, none of the glycan-interfering treatments used here increased the staining for β1 integrin in cells transfected with empty vector (Figure 3-5 A). Also, these treatments did not cause the permeabilization of cells, allowing us to attribute changes in staining to alterations at the cell surface (Figure 3-5 B). Staining for β1 integrin on GP-expressing cells was increased by incubation with PNGaseF, an endoglycosidase that cleaves all N-linked sugar moieties (Figure 3-5 D left). Similarly, staining for β1 integrin was increased by incubation with neuraminidase, an exoglycosidase that cleaves sialic acid, which is a common component of mucin sugars. (Figure 3-5 D, middle). When GP-expressing cells were incubated with both PNGaseF and neuraminidase, an additive effect was seen and β1 integrin staining was further increased (Figure 3-5 D, right). The effect of glycosidase

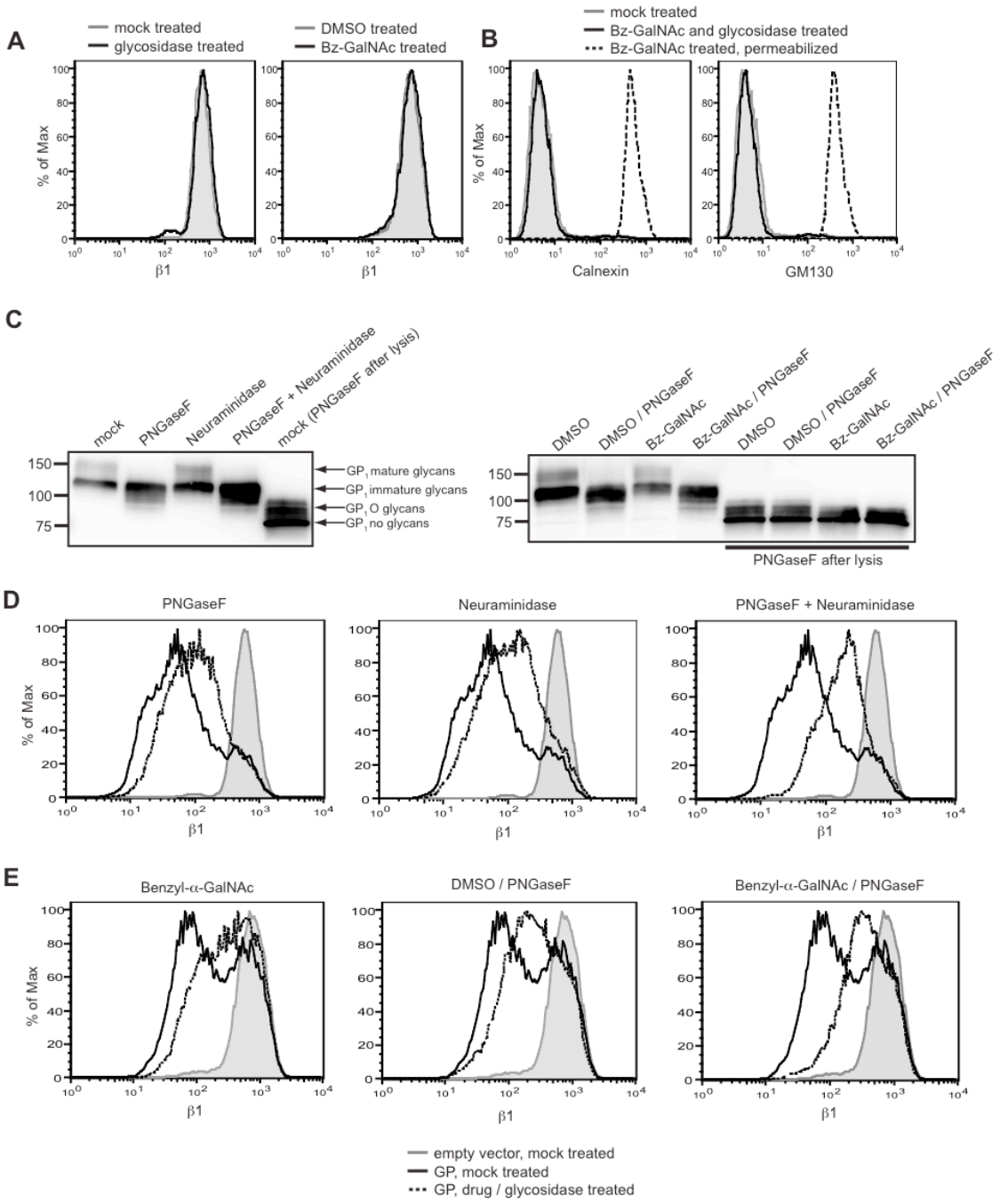

Figure 3-5 Surface N- and O- linked glycans contribute to GP-mediated shielding. (A, left plot) Cells transfected with empty vector were mock incubated (grey shading) or incubated with neuraminidase and PNGaseF (black trace), stained for β1 integrin and assayed by flow cytometry. (A, right plot) Cells were treated with DMSO, transfected with empty vector, and mock incubated (grey shading) or treated with benzyl-

α-GalNAc (bz-GalNAc), transfected with empty vector, and incubated with PNGaseF (black trace), then stained for β1 integrin and assayed by flow cytometry. (B) Cells were left untreated and untransfected (grey shading), or treated with benzyl-α-GalNAc, transfected with vector encoding GP, and incubated with PNGaseF (black trace), then assayed by flow cytometry for the internal proteins GM130 and calnexin to show the effect of these treatments on cell permeabilization. As a positive control, benzyl-α-GalNAc-treated, fixed/permeabilized cells are shown (dashed trace). (C, D) Floating cells in cultures transfected with vector encoding GP were mock incubated or incubated with neuraminidase and/or PNGaseF, then analyzed by western blot with rabbit polyclonal antibodies to GP (C, left blot) or stained for β1 integrin and assayed by flow cytometry (D). (C, E) Cells were treated with DMSO or bz-GalNAc, then transfected with empty vector, or vector encoding GP. Cells were then mock-incubated, or incubated with PNGaseF, then analyzed by western blot (C, right blot) or stained for β1 integrin and assayed by flow cytometry (E). For D and E, mock-incubated cells or DMSO-treated cells transfected with empty vector= grey shading; GP-transfected and DMSO-treated or mock-incubated cells= black traces; GP-transfected and bz-GalNAc- and glycosidase-treated cells= dashed traces. In western blot panels (C), selected samples were lysed and denatured before incubation with PNGaseF for comparison, as indicated.

treatment on cellular GP was also analyzed by western blot (Figure 3-5 C, left). PNGaseF treatment results in loss of the top band of GP_1, which is the maturely- glycosylated form and the appearance of bands which co-migrate with GP_1 that has been PNGaseF treated under denaturing conditions, but which still contains O glycosylation. Treatment with neuraminidase did not result in a perceivable shift in migration of GP_1; this is likely due to the small mass of these glycans and the resolution of the gel. These data indicate a direct role for N-linked glycans in GP-mediated loss of β1 integrin staining.

To directly address the role of O glycosylation in host protein down-modulation by EBOV GP, O glycosylation was perturbed by pre-incubating cells with benzyl-α-GalNAc or the control vehicle DMSO. This compound is a competitive inhibitor of β1,3-galactosyltransferase, which prevents the modification of core O glycan structures, resulting in shorter O-linked glycans and reduced sialyation [29,30,31]. Cells pre-treated with benzyl-α-GalNAc, then transfected with vector encoding GP showed increased staining for β1 integrin compared to DMSO treated cells, consistent with a role for O glycoslyation in the shielding of epitopes by the GP mucin domain (Figure 3-5 E, left plot). In cells pre-treated with benzyl-α-GalNAc and expressing GP, incubation with PNGaseF further increased staining for β1 integrin (Figure 3-5 E, right plot). Cells pre-treated with benzyl-α-GalNAc were also incubated with O-glycosidase, which can cleave unmodified core GalNAc structures; however, no further increase in β1 integrin was observed (data not shown). This is perhaps due to remaining modification of the core O glycans. The effect of these treatments on GP glycosylation was analyzed by western blot (Figure 3-5 C, right blot). Treatment with benzyl-α-GalNAc results in a modest increase

in mobility for bands corresponding to GP containing O glycosylation, which are most easily seen in samples that have been PNGase-treated after cell lysis. Our data here suggest that the mass of O glycosylation is reduced, but not fully eliminated. This is expected, as benzyl-α-GalNAc only reduces mucin modification, but does not prevent the synthesis of initial core glycans. Taken together, these data demonstrate that surface N- and O- linked glycans, presumably on EBOV GP, contribute to the ability of GP to mask surface β1 integrin epitopes.

EBOV GP expression blocks MHC1 mediated T cell activation

In cells expressing GP, we observed that staining for MHC1 is blocked regardless of the epitope examined (Figure 3-6). Given the ability of EBOV GP to mask spatially separate epitopes on MHC1, we wanted to address whether this had functional consequences for MHC1. Human OV79 cells expressing the HIV Gag-derived peptide SLYNTVATL (SL9) were used to test the effect of EBOV GP on MHC1 antigen presentation. These cells present the SL9 antigen using a stably expressed MHC1, HLA-A2. The OV79- SL9 cells were mock transduced or transduced with adenoviral vectors encoding GFP (AdGFP) or GFP and EBOV GP (AdGP), which resulted in nearly 100% of cells expressing GFP (Figure 3-7 A). Expression of EBOV GP dramatically reduced MHC1 levels in these cells whereas the control GFP vector had no effect on MHC1 expression (Figure 3-7 B). Primary human CD8 T cells transduced with a lentiviral vector expressing a T cell receptor (868TCRwt) specific for SL9 were used to assess antigen presentation by GP-expressing OV79 cells. T cell activation was measured by

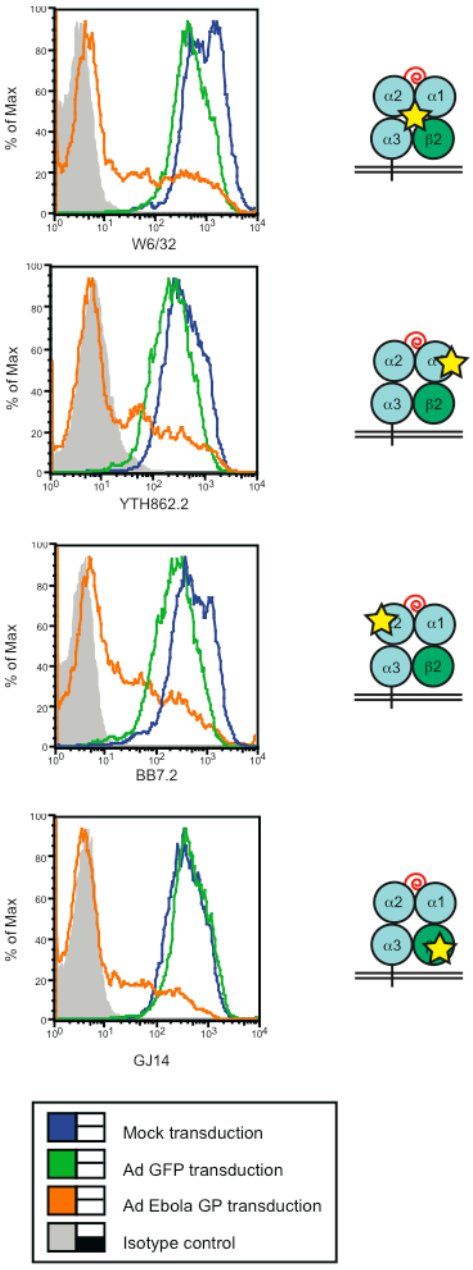

Figure 3-6 EBOV GP masks multiple epitopes on MHC1. OV79 SL9 target cells were mock transduced or transduced with Adenoviral vectors expressing GFP (Ad GFP) or GFP and EBOV GP (Ad GP) at an MOI of 300. 48 h after transduction, cells were indirectly stained for different epitopes on MHC1 with primary antibody clones W6/32, YTH862.2, BB7.2 and GJ14 and detected with Alexa Fluor 647-conjugated secondary antibodies; isotype antibody= grey peak; mock transduction= blue trace; Ad GFP= green trace; Ad GP= orange trace. The approximate location of each epitope is marked by the yellow star in a cartoon depiction of MHC1 to the right of each graph. The W6/32 clone recognizes the MHC1 heavy chain and the β2 microglobulin. The YTH862.2 clone recognizes the α1 domain of the MHC1 heavy chain. The BB7.2 clone is specific for HLA-A2 and recognizes the α2 domain of the heavy chain. The GJ14 clone recognizes the β2 microglobulin.

intracellular staining for production of the cytokine MIP-1β in $CD8^+$ 868TCRwt^+ expressing cells (Figure 3-7 C). Production of MIP-1β has been shown to be the most sensitive indicator of HIV-specific CD8 T cell activation [32]. Quantification of the CD8 activation results demonstrates that expression of EBOV GP had a profound effect on antigen presentation by the target cells, reducing T cell responses to nearly background levels (Figure 3-7 D). In contrast, the AdGFP control cells only modestly reduced the number of responding T cells. Similar results were obtained using 293T target cells (data not shown). Thus EBOV GP expression not only masks epitopes on MHC and other surface proteins, it also functionally inactivates them.

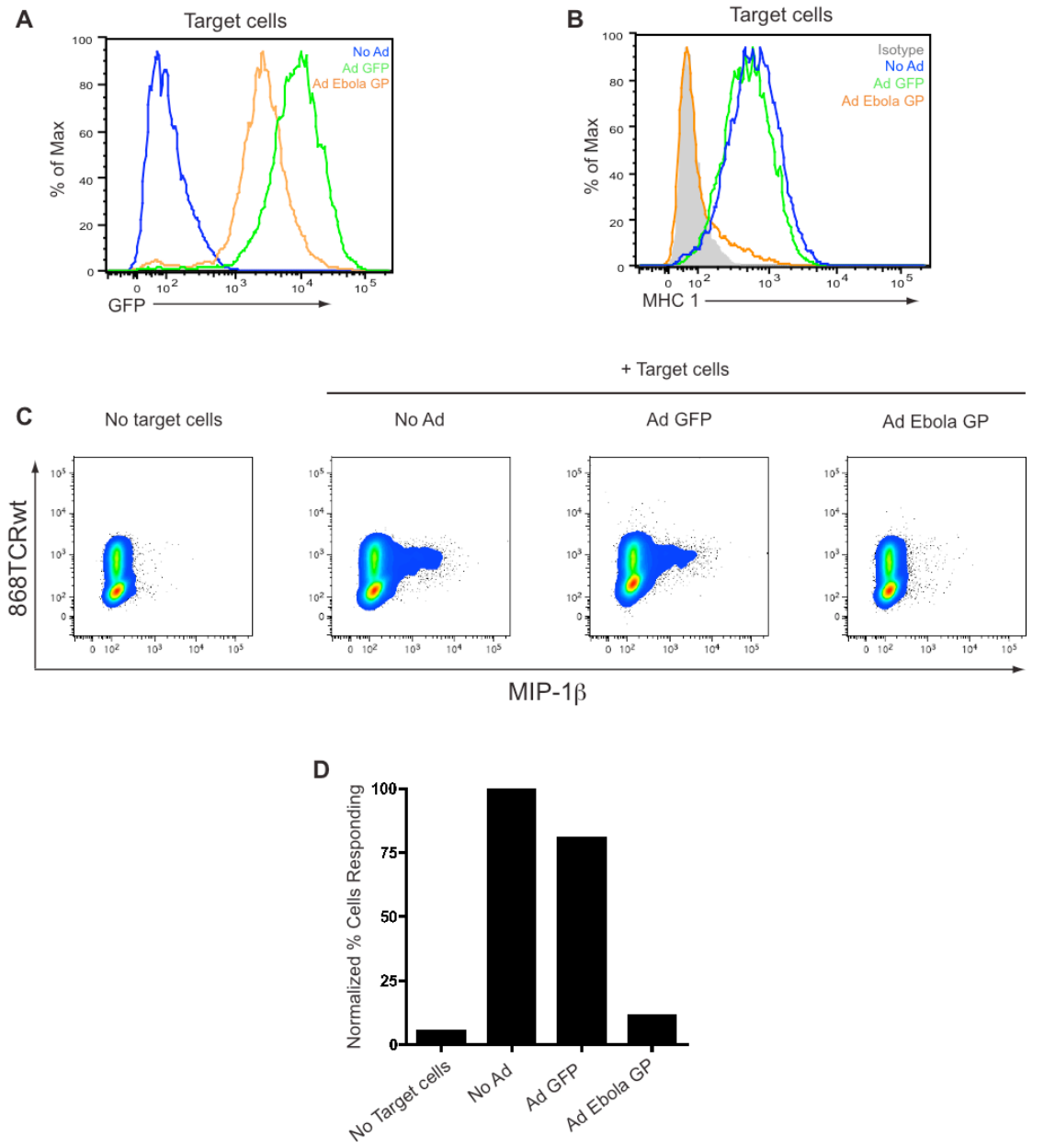

Figure 3-7 EBOV GP-induced disruption of MHC1 prevents the activation of CD8$^+$ T cells. OV79 SL9 target cells were mock transduced (no Ad) or transduced with Adenoviral vectors expressing GFP (Ad GFP) or GFP and EBOV GP (Ad GP) at an MOI of 300. 48 h after transduction, cells were assayed for GFP expression (A); No Ad= blue trace; Ad GFP= green trace; Ad GP= orange trace. Cells were also stained for MHC1 (B); isotype antibody= shaded peak; No Ad= blue trace; Ad GFP= green trace; Ad GP= orange trace. In parallel, CD8 T cells expressing a transgenic TCR (868TCRwt) that recognizes the SL9 HLA-A2 complex were incubated alone or with mock- (no Ad) or

Ad- transduced target cells in a 2:1 ratio. After co-culture, T cells were surface stained for CD8, then fixed and permeabilized, and stained for 868TCRwt and MIP-1β with APC-H7, FITC, and PE- conjugated antibodies, respectively, and assayed by flow cytometry. (C) $CD8^+$ and $868TCRwt^+$ events were analyzed for MIP-1β staining. (D) Bar graph depicts percent cells positive for MIP-1β, normalized to the No Ad target cell sample.

3.5 Discussion

An important component of the virus host interaction is viral modulation of host functions. Many viruses alter expression and/or function of host surface proteins to affect signaling, immune surveillance, or viral superinfection. EBOV GP expression in cell culture has been observed by several groups to cause dramatic changes in cell adhesion and reduction in surface protein staining by flow cytometry [10,12,14,16]. EBOV infection causes a similar reduction of β1 integrin and MHC1 staining by flow cytometry, suggesting that observations from transient GP expression are not simply artifacts of overexpression [3]. EBOV GP-induced effects have previously been assumed to result from removal of surface proteins from the plasma membrane. In this study we analyzed the mechanism of down-modulation of host surface proteins by the EBOV viral glycoprotein, GP. We show that reduction in surface staining for the host proteins MHC1 and β1 integrin is not accompanied by decreases in the total cellular levels of these proteins. Moreover, the observed self down-modulation of EBOV GP does not result in relocalization of GP away from the plasma membrane. Using epitopes placed at various locations in EBOV GP we find that the observed GP surface levels appear to differ based on epitope position relative to the mucin domain and the globular regions of the EBOV GP. A similar observation has been made using a series of monoclonal antibodies to EBOV GP [33]. Additionally, the apparent down-modulation of surface proteins is reversed by removal of the EBOV GP_1 subunit by reduction or by enzymatic digestion of the carbohydrate modification on EBOV GP. Finally, our data demonstrate that EBOV GP expression dramatically impairs antigen presentation by host cells. Taken together

these data support a model in which EBOV GP utilizes a steric occlusion mechanism to downmodulate accessibility and function of host surface proteins.

The ability of viruses to affect host surface proteins has been well documented. For example, viruses may down-regulate their cellular receptor, as in the case of HIV down-regulation of CD4 and measles virus down-regulation of the complement regulatory protein [34,35]. Other common targets for virus mediated down-modulation are surface proteins related to immune surveillance. MHC1 is known to be down-regulated from the cell surface by many viral proteins: HIV nef, Adenovirus E19, and KSHV K3 and K5, to name a few [36,37,38]. Activating ligands for natural killer (NK) cells have also been shown to be actively down-regulated by KSHV and Hepatitis C virus [39,40]. Multiple mechanisms and cellular pathways have been implicated in viral dysregulation of the various host surface molecules (reviewed for MHC1 in [41]). The model demonstrated here of glycan mediated steric occlusion by EBOV GP represents, to our knowledge, a unique mechanism for viral regulation of host surface proteins. Indeed, a similar steric masking model has recently been proposed for EBOV GP [33]. The polydnavirus, *Microplitis demolitor* bracovirus expresses a mucin domain-containing glycoprotein which can abrogate cell adhesion and thus may utilize a mechanism similar to that proposed here for EBOV [42].

Our observation that enzymatic removal of carbohydrate modification can relieve down-modulation, coupled with prior observations that the mucin domain of EBOV GP is sufficient for down-regulation [8,15], suggests that the steric occlusion observed is mediated, at least in part, by N- and O-linked modification of EBOV GP. A similar

glycan mediated steric hindrance model has been proposed for cellular mucin proteins, which can disrupt a variety of cell-cell interactions at the plasma membrane [43,44,45,46,47]. For the cellular mucin proteins, densely-arrayed O-linked glycans are critical for disruption of cell adhesion, with different core glycan structure and subsequent modifications influencing the function and anti-adhesive properties of the protein [48]. Additionally, the number of mucin tandem repeats positively correlates with the anti-adhesive properties of Muc1 [47]. Similarly, we have shown that sequential removal of glycosylation sites in the mucin domain of EBOV GP led to a step-wise reduction in cell detachment suggesting that such modifications within GP are involved in down-modulation [12]. The O-linked glycosylation found on the EBOV GP mucin domain may promote an extended conformation as is seen for cellular mucin proteins [26] allowing this domain in GP to act as an approximately 150 residue long flexible rod that can protrude and mask epitopes in the immediate vicinity.

The ability of carbohydrate modification to protect epitopes on the surface of a viral glycoprotein is well established. Indeed, a glycan shield model has been proposed for other viral glycoproteins, most notably HIV, as a mechanism to avoid host immune recognition [49]. An extended glycosylated protrusion provided by the mucin domain may be a characteristic feature that distinguishes EBOV GP from other viral glycoproteins where the glycan shield does not cause steric occlusion of host factors. Another feature of the proposed model is that EBOV GP must localize in close proximity to the affected proteins; perhaps within plasma membrane microdomains inhabited by the host proteins. This requirement may explain the critical threshold for the observed GP

effects as well as the variety of proteins regulated by EBOV GP. It may be that the ability to occupy these microdomains is, in addition to the extensive carbohydrate modification, a characteristic feature of EBOV GP. Based upon our results it appears likely, therefore, that the heavily glycosylated EBOV GP acts as a glycan shield to physically occlude access to nearby host proteins, and GP itself, thereby impairing host protein function.

It is intriguing to consider the role in EBOV replication or pathogenesis of GP-induced steric occlusion of surface proteins. Based upon our observations of proteins at the plasma membrane it is plausible that EBOV GP functions to shield epitopes on the surface of virions thereby contributing to infection and/or persistence in the natural reservoir. Notably the KZ52 monoclonal antibody employed in these studies is neutralizing but fails to protect nonhuman primates from EBOV infection [23,50]. Perhaps variation in GP density on virions produced in vivo differentially affects the neutralization sensitivity of viruses in nonhuman primates. Additionally, the ability of GP to mask MHC1 and inhibit cell-cell adhesion may be a strategy for avoiding CD8 T cell-mediated killing of infected cells. Our data demonstrating that GP-expressing cells do not effectively activate CD8 T cells supports this hypothesis. Interestingly, this mechanism is proposed for adenocarcinomas, in which cellular mucin protein overexpression can result in metastasis due to loss of adhesion, and has been shown to prevent recognition and killing by NK and cytotoxic T cells [44,51,52]. However, the rapid time course of EBOV infection and its impairment of adaptive responses may render escape from CD8 cells unnecessary in humans. Instead, protection from NK cells

may be more important and the ability of EBOV GP to affect NK cell recognition should be explored. Alternatively, the ability to mask MHC1 may be more critical for viral infection or persistence in the natural reservoir for EBOV. Finally, it is known that the interface between the innate and adaptive immune response is affected during EBOV infection (reviewed in [2]). We have previously shown that EBOV GP causes rounding in macrophages [12]. It is possible that EBOV GP shielding and inhibition of adhesion molecules or other immune regulatory proteins on professional antigen presenting cells such as macrophage or dendritic cells plays a role in the immune dysfunction characteristic of EBOV infection.

3.6 Acknowledgements

The authors would like to thank Christian Fuchs for technical assistance, Erica Ollmann Saphire and Dennis Burton for providing the KZ52 antibody, Yoshihiro Kawaoka for providing anti-GP monoclonal antibodies for IF, and Andrew Rennekamp and Rachel Kaletsky for helpful discussion. This work was funded by Public Health Service grants T32GM07229, T32AI055400 (JF), K12GM081259 (AV-R), U19AI082628-01 (JLR), P01AI080192 (JLR) and R01-AI43455 (PB).

3.7 References

1. Sanchez A, Khan AS, Zaki SR, Nabel GJ, Ksiazek TG, et al. (2001) Filoviridae: Marburg and Eboila Viruses. In: Knipe DM, Howley PM, Griggen DE, Lamb RA, Martin MA et al., editors. Fields Virology: Lippincott, Williams & Wilkins. pp. 1279-1304.
2. Mahanty S, Bray M (2004) Pathogenesis of filoviral haemorrhagic fevers. The Lancet Infectious Diseases 4: 487-498.
3. Alazard-Dany N, Volchkova V, Reynard O, Carbonnelle C, Dolnik O, et al. (2006) Ebola virus glycoprotein GP is not cytotoxic when expressed constitutively at a moderate level. J Gen Virol 87: 1247-1257.
4. Sanchez A, Trappier SG, Mahy BW, Peters CJ, Nichol ST (1996) The virion glycoproteins of Ebola viruses are encoded in two reading frames and are expressed through transcriptional editing. Proceedings of the National Academy of Sciences of the United States of America 93: 3602-3607.
5. Volchkova VA, Feldmann H, Klenk HD, Volchkov VE (1998) The nonstructural small glycoprotein sGP of Ebola virus is secreted as an antiparallel-orientated homodimer. Virology 250: 408-414.
6. Volchkov VE, Feldmann H, Volchkova VA, Klenk HD (1998) Processing of the Ebola virus glycoprotein by the proprotein convertase furin. Proc Natl Acad Sci U S A 95: 5762-5767.
7. Jeffers SA, Sanders DA, Sanchez A (2002) Covalent modifications of the ebola virus glycoprotein. J Virol 76: 12463-12472.
8. Yang ZY, Duckers HJ, Sullivan NJ, Sanchez A, Nabel EG, et al. (2000) Identification of the Ebola virus glycoprotein as the main viral determinant of vascular cell cytotoxicity and injury. Nat Med 6: 886-889.
9. Chan SY, Ma MC, Goldsmith MA (2000) Differential induction of cellular detachment by envelope glycoproteins of Marburg and Ebola (Zaire) viruses. J Gen Virol 81: 2155-2159.
10. Takada A, Watanabe S, Ito H, Okazaki K, Kida H, et al. (2000) Downregulation of beta1 integrins by Ebola virus glycoprotein: implication for virus entry. Virology 278: 20-26.
11. Volchkov VE, Volchkova VA, Muhlberger E, Kolesnikova LV, Weik M, et al. (2001) Recovery of infectious Ebola virus from complementary DNA: RNA editing of the GP gene and viral cytotoxicity. Science 291: 1965-1969.
12. Simmons G, Wool-Lewis RJ, Baribaud F, Netter RC, Bates P (2002) Ebola virus glycoproteins induce global surface protein down-modulation and loss of cell adherence. J Virol 76: 2518-2528.
13. Ray RB, Basu A, Steele R, Beyene A, McHowat J, et al. (2004) Ebola virus glycoprotein-mediated anoikis of primary human cardiac microvascular endothelial cells. Virology 321: 181-188.
14. Sullivan NJ, Peterson M, Yang ZY, Kong WP, Duckers H, et al. (2005) Ebola virus glycoprotein toxicity is mediated by a dynamin-dependent protein-trafficking pathway. J Virol 79: 547-553.

15. Francica JR, Matukonis MK, Bates P (2009) Requirements for cell rounding and surface protein down-regulation by Ebola virus glycoprotein. Virology 383: 237-247.
16. Zampieri CA, Fortin JF, Nolan GP, Nabel GJ (2007) The ERK mitogen-activated protein kinase pathway contributes to Ebola virus glycoprotein-induced cytotoxicity. J Virol 81: 1230-1240.
17. Wool-Lewis RJ, Bates P (1999) Endoproteolytic processing of the ebola virus envelope glycoprotein: cleavage is not required for function. J Virol 73: 1419-1426.
18. Bertozzi CC, Chang CY, Jairaj S, Shan X, Huang J, et al. (2006) Multiple initial culture conditions enhance the establishment of cell lines from primary ovarian cancer specimens. In Vitro Cell Dev Biol Anim 42: 58-62.
19. Suhoski MM, Golovina TN, Aqui NA, Tai VC, Varela-Rohena A, et al. (2007) Engineering artificial antigen-presenting cells to express a diverse array of co-stimulatory molecules. Mol Ther 15: 981-988.
20. Parry RV, Rumbley CA, Vandenberghe LH, June CH, Riley JL (2003) CD28 and inducible costimulatory protein Src homology 2 binding domains show distinct regulation of phosphatidylinositol 3-kinase, Bcl-xL, and IL-2 expression in primary human CD4 T lymphocytes. J Immunol 171: 166-174.
21. Varela-Rohena A, Molloy PE, Dunn SM, Li Y, Suhoski MM, et al. (2008) Control of HIV-1 immune escape by CD8 T cells expressing enhanced T-cell receptor. Nat Med 14: 1390-1395.
22. Lin G, Simmons G, Pohlmann S, Baribaud F, Ni H, et al. (2003) Differential N-linked glycosylation of human immunodeficiency virus and Ebola virus envelope glycoproteins modulates interactions with DC-SIGN and DC-SIGNR. J Virol 77: 1337-1346.
23. Maruyama T, Rodriguez LL, Jahrling PB, Sanchez A, Khan AS, et al. (1999) Ebola virus can be effectively neutralized by antibody produced in natural human infection. J Virol 73: 6024-6030.
24. Bavari S, Bosio CM, Wiegand E, Ruthel G, Will AB, et al. (2002) Lipid raft microdomains: a gateway for compartmentalized trafficking of Ebola and Marburg viruses. J Exp Med 195: 593-602.
25. Lee JE, Fusco ML, Hessell AJ, Oswald WB, Burton DR, et al. (2008) Structure of the Ebola virus glycoprotein bound to an antibody from a human survivor. Nature 454: 177-182.
26. Jentoft N (1990) Why are proteins O-glycosylated? Trends Biochem Sci 15: 291-294.
27. Neumann G, Feldmann H, Watanabe S, Lukashevich I, Kawaoka Y (2002) Reverse genetics demonstrates that proteolytic processing of the Ebola virus glycoprotein is not essential for replication in cell culture. J Virol 76: 406-410.
28. Dolnik O, Volchkova V, Garten W, Carbonnelle C, Becker S, et al. (2004) Ectodomain shedding of the glycoprotein GP of Ebola virus. Embo J 23: 2175-2184.

29. Kuan SF, Byrd JC, Basbaum C, Kim YS (1989) Inhibition of mucin glycosylation by aryl-N-acetyl-alpha-galactosaminides in human colon cancer cells. J Biol Chem 264: 19271-19277.
30. Huang J, Byrd JC, Yoon WH, Kim YS (1992) Effect of benzyl-alpha-GalNAc, an inhibitor of mucin glycosylation, on cancer-associated antigens in human colon cancer cells. Oncol Res 4: 507-515.
31. Huet G, Hennebicq-Reig S, de Bolos C, Ulloa F, Lesuffleur T, et al. (1998) GalNAc-alpha-O-benzyl inhibits NeuAcalpha2-3 glycosylation and blocks the intracellular transport of apical glycoproteins and mucus in differentiated HT-29 cells. J Cell Biol 141: 1311-1322.
32. Betts MR, Nason MC, West SM, De Rosa SC, Migueles SA, et al. (2006) HIV nonprogressors preferentially maintain highly functional HIV-specific CD8+ T cells. Blood 107: 4781-4789.
33. Reynard O, Borowiak M, Volchkova VA, Delpeut S, Mateo M, et al. (2009) Ebolavirus glycoprotein GP masks both its own epitopes and the presence of cellular surface proteins. J Virol 83: 9596-9601.
34. Willey RL, Maldarelli F, Martin MA, Strebel K (1992) Human immunodeficiency virus type 1 Vpu protein induces rapid degradation of CD4. J Virol 66: 7193-7200.
35. Schneider-Schaulies J, Schnorr JJ, Brinckmann U, Dunster LM, Baczko K, et al. (1995) Receptor usage and differential downregulation of CD46 by measles virus wild-type and vaccine strains. Proc Natl Acad Sci U S A 92: 3943-3947.
36. Schwartz O, Marechal V, Le Gall S, Lemonnier F, Heard JM (1996) Endocytosis of major histocompatibility complex class I molecules is induced by the HIV-1 Nef protein. Nat Med 2: 338-342.
37. Andersson M, Paabo S, Nilsson T, Peterson PA (1985) Impaired intracellular transport of class I MHC antigens as a possible means for adenoviruses to evade immune surveillance. Cell 43: 215-222.
38. Ishido S, Wang C, Lee BS, Cohen GB, Jung JU (2000) Downregulation of major histocompatibility complex class I molecules by Kaposi's sarcoma-associated herpesvirus K3 and K5 proteins. J Virol 74: 5300-5309.
39. Wen C, He X, Ma H, Hou N, Wei C, et al. (2008) Hepatitis C virus infection downregulates the ligands of the activating receptor NKG2D. Cell Mol Immunol 5: 475-478.
40. Thomas M, Boname JM, Field S, Nejentsev S, Salio M, et al. (2008) Down-regulation of NKG2D and NKp80 ligands by Kaposi's sarcoma-associated herpesvirus K5 protects against NK cell cytotoxicity. Proc Natl Acad Sci U S A 105: 1656-1661.
41. Hewitt EW (2003) The MHC class I antigen presentation pathway: strategies for viral immune evasion. Immunology 110: 163-169.
42. Beck M, Strand MR (2005) Glc1.8 from Microplitis demolitor bracovirus induces a loss of adhesion and phagocytosis in insect high five and S2 cells. J Virol 79: 1861-1870.

43. Wesseling J, van der Valk SW, Vos HL, Sonnenberg A, Hilkens J (1995) Episialin (MUC1) overexpression inhibits integrin-mediated cell adhesion to extracellular matrix components. J Cell Biol 129: 255-265.
44. Komatsu M, Yee L, Carraway KL (1999) Overexpression of sialomucin complex, a rat homologue of MUC4, inhibits tumor killing by lymphokine-activated killer cells. Cancer Res 59: 2229-2236.
45. Pino V, Ramsauer VP, Salas P, Carothers Carraway CA, Carraway KL (2006) Membrane mucin Muc4 induces density-dependent changes in ERK activation in mammary epithelial and tumor cells: role in reversal of contact inhibition. J Biol Chem 281: 29411-29420.
46. Hollingsworth MA, Swanson BJ (2004) Mucins in cancer: protection and control of the cell surface. Nat Rev Cancer 4: 45-60.
47. Wesseling J, van der Valk SW, Hilkens J (1996) A mechanism for inhibition of E-cadherin-mediated cell-cell adhesion by the membrane-associated mucin episialin/MUC1. Mol Biol Cell 7: 565-577.
48. Fukuda M (2002) Roles of mucin-type O-glycans in cell adhesion. Biochim Biophys Acta 1573: 394-405.
49. Wei X, Decker JM, Wang S, Hui H, Kappes JC, et al. (2003) Antibody neutralization and escape by HIV-1. Nature 422: 307-312.
50. Oswald WB, Geisbert TW, Davis KJ, Geisbert JB, Sullivan NJ, et al. (2007) Neutralizing antibody fails to impact the course of Ebola virus infection in monkeys. PLoS Pathog 3: e9.
51. McGuckin MA, Walsh MD, Hohn BG, Ward BG, Wright RG (1995) Prognostic significance of MUC1 epithelial mucin expression in breast cancer. Hum Pathol 26: 432-439.
52. Sherblom AP, Moody CE (1986) Cell surface sialomucin and resistance to natural cell-mediated cytotoxicity of rat mammary tumor ascites cells. Cancer Res 46: 4543-4546.

CHAPTER 4 – A STUDY OF SHIELDING OF THE KZ52 EPITOPE ON THE EBOLA VIRUS GLYCOPROTEIN

Joseph R. Francica[1] and Paul Bates[1]

[1]Department of Microbiology, University of Pennsylvania School of Medicine
225 Johnson Pavilion 3610 Hamilton Walk, Philadelphia, PA 19104-6076

4.1 Abstract

The Ebola virus (EBOV) is highly pathogenic in humans and non-human primates with mortality rates reaching 90%. Our understanding of EBOV pathogenesis is limited, though it is generally understood that the immune response is severely disrupted during infection. Terminally-infected patients are unable to mount a significant adaptive immune response and show low or no significant EBOV specific antibody production. The underlying mechanisms for this immune dysfunction are not completely understood but are likely complex. In previous reports we have demonstrated that a neutralizing antibody, KZ52, which is directed against the EBOV glycoprotein (GP), is sterically blocked from binding to GP at the cell surface by heavily-glycosylated domains within GP, itself. In the current study, we address the possibility that steric occlusion of the KZ52 antibody may also occur on the surface of viral particles. First, we characterize a construct of GP that undergoes processing in the secretory system to remove the mucin and glycan cap domains of GP. This "primed GP" allowed us to identify the glycan cap as responsible for the shielding of the KZ52 epitope at the cell surface. We then demonstrate that full-length GP interferes with the amount of antibody that can bind on retroviral particles, indicating that steric occlusion occurs on the virion surface.

Interestingly, despite differences in antibody access, neutralization of retroviral particles bearing occluding or non-occluding forms of GP seems unaffected. These data suggest a novel role for the glycosylated domains of GP in blocking antibody access to viral particles and warrant further studies into this mechanism to expand our understanding of the interplay between GP and the immune response to EBOV.

4.2 Introduction

The Ebola virus (EBOV) is a member of the family, *Filoviridae*, and is the etiological agent of Ebola hemorrhagic fever (EHF). Generally, EHF is associated with extremely high levels of morbidity and mortality in humans and nonhuman primates, although different subtypes of EBOV are differently pathogenic in humans. The five subtypes of EBOV- from most to least pathogenic- are Zaire, Sudan, Bundibugyo, Côte d'Ivoire, and Reston [1,2]. The basis for the high pathogenicity of certain subtypes of EBOV is unclear, however immune dysregulation likely plays a role [3]. It has been noted during outbreaks of EHF, that infected patients who succumb to EBOV show little or no signs of adaptive immunity. These patients do not make EBOV- specific antibodies and do not undergo class switching from IgM to IgG, an indicator of a productive B cell response [4,5,6]. In contrast, patients who survived EHF were able to make IgG responses, which have been observed to be mostly against VP40 and NP [5]. Although it is unclear what leads to a nominal or aberrant humoral response, it has been observed in both humans and experimentally-infected primates that EBOV infection induces a significant bystander apoptosis of lymphocytes [4,5,6,7,8].

Interestingly, the role of antibodies in mediating protection to EBOV is unclear. Several studies have demonstrated that the passive transfer of GP-specific monoclonal antibodies to mice, or hyperimmune equine IgG to guinea pigs and mice can protect against EBOV challenge [9,10,11]. However, other studies have found no efficacy in passive antibody transfer of polyclonal antibodies to guinea pigs or mice [12,13]. The KZ52 antibody, a neutralizing monoclonal antibody isolated from a human survivor, can

be administered to protect guinea pigs [14]. However, the passive transfer of KZ52 antibodies does not protect nonhuman primates [15]. And although one study has reported efficacy of infusion of convalescent patient blood to EHF patients during an outbreak, other factors may have played a role in the recovery of these patients and similar studies in primate models have been unable to repeat this finding [16,17]. Furthermore, several vaccine studies in both mice and macaques have concluded that cellular- not humoral- immunity is a correlate of vaccine protection against EBOV [13,18,19].

In the present study, we examined the interaction of the KZ52 antibody with its epitope on the main EBOV glycoprotein, GP. GP is actually the minor product of the glycoprotein gene; the major product is a dimeric, secreted form (sGP) whose function remains unclear [20,21]. Full-length, trimeric, membrane-bound GP results from transcriptional editing of the glycoprotein gene by the viral polymerase [20,22]. This form is expressed at the cell surface, is incorporated into the virion, and drives viral attachment and membrane fusion [20]. GP is initially translated as a precursor (GP_0), which is then cleaved by furin within the Golgi into two subunits, a surface subunit, GP_1 and a membrane-spanning subunit, GP_2 [23]. These subunits remain covalently connected through a single intermolecular cysteine bond [24]. During viral entry, GP_1 is proteolyzed by endosomal cathepsins, which removes the glycosylated glycan cap and mucin domains and exposes the receptor-binding domain (RBD) [25,26,27,28].

Expression of GP has been shown to cause effects in cell culture on host surface proteins similar to those observed during viral infection, and so is proposed to be an

important determinant of viral pathogenesis [22,29,30,31]. GP expression in cultured cells disrupts cell adhesion resulting in loss of cell-cell contacts as well as cell rounding and loss of attachment to the culture substrate [29,31,32]. By flow cytometry, cells expressing GP display dramatically lowered levels of various surface proteins, including several members of the integrin family and MHC class I [31,32,33]. These effects of EBOV GP are known to be caused by a highly glycosylated region in GP_1, the mucin domain [29,32,33]. In the previous chapters of this dissertation, we demonstrate that the mucin domain of GP sterically shields affected surface proteins from antibody recognition, giving the appearance of a loss of expression by surface staining flow cytometry. Interestingly, we found that the GP_1 subunit also shields the epitope for the KZ52 antibody, preventing its binding to GP at the cell surface.

In the present study we analyze the requirements for the shielding of the KZ52 epitope by GP and hypothesize that such shielding may occur on the surface of viral particles. We have found that the glycan cap seems to be necessary for blocking antibody access to the KZ52 epitope at the cell surface. We further demonstrate that a form of GP lacking this domain and the mucin domain shows greater antibody binding on pseudoviral particles, although a modulation of neutralization was not observed. These data impel further research into this model as a potential immune evasion mechanism by EBOV.

4.3 Materials and Methods

Plasmids, cell culture and transfections

For GP studies, cDNA encoding the membrane-anchored form of Zaire EBOV GP (Mayinga strain, accession number U23187) was used. GP containing a deletion of the mucin domain (GPΔmuc), amino acids 302-462 has been previously described [32]. For furin processed construct (primed GP), the amino acids VNAT at positions 203-206 were replaced with the amino acids RRKR. All constructs contain a C-terminal V5-His tag and are cloned into the pCAGGS expression vector. For over-expression of furin, cDNA encoding human furin was described previously, but was sub-cloned into the pCDNA3.1 expression vector for use here [34].

293T cells were cultured in DMEM (Gibco) with 10% fetal bovine serum (HyClone) and penicillin/streptomycin (Gibco) at 37 ºC with 5% CO_2. For flow cytometry and western blotting, 293T cells were plated in 6-well plates one day prior to transfection. Cells were transiently transfected by Lipofectamine 2000 according to manufacturer's directions with 4 μg DNA per well. For pseudovirus production, 293T cells were plated in 10 cm plates one day prior to transfection. Cells were then transfected with varying amounts of DNA by calcium-phosphate precipitation; media was replaced 5 hours post transfection. For pseudovirion neutralization assay, cells were plated in Biocoat 96-well plates (Becton & Dickinson) one day prior to infection. One hour prior to infection, cells were replaced with fresh media.

Cell lysates and western blotting

Transfected cells were removed by resuspension in the culturing media. Cells were pelleted at 4 ºC for 3 minutes at 1300 x g. Pellets were resuspended in 1% Triton X-100 buffer with complete protease inhibitor cocktail (Roche) for 5 minutes at room temperature. Lysates were cleared by centrifugation at 4 ºC at 20,800 x g. 30 µl samples were mixed with reducing SDS buffer, boiled for 5 minutes, and separated on a 4-15% Criterion PAGE gel (Bio-Rad). Proteins were transferred to PVDF (Millipore) at a 400 mA constant current. Membranes were blocked in 5% milk in TBS. For detection of GP, membranes were probed with rabbit polyclonal anti-GP sera which recognizes the GP_1 subunit, in blocking buffer [35]. For detection of V5 epitopes, membranes were probed with rabbit anti- V5 antibodies (Bethyl Labs), in blocking buffer. For detection of the mucin domain, membranes were probed with the 13F6 mouse monoclonal antibody in blocking buffer [11]. Proteins were detected with stabilized goat anti- mouse or rabbit HRP conjugated antibodies (Pierce), in blocking buffer. For detection of the human KZ52 antibody, membranes were probed with anti- human HRP-conjugated antibodies (Jackson ImmunoResearch Laboratories), in blocking buffer. Membranes were visualized with SuperSignal Femto substrate (Pierce).

Flow cytometry

293T cells were detached from the plate 24 hours post transfection with PBS -/-, 0.5 mM EDTA and combined with floating cells in culture media. Cells were pelleted at 4 ºC at 250 x g, then resuspended in flow wash buffer (PBS -/- with 1% bovine calf

serum and 0.05% NaAzide) and aliquoted for staining. For detection of EBOV GP, cells were stained with the human MAb, KZ52 [36] and detected with FITC anti-human IgG (PharMingen). For detection of β1 integrin, cells were stained with anti-human CD29 PE-Cy5 conjugate (eBioscience); for detection of MHC1, cells were stained with anti- HLA-ABC PE-Cy5 conjugate (eBioscience). For fixation and permeabilization, cells were resuspended in Cytofix/Cytoperm (BD Biosciences) for 20 minutes on ice, followed by washing with Permwash (BD Biosciences). Antibodies where then diluted in Permwash buffer. All staining was performed on ice, followed by washing. Live cell gates were drawn based on forward and side scatter. For each sample, 10,000 events in the live cell gate were collected and analyzed. Data were collected on a Becton Dickinson FACSCalibur and analyzed using FlowJo software (Tree Star, Inc.).

Production of lentiviral luciferase pseudovirions

Human immunodeficiency virus (HIV) luciferase-encoding pseudotyped particles were produced as previously described [28]. Briefly, 293T cells were transfected with 10 μg of a luciferase-encoding HIV plasmid (pNL-luc) and 10 μg of additional HIV Gag-Pol-encoding plasmid (psPAX). The following amounts of plasmid were co-transfected to pseudotype the indicated glycoproteins: 10-20 μg of GP, 8 μg of GPΔmuc, 20 μg of primed GP or 6 μg of pCB6-VSV(G). Viral supernatants were collected 48 hours posttransfection, and pre-cleared by centrifugation at 250 x g at 4 ºC for 2 minutes. Supernatant was then filtered through a 0.45 μm syringe filter, then concentrated through

a 20% sucrose cushion by ultracentrifugation at 28,000 rpm in an SW28 rotor for 2 hours at 4°C. Pelleted virions were resuspended in PBS overnight at 4°C.

Pseudovirion and glycoprotein normalization

HIV pseudovirions were normalization using p24 levels. Relative glycoprotein incorporation was determined using a V5 epitope tag on the GP_2 C terminus. Fluorescent western blot analysis was employed to quantify p24 and V5 as follows: For each sample, 15 µl of pseudovirions (in triplicate lanes) were mixed with reducing SDS buffer, boiled for 5 minutes, and separated on a 4-15% Criterion PAGE gel (Bio-Rad). Proteins were transferred to PVDF (Millipore) at a 400 mA constant current. Membranes were blocked in 5% milk in TBS. p24 levels were probed with mouse anti- p24 monoclonal antibody 241-D (NIH AIDS Reagent Program); V5 levels were probed with rabbit anti- V5 polyclonal antibodies (Bethyl Labs). Anti- mouse IRDye800CW antibodies (1:5,000; Rockland) and anti- rabbit Alexa Fluor 680 (1:10,000; Invitrogen) were then used to detect p24 and V5, respectively. Blots were scanned using an Odyssey infrared imaging system (LI-COR) and band intensities were quantified using LI-COR software. Triplicate lane bands were averaged to give relative sample quantities, measured in relative fluorescent units, RFUs. Average p24 RFUs were used to normalize across samples. For evaluation of glycoprotein incorporation, the ratio of V5 to p24 RFUs were calculated so that a higher quotient indicates better incorporation and a lower quotient indicates poorer incorporation.

Pseudovirion immunoprecipitation

Pseudovirions were diluted in eppendorf tubes in flow wash buffer (PBS -/- with 1% bovine calf serum and 0.05% NaAzide) or 1% NP40 buffer to a final volume of 350 µl and incubated with 3 µg of KZ52, mouse anti- V5 (Invitrogen), or mouse anti- HA (12CA5, Roche) antibodies for 1 hour at 4 ºC, rocking. Antibodies were captured by adding 12.5 µl Protein A Dynabeads (Invitrogen), pre-washed in the appropriate buffer, and incubating for 2 hours at 4 ºC, rocking. Complexes were isolated using a MACS separation magnet (Miltenyi Bioech) and washed twice with the appropriate buffer. Samples were then analyzed by western blotting as described above.

Pseudovirion bound antibody analysis

Pseudovirions were diluted in flow wash and incubated with antibodies as described above. Samples were then further diluted to 3.5 ml in PBS and layered above a 1.5 ml 20% sucrose cushion in Ultra-Clear centrifuge tubes **(**Beckman) and centrifuged in a SW55 rotor at 54,000 rpm for 36 minutes at 4 ºC. Supernatants were decanted and pelleted pseudovirions were resuspended in 1% Triton X-100 lysis buffer for 5 minutes at room temperature. Protein A Dynabeads were then added and used for immunoprecipitation as described above.

Pseudovirion neutralization

Samples were normalized for p24 levels. Pseudovirions were diluted in media and mixed with serially-diluted KZ52 antibody, or media as a control, in a combined

volume of 50 µl. Pseudovirion/antibody mixtures were incubated on ice for 20 minutes. Pseudovirions were then added to cells for a combined volume of 100 µl. Indicated antibody concentrations are relative to final combined 100 µl volume. All samples were performed in triplicate. 48 hours after infection, supernatants were removed and cells were lysed in 100 µl 0.5% Triton X-100 for 5 minutes at room temperature. 50 µl from each well was then transferred to a 96-well black, solid bottom plate. 100 µl firefly luciferase substrate (Promega) was added to each well and the plate was assayed on a luminometer (Dynex / Thermo). Percent normalized infection values were calculated by setting the relative luciferase values from the no antibody sample to 100%.

4.4 Results

GP mucin and glycan cap domains can be proteolytically removed during secretion

We have previously demonstrated that EBOV GP from the highly-pathogenic Zaire subtype sterically shields the epitopes of several host proteins at the cell surface, as well as epitopes on GP itself (Figure 3-3). We have also shown that the mucin domain is necessary and sufficient to shield these host proteins (Chapter 2). However, the critical domain(s) on GP responsible for shielding the KZ52 epitope has not been elucidated. Removal of the entire GP_1 surface subunit restores KZ52 staining at the cell surface (Figure 3-4), however, GP_1 contains several domains: the mucin domain, glycan cap, RBD-containing head region, and the GP_1 base, which makes contacts with the KZ52 antibody (Figure 1-4 and [25]). The glycan cap contains 4 bulky N-linked glycosylation sites that are positioned such that they could shield the RBD. Therefore, it was beneficial to create a construct that lacked both the glycan cap and the mucin domain so that we could evaluate the potential of this domain to shield epitopes on GP. Although genetic deletion of the mucin domain is viable, genetic deletion of both the mucin domain and the glycan cap does not result in properly folded protein (P.B., unpublished observation). Therefore, we created a GP construct in which amino acid residues from 203-206 were mutated to a recognition sequence for the cellular protein convertase, furin (Figure 4-1 A). This sequence is located within a disordered loop in GP, and is 4 residues downstream of the primary site of cathepsin cleavage during entry, which removes the mucin and glycan cap domains [25,27]. When this construct is expressed in cells, GP is

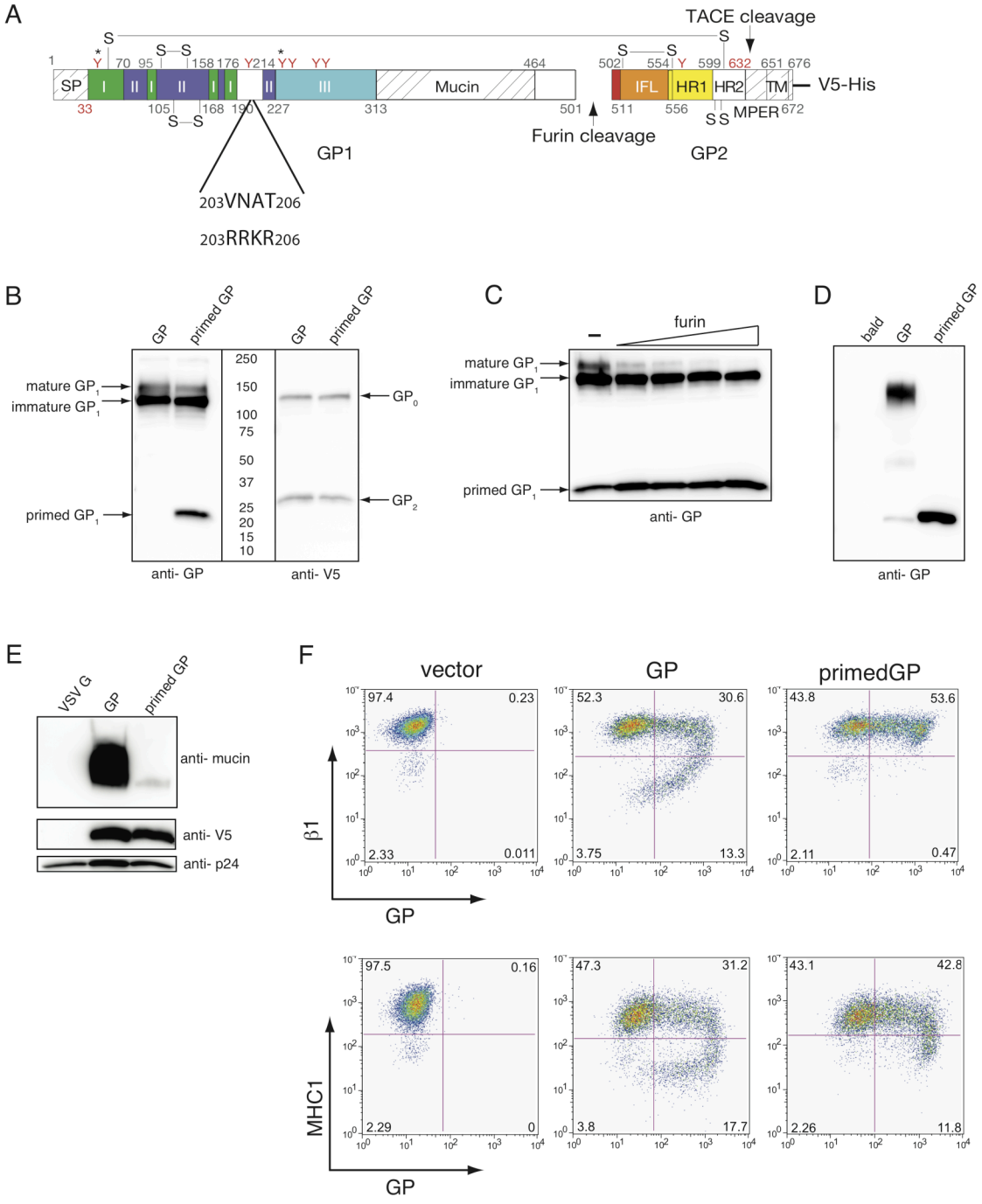

Figure 4-1 Characterization of primed GP construct. (A) Diagram of EBOV GP domains, modified from [25]. Primed GP construct was created by mutating amino acid resides 203-206 to RRKR. Construct also encodes a C-terminal V5-His tag. (B) GP and primed GP expression. 293T cells were transfected with plasmid encoding GP or primed GP. 24 h post transfection, cells were lysed in Triton X-100, resolved by SDS-PAGE

under reducing conditions, transferred to PVDF, and blotted for GP using polyclonal rabbit anti-GP antibodies (left blot) or polyclonal rabbit anti- V5 antibodies (right blot). (C) Primed GP construct was expressed alone or co-transfected with increasing concentrations of plasmid encoding human furin. Cell lysates were harvested and resolved by SDS-PAGE and blotted for GP using rabbit polyclonal antibodies as above. (D) Incorporation of GP and primed GP into lentiviral pseudovirions. Bald pseudovirions or pseudovirions bearing GP or primed GP were produced and purified as described in materials and methods. Aliquots were then resolved by SDS-PAGE and blotted for GP using rabbit polyclonal antibodies as above. (E) The glycan cap and mucin domain are removed from pseudovirions bearing primed GP. Pseudovirions bearing VSV G, EBOV GP, or primed GP were produced and purified as above. Aliquots were then resolved by SDS-PAGE and blotted for the mucin domain using the 13F6 antibody, for GP_2 using anti- V5 antibodies, and for the lentiviral capsid using anti- p24 antibodies. (F) Primed GP does not shield surface proteins. 293T cells were transfected with empty pCAGGS (vector) or vector encoding GP or primed GP. Floating and adherent cells were harvested 24 h after transfection, pooled, and stained for GP using the KZ52 antibody, followed by FITC-labeled secondary antibodies, and co-stained for β1 integrin or MHC1 with PE-Cy5 conjugated monoclonal antibodies and assayed by flow cytometry.

processed by endogenous furin to produce an approximately 24 kDa fragment that corresponds to GP_1 that lacks the mucin domain and glycan cap and has been termed, primed GP (Figure 4-1 B and [37]). The primed GP construct is well-expressed and stable in cells, compared to wild-type GP, however, processing from the mature form of GP to the primed form by endogenous furin is incomplete (Figure 4-1 B, left blot). To increase processing, furin was over-expressed with the primed GP construct,which resulted in nearly complete processing of mature GP to primed GP (Figure 4-1 C). Primed GP was well incorporated into HIV pseudovirions, in which no mature, unprocessed GP could be detected by western blot (Figure 1-4 D). Similarly, antibodies recognizing the mucin domain react with pseudovirions bearing full-length GP but not primed GP, indicating this domain has been removed (Figure 1-4 E).

Primed GP does not shield epitopes at the cell surface

In the Primed GP construct, the mucin domain and glycan cap have been cleaved from the full-length protein. If these domains are physically separated from the remaining GP_1 domains at the cell surface, primed should not be capable of shielding host surface proteins. To evaluate this, we expressed primed GP in 293T cells and surface stained them for β1 integrin and major histocompatibility complex class 1 (MHC1) and for GP. As shown in Figure 4-1 F, GP causes dramatic shielding of β1 and MHC1, resulting of cells that stain dimly for these proteins, while primed GP does not display this effect. These data indicate that the mucin and glycan cap domains have been removed from their normal position in GP_1.

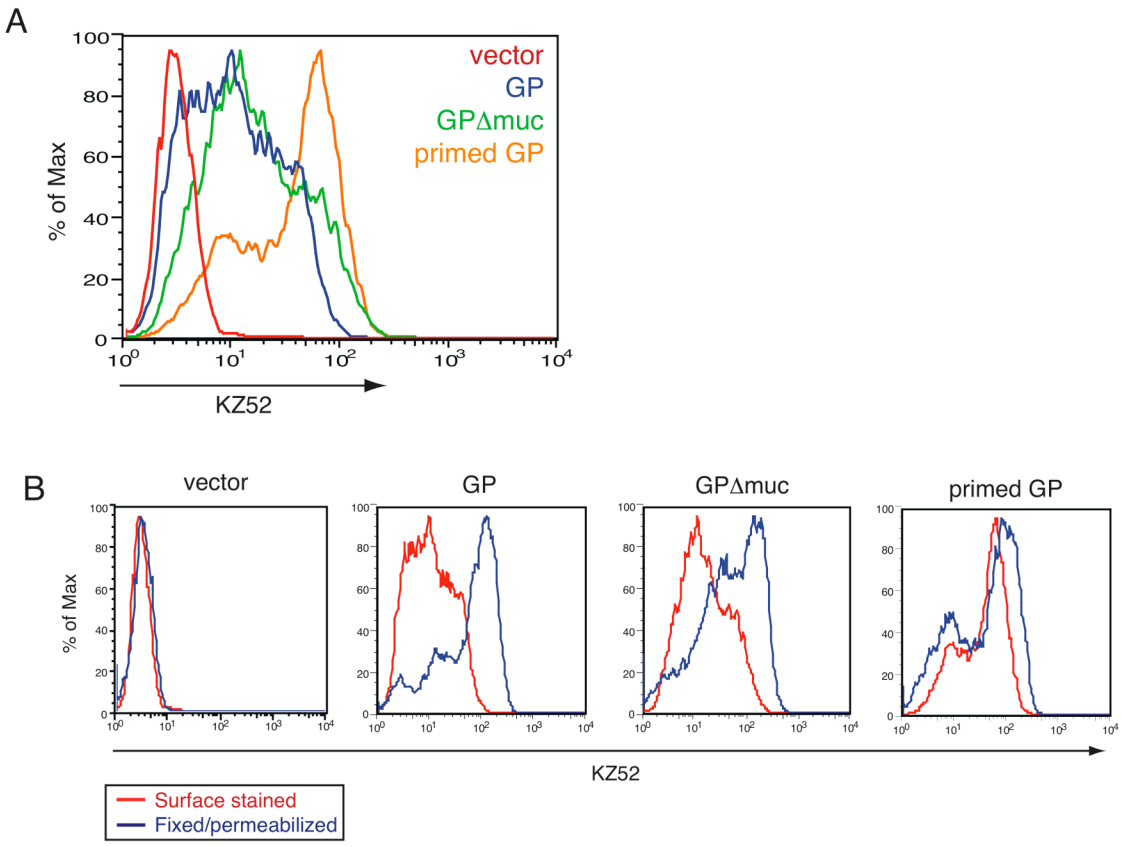

Figure 4-2 Primed GP does not shield the KZ52 epitope at the cell surface. (A) 293T cells were transfected with empty pCAGGS (vector) or vector encoding GP, GPΔmuc, or primed GP. Floating and adherent cells were harvested 24 h after transfection, pooled, and stained for GP using the KZ52 antibody, followed by FITC-labeled secondary antibodies and assayed by flow cytometry. (B) To evaluate each form of GP's ability to shield the KZ52 epitope, samples from (A) were fixed and permeabilized in parallel, then stained for KZ52 and assayed by flow cytometry. To make a direct comparison between surface stained and fixed/permeabilized samples, FL-1 channel voltages were set to overlap each other using the empty vector samples (left-most plot).

We next wanted to address whether the glycan cap played a role in shielding the KZ52 epitope at the cell surface. 293T cells were transfected with plasmid encoding GP, GP lacking the mucin domain (GPΔmuc), or primed GP. 24 hours after transfection, cells were harvested and stained for GP with the KZ52 antibody and assayed by flow cytometry (Figure 4-2 A). As we have previously shown (Figure 3-3), GP shields this epitope at the cell surface. The mucin domain seems to be dispensable for this effect, because GPΔmuc shows similar levels of surface staining for KZ52 as GP. Interestingly, primed GP displays much higher levels of staining, with the majority of cells showing uniformly bright staining. Because the difference between GPΔmuc and primed GP is the presence or absence of the glycan cap, we conclude that this domain is critical for the shielding of the KZ52 epitope at the cell surface.

To further evaluate the role of the glycan cap in shielding epitopes on GP, we attempted to rescue staining of the occluded KZ52 epitope. We have previously shown that treatment of GP-expressing cells with saponin will rescue KZ52 staining (Figure 3-2). This effect appears to be a result of saponin binding to cholesterol at the plasma membrane, and not due to the fact that the cells become permeabilized (J.R.F., unpublished observations). Therefore, we can gauge the ability of each GP construct to shield the KZ52 epitope by pre-treating cells with a saponin solution. This treatment dramatically increases staining in cells expressing GP or GPΔmuc, indicating that these constructs had shielded the KZ52 epitope (Figure 4-2 B). In contrast, saponin treatment does not significantly alter the high level of KZ52 staining in cells expressing primed GP.

These data indicate that primed GP does not shield the KZ52 epitope and further support the conclusion that the glycan cap is necessary for this shielding.

EBOV GP imposes steric constraints on lentiviral pseudovirions

Because full-length GP is capable of shielding the KZ52 epitope at the cell surface, we hypothesized there may be comparable steric occlusion on viral particles. For these experiments, primed GP was used as a control because it is unable to sterically occlude epitopes at the cell surface, as previously demonstrated. To address this question, we performed immunoprecipitations (IPs) of intact pseudovirion preparations diluted in a PBS-based buffer by incubating pseudovirions with KZ52 then immunoprecipitating antibody-particle complexes with protein A. It had been previously reported that KZ52 antibodies could IP intact pseudovirions bearing GP, but not particles that had been *in vitro* treated with cathepsin L to produce primed GP [38]. In contrast to that report, we found that KZ52 was not able to immunoprecipitate particles bearing GP, whereas KZ52 particles bearing primed GP were effectively recognized (Figure 4-3 A). These IPs had extremely low background, as judged by IP with control anti- HA antibodies. Also, the pseudovirion preparations used here contained only a small fraction of ruptured particles, as judged by IP with anti- V5 antibodies, which will only IP GP that is not protected by a viral lipid envelope. Therefore, it appeares that the mucin domain and glycan cap of GP prevent the necessary protein A-antibody-virion interactions from occurring. This is further supported by the fact that such interactions could be restored when particles were lysed and

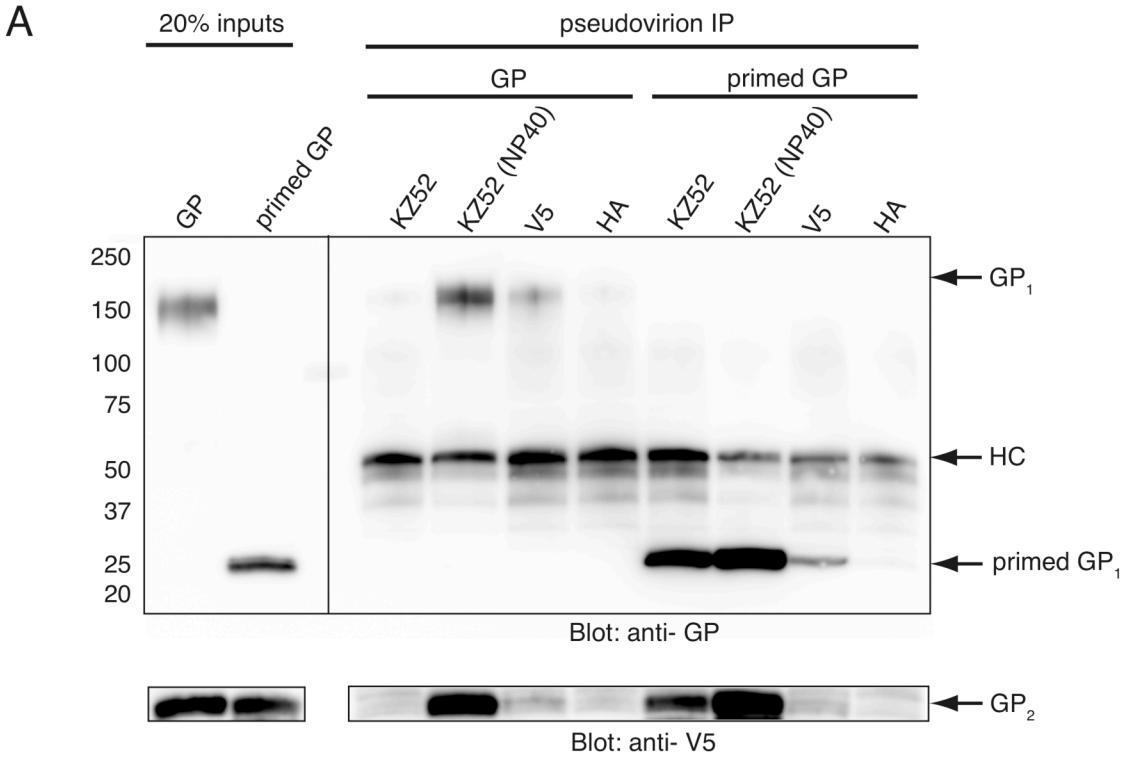
A
20% inputs
pseudovirion IP
GP
primed GP
GP
primed GP
KZ52
KZ52 (NP40)
V5
HA
KZ52
KZ52 (NP40)
V5
HA
250
150
100
75
50
37
25
20
GP1
HC
primed GP1
Blot: anti- GP
GP2
Blot: anti- V5

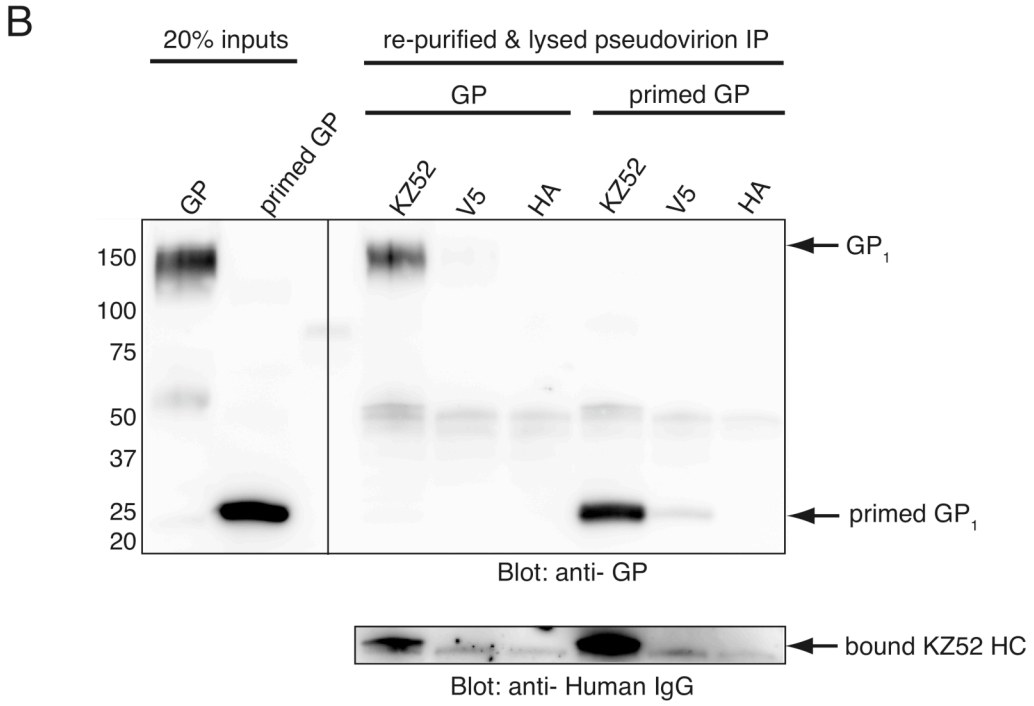
B
20% inputs
re-purified & lysed pseudovirion IP
GP
primed GP
GP
primed GP
KZ52
V5
HA
KZ52
V5
HA
150
100
75
50
37
25
20
GP1
primed GP1
Blot: anti- GP
bound KZ52 HC
Blot: anti- Human IgG

Figure 4-3 Steric occlusion by GP on lentiviral pseudovirions. (A) Lentiviral pseudovirions bearing GP or primed GP were incubated with KZ52, anti- V5, or anti- HA antibodies in PBS buffer, or incubated with KZ52 antibodies in NP40 buffer. Dynabeads conjugated to protein A were then added to IP pseudovirions. Beads were boiled in reducing buffer, resolved by SDS-PAGE, transferred to PVDF, and blotted for GP using polyclonal rabbit anti-GP antibodies (top panel) or polyclonal rabbit anti- V5 antibodies (bottom panel). The anti- V5 IP indicates the amount of disrupted particles in each sample; the anti- HA IP indicates non-specific binding. (B) To determine the amount of antibody bound to GP or primed GP pseudovirions, KZ52, V5, or HA antibodies were bound to particles in PBS buffer, then purified away from unbound antibodies through a 20% sucrose cushion. Pelleted particles were resuspended in Triton-X100 lysis buffer, then immunoprecipitated and resolved by SDS-PAGE as described above. Membranes were probed for GP with polyclonal rabbit anti-GP antibodies (top panel), and probed for bound KZ52 antibody with anti- human IgG antibodies (bottom panel). For pseudovirion preparations used in this experiment, primed GP was found to incorporate at levels 70% of that of GP.

immunoprecipitated in a buffer containing NP40 detergent (Figure 4-3 A). These results are consistent regardless of whether one visualizes the GP_1 (top panel) or GP_2 (bottom panel) subunits.

Although we have shown that GP prevents the IP of intact virions using the KZ52 antibody, this experiment does not address whether GP prevents the KZ52 antibody from binding, or whether it prevents protein A from interacting with bound antibody. To further probe this question, we performed a similar experiment, but first purified intact pseudovirions away from unbound antibody. These re-purified particles were then lysed and IPs were carried out in buffer containing detergent. As Figure 4-3 B shows, the amount of bound KZ52 antibody is greater on particles bearing primed GP, compared to particles bearing full-length GP (bottom panel). This bound antibody was capable of immunoprecipitating both primed GP and full-length GP once the particles were lysed (top panel). These data suggest that steric occlusion by GP may serve to interfere with antibody binding. Additionally, because bound KZ52 can be detected on GP-bearing pseudovirions, shielding by GP is also likely also preventing access of protein A to bound antibodies.

Impact of GP shielding on neutralization by KZ52

We have observed that antibody access to lentiviral pseudotyped particles may be limited by the mucin and glycan cap domains on GP. Therefore, we wanted to assess whether this impacted the amount of antibody required to neutralize these pseudovirions. KZ52 has been shown to neutralize replicating EBOV with an IC_{50} of 0.3 μg/ml as well

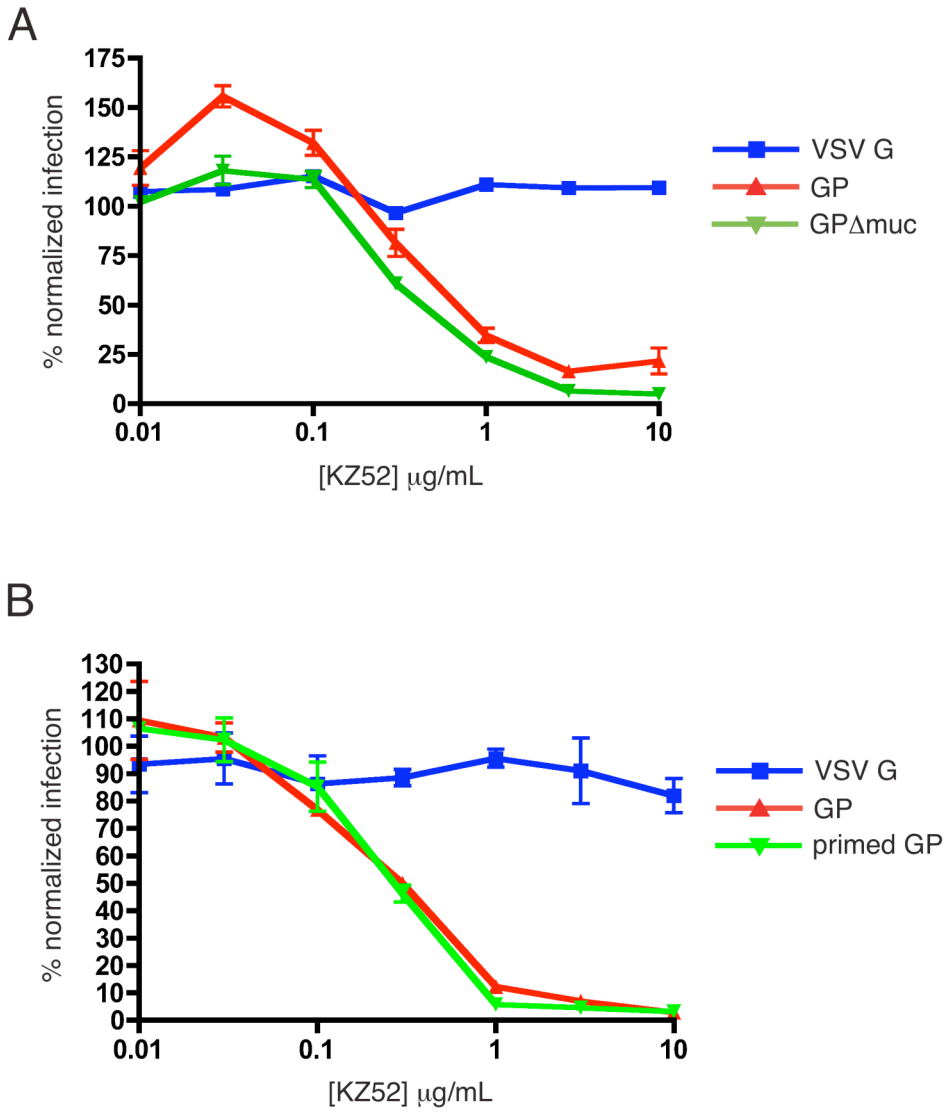

Figure 4-4 Neutralization of lentiviral pseudovirions by the KZ52 antibody. Lentiviral pseudotyped particles encoding luciferase and bearing VSV G, GP and GPΔmuc (A) or primed GP (B) glycoproteins were incubated with KZ52 antibodies over a range of concentrations then applied to 293T cells. 48 h after infection, supernatants were removed, cells were lysed in Triton-X100 and firefly luciferase substrate was added. Luciferase activity was measured by luminometer. All samples were performed in triplicate and were normalized to infection of pseudovirions incubated without antibody. Data shown are representative of at least two independent experiments. For pseudovirions preparations used in this experiment, GPΔmuc was incorporated at levels 105% of that of GP; primed GP was incorporated at levels 98% of that of GP.

as lentiviral pseudotypes bearing GP; however, a recent report found that cathepsin L-processed pseudotypes bearing GP could not be neutralized by KZ52 [36,38]. We compared the neutralization of pseudotypes bearing GP or GPΔmuc (Figure 4-4 A) and GP or primed GP (Figure 4-4 B). KZ52 efficiently neutralized pseudotypes bearing all three forms of the EBOV glycoprotein, but not those bearing VSV G. The IC_{50} values for these neutralization profiles were all approximately 0.3 μg/ml, comparable to that observed with EBOV. Therefore, we conclude that the observed steric occlusion by the mucin domain and glycan cap of GP does not impact the neutralization sensitivity of HIV pseudovirions.

4.5 Discussion

In this study we have examined the ability of the highly-glycosylated mucin and glycan cap domains in GP to modulate access to the neutralizing epitope bound by the KZ52 antibody. Our hypothesis that the glycan cap might play a critical role in providing steric occlusion necessitated the creation of a mutant form of GP lacking this domain. In creating the primed GP construct, we are able to transport a form of GP to the cell surface that resembles the structure of GP after it is processed by endosomal cathepsins during entry (for which the term, primed GP, was first coined) [25,27,37]. Because this primed GP can be easily incorporated into budding pseudotyped particles (Figure 4-1 D), this construct should be highly useful in the study of viral entry. It presumably adopts the same confirmation as cathepsin-processed GP, but obviates the need for *in vitro* cathepsin treatment, which can be heterogeneous and is prone to over-processing. A chimeric GP-Fc protein that encompasses the region found in primed GP has been produced in soluble monomeric form and has been shown to bind to the surface of susceptible cells [37]. In contrast, the primed GP construct described here is trimeric because it is initially synthesized and folded as full-length GP. If the quaternary structure of trimeric GP is important for receptor engagement or structural rearrangement, this primed GP construct may prove useful in EBOV entry studies. This idea is conceptually supported by the crystal structure of GP, which shows that GP_2 subunits interact with GP_1 subunits on neighboring monomers [25].

It is interesting to note that this study has produced results that would seem to contradict a previously published study by Shedlock and colleagues in two particular

areas [38]. In their study, they examined the ability of the KZ52 antibody to bind and IP intact pseudovirions bearing GP and cathepsin L-processed GP; unprocessed GP was able to be immunoprecipitated, while cathepsin L-processed GP was not. However, in Figure 4-3 A, we show evidence that GP is unable to be immunoprecipitated unless detergent is added to the IP to solubilize the glycoproteins. It is possible that our full-length GP is incorporated to higher levels in our pseudovirion preparations than in the previous study, giving rise to our conclusion that GP provides a steric shield on particles. This may not be true, however, as the amount of GP-encoding plasmid was actually scaled back from our usual preparation to better match the incorporation level of primed GP. The other discrepancy between our data and the study by Shedlock *et al*., is their report that pseudovirions bearing cathepsin L-processed GP can neither be immunoprecipitated nor neutralized by the KZ52 antibody. This finding is somewhat surprising because cathepsin processing does not directly involve the residues that form the KZ52 epitope [25,27]. Our data in figures 4-3 A and 4-4 B clearly demonstrate that primed GP, which should faithfully mimic the cathepsin-processed form, is readily immunoprecipitated and neutralized by KZ52. One possible explanation then, is that the primed GP construct described here stability preserves the KZ52 epitope, while cathepsin treatment of GP yields a more unstable primed form. This could occur by over-processing with cathepsin L, which can further degrade the primed GP form (P.B. and R. Kaletsky, unpublished observation), or could result from the fact that our construct is cleaved by furin at residue 206, while cathepsins process GP at residue 202 [27]. Perhaps these extra 4 amino acids serve to further stabilize the KZ52 epitope.

In Figures 4-2 and 4-3, we have endeavored to demonstrate that the mucin domain and glycan cap are capable of imposing steric constraints on the KZ52 epitope, both at the cell surface and on the virion surface. Interestingly, we show that by removing the glycan cap, through expression of primed GP, KZ52 staining is restored to high levels that are comparable to the rescue seen after fixation and permeabilization of cells expressing GP or GPΔmuc (Figure 4-2). Although these data indicate that the glycan cap is critical to the shielding of the KZ52 epitope at the cell surface, the mechanism by which this domain promotes shielding is unknown. The glycan cap contains 4 N-linked sugar moieties, and we have shown that N-liked glycosylation plays a role in shielding surface epitopes (Figure 3-5). However, the glycan cap sits on top of the GP head domain in a position unlikely to directly occlude the KZ52 epitope [25]. The glycan cap might instead serve to maintain a certain density or arrangement of GP trimers at the cell surface, which might lead to occlusion of the KZ52 epitope.

Additionally, these studies demonstrate that the presence of the mucin and glycan cap domains partially prevent binding of KZ52 antibodies to the surface of pseudovirions and significantly prevent their immunoprecipitation (Figure 4-3). These data suggest that our model of a GP-mediated glycan shield at the cell surface may also apply to the virion surface. This concept may be best described for HIV, in which a similar glycan shield model has been described [39]. Glycosylation sites on HIV envelope have been observed to mutate in response to antibody pressure, and their removal has been shown to increase antibody sensitivity [39,40]. EBOV GP glycosylation may act in a similar manner to modulate antibody binding (Figure 4-3 B); however, our neutralization data have not

revealed any difference in KZ52 sensitivity between forms of GP that possess or lack the ability to shield. It is possible that the amount of antibody that is able to bind GP pseudovirions is fully sufficient to neutralize particles so that any increase in antibody opsonization does not impact neutralization. However, it is also important to note that these assays have been performed using lentiviral pseudotyped particles, which are relatively easy to produce and assay for infectivity, but may not accurately reflect the arrangement or density of glycoprotein trimers on the surface of filoviral particles. For a more biologically relevant comparison, neutralization assays should be performed using filamentous virus-like particles.

The ability of GP to shield the virion surface could impact pathogenesis in several ways. The modulation of antibody binding to neutralizing epitopes could prolong the clearance of virus by the humoral response. This strategy could explain, in part, the observations that the infusion of convalescent blood or passive transfer of antibodies- including the KZ52 antibody studied here- can fail to protect experimentally infected animals [12,13,15,16]. Virion shielding might also be critical in the natural animal reservoir, proposed to be several species of fruit bats, in which EBOV may need to successfully evade the adaptive immune response over a long time [41]. Additionally, the ability of GP to shield the virion surface could impact the ability of the innate immune response to clear the virus. Complement-mediated neutralization can occur with antibodies through the classical pathway, without antibody opsonization through the alternative pathway, or through interactions with mannose binding lectin (MBL) [42,43]. Indeed, the glycans on GP have been found to contain significant amounts of mannose,

and one study has reported that GP-bearing pseudotypes can be neutralized by complement, in part through the MBL pathway [44,45,46]. However, it is possible that the ability to sterically shield the virion surface provides partial protection from complement. It may be interesting to compare the effects of complement-mediated neutralization on pseudotypes bearing GP or primed GP. Taken together, these data indicate that highly-glycosylated domains within GP can place steric constraints on the cell and virion surface, and suggest further study should be conducted into the effects this may have on the recognition and neutralization of EBOV by the immune system.

4.6 Acknowledgements

The authors would like to acknowledge Rachel Kaletsky and Caitlin Alyse Baiduc for experimental assistance. The authors would also like to thank Erica Ollmann Saphire and Dennis Burton for providing the KZ52 antibody, and Devon Shedlock for helpful discussion. This work was funded by Public Health Service grants T32GM07229, T32AI055400 (JF) and R01-AI43455 (PB).

4.7 References

1. Sanchez A, Khan AS, Zaki SR, Nabel GJ, Ksiazek TG, et al. (2001) Filoviridae: Marburg and Eboila Viruses. In: Knipe DM, Howley PM, Griggen DE, Lamb RA, Martin MA et al., editors. Fields Virology: Lippincott, Williams & Wilkins. pp. 1279-1304.
2. Towner JS, Sealy TK, Khristova ML, Albarino CG, Conlan S, et al. (2008) Newly discovered ebola virus associated with hemorrhagic fever outbreak in Uganda. PLoS Pathog 4: e1000212.
3. Mahanty S, Bray M (2004) Pathogenesis of filoviral haemorrhagic fevers. The Lancet Infectious Diseases 4: 487-498.
4. Sanchez A, Lukwiya M, Bausch D, Mahanty S, Sanchez AJ, et al. (2004) Analysis of human peripheral blood samples from fatal and nonfatal cases of Ebola (Sudan) hemorrhagic fever: cellular responses, virus load, and nitric oxide levels. J Virol 78: 10370-10377.
5. Baize S, Leroy EM, Georges-Courbot MC, Capron M, Lansoud-Soukate J, et al. (1999) Defective humoral responses and extensive intravascular apoptosis are associated with fatal outcome in Ebola virus-infected patients. Nat Med 5: 423-426.
6. Ksiazek TG, Rollin PE, Williams AJ, Bressler DS, Martin ML, et al. (1999) Clinical virology of Ebola hemorrhagic fever (EHF): virus, virus antigen, and IgG and IgM antibody findings among EHF patients in Kikwit, Democratic Republic of the Congo, 1995. J Infect Dis 179 Suppl 1: S177-187.
7. Geisbert TW, Hensley LE, Larsen T, Young HA, Reed DS, et al. (2003) Pathogenesis of Ebola hemorrhagic fever in cynomolgus macaques: evidence that dendritic cells are early and sustained targets of infection. Am J Pathol 163: 2347-2370.
8. Reed DS, Hensley LE, Geisbert JB, Jahrling PB, Geisbert TW (2004) Depletion of peripheral blood T lymphocytes and NK cells during the course of ebola hemorrhagic Fever in cynomolgus macaques. Viral Immunol 17: 390-400.
9. Takada A, Ebihara H, Jones S, Feldmann H, Kawaoka Y (2007) Protective efficacy of neutralizing antibodies against Ebola virus infection. Vaccine 25: 993-999.
10. Jahrling PB, Geisbert TW, Geisbert JB, Swearengen JR, Bray M, et al. (1999) Evaluation of immune globulin and recombinant interferon-alpha2b for treatment of experimental Ebola virus infections. J Infect Dis 179 Suppl 1: S224-234.
11. Wilson JA, Hevey M, Bakken R, Guest S, Bray M, et al. (2000) Epitopes involved in antibody-mediated protection from Ebola virus. Science 287: 1664-1666.
12. Pushko P, Bray M, Ludwig GV, Parker M, Schmaljohn A, et al. (2000) Recombinant RNA replicons derived from attenuated Venezuelan equine encephalitis virus protect guinea pigs and mice from Ebola hemorrhagic fever virus. Vaccine 19: 142-153.
13. Olinger GG, Bailey MA, Dye JM, Bakken R, Kuehne A, et al. (2005) Protective cytotoxic T-cell responses induced by venezuelan equine encephalitis virus replicons expressing Ebola virus proteins. J Virol 79: 14189-14196.

14. Parren PW, Geisbert TW, Maruyama T, Jahrling PB, Burton DR (2002) Pre- and postexposure prophylaxis of Ebola virus infection in an animal model by passive transfer of a neutralizing human antibody. J Virol 76: 6408-6412.
15. Oswald WB, Geisbert TW, Davis KJ, Geisbert JB, Sullivan NJ, et al. (2007) Neutralizing antibody fails to impact the course of Ebola virus infection in monkeys. PLoS Pathog 3: e9.
16. Jahrling PB, Geisbert JB, Swearengen JR, Larsen T, Geisbert TW (2007) Ebola hemorrhagic fever: evaluation of passive immunotherapy in nonhuman primates. J Infect Dis 196 Suppl 2: S400-403.
17. Mupapa K, Massamba M, Kibadi K, Kuvula K, Bwaka A, et al. (1999) Treatment of Ebola hemorrhagic fever with blood transfusions from convalescent patients. International Scientific and Technical Committee. J Infect Dis 179 Suppl 1: S18-23.
18. Wilson JA, Hart MK (2001) Protection from Ebola virus mediated by cytotoxic T lymphocytes specific for the viral nucleoprotein. J Virol 75: 2660-2664.
19. Hensley LE, Mulangu S, Asiedu C, Johnson J, Honko AN, et al. Demonstration of cross-protective vaccine immunity against an emerging pathogenic Ebolavirus Species. PLoS Pathog 6: e1000904.
20. Sanchez A, Trappier SG, Mahy BW, Peters CJ, Nichol ST (1996) The virion glycoproteins of Ebola viruses are encoded in two reading frames and are expressed through transcriptional editing. Proceedings of the National Academy of Sciences of the United States of America 93: 3602-3607.
21. Volchkova VA, Feldmann H, Klenk HD, Volchkov VE (1998) The nonstructural small glycoprotein sGP of Ebola virus is secreted as an antiparallel-orientated homodimer. Virology 250: 408-414.
22. Volchkov VE, Volchkova VA, Muhlberger E, Kolesnikova LV, Weik M, et al. (2001) Recovery of infectious Ebola virus from complementary DNA: RNA editing of the GP gene and viral cytotoxicity. Science 291: 1965-1969.
23. Volchkov VE, Feldmann H, Volchkova VA, Klenk HD (1998) Processing of the Ebola virus glycoprotein by the proprotein convertase furin. Proc Natl Acad Sci U S A 95: 5762-5767.
24. Jeffers SA, Sanders DA, Sanchez A (2002) Covalent modifications of the ebola virus glycoprotein. J Virol 76: 12463-12472.
25. Lee JE, Fusco ML, Hessell AJ, Oswald WB, Burton DR, et al. (2008) Structure of the Ebola virus glycoprotein bound to an antibody from a human survivor. Nature 454: 177-182.
26. Chandran K, Sullivan NJ, Felbor U, Whelan SP, Cunningham JM (2005) Endosomal proteolysis of the Ebola virus glycoprotein is necessary for infection. Science 308: 1643-1645.
27. Hood CL, Abraham J, Boyington JC, Leung K, Kwong PD, et al. Biochemical and structural characterization of cathepsin L-processed Ebola virus glycoprotein: implications for viral entry and immunogenicity. J Virol 84: 2972-2982.
28. Kaletsky RL, Simmons G, Bates P (2007) Proteolysis of the Ebola virus glycoproteins enhances virus binding and infectivity. J Virol 81: 13378-13384.

29. Yang ZY, Duckers HJ, Sullivan NJ, Sanchez A, Nabel EG, et al. (2000) Identification of the Ebola virus glycoprotein as the main viral determinant of vascular cell cytotoxicity and injury. Nat Med 6: 886-889.
30. Chan SY, Ma MC, Goldsmith MA (2000) Differential induction of cellular detachment by envelope glycoproteins of Marburg and Ebola (Zaire) viruses. J Gen Virol 81: 2155-2159.
31. Takada A, Watanabe S, Ito H, Okazaki K, Kida H, et al. (2000) Downregulation of beta1 integrins by Ebola virus glycoprotein: implication for virus entry. Virology 278: 20-26.
32. Simmons G, Wool-Lewis RJ, Baribaud F, Netter RC, Bates P (2002) Ebola virus glycoproteins induce global surface protein down-modulation and loss of cell adherence. J Virol 76: 2518-2528.
33. Sullivan NJ, Peterson M, Yang ZY, Kong WP, Duckers H, et al. (2005) Ebola virus glycoprotein toxicity is mediated by a dynamin-dependent protein-trafficking pathway. J Virol 79: 547-553.
34. Wool-Lewis RJ, Bates P (1999) Endoproteolytic processing of the ebola virus envelope glycoprotein: cleavage is not required for function. J Virol 73: 1419-1426.
35. Lin G, Simmons G, Pohlmann S, Baribaud F, Ni H, et al. (2003) Differential N-linked glycosylation of human immunodeficiency virus and Ebola virus envelope glycoproteins modulates interactions with DC-SIGN and DC-SIGNR. J Virol 77: 1337-1346.
36. Maruyama T, Rodriguez LL, Jahrling PB, Sanchez A, Khan AS, et al. (1999) Ebola virus can be effectively neutralized by antibody produced in natural human infection. J Virol 73: 6024-6030.
37. Dube D, Brecher MB, Delos SE, Rose SC, Park EW, et al. (2009) The primed ebolavirus glycoprotein (19-kilodalton GP1,2): sequence and residues critical for host cell binding. J Virol 83: 2883-2891.
38. Shedlock DJ, Bailey MA, Popernack PM, Cunningham JM, Burton DR, et al. Antibody-mediated neutralization of Ebola virus can occur by two distinct mechanisms. Virology 401: 228-235.
39. Wei X, Decker JM, Wang S, Hui H, Kappes JC, et al. (2003) Antibody neutralization and escape by HIV-1. Nature 422: 307-312.
40. McCaffrey RA, Saunders C, Hensel M, Stamatatos L (2004) N-linked glycosylation of the V3 loop and the immunologically silent face of gp120 protects human immunodeficiency virus type 1 SF162 from neutralization by anti-gp120 and anti-gp41 antibodies. J Virol 78: 3279-3295.
41. Leroy EM, Kumulungui B, Pourrut X, Rouquet P, Hassanin A, et al. (2005) Fruit bats as reservoirs of Ebola virus. Nature 438: 575-576.
42. Ikeda K, Sannoh T, Kawasaki N, Kawasaki T, Yamashina I (1987) Serum lectin with known structure activates complement through the classical pathway. J Biol Chem 262: 7451-7454.
43. Hirsch RL (1982) The complement system: its importance in the host response to viral infection. Microbiol Rev 46: 71-85.

44. Ritchie G, Harvey DJ, Stroeher U, Feldmann F, Feldmann H, et al. Identification of N-glycans from Ebola virus glycoproteins by matrix-assisted laser desorption/ionisation time-of-flight and negative ion electrospray tandem mass spectrometry. Rapid Commun Mass Spectrom 24: 571-585.
45. Powlesland AS, Fisch T, Taylor ME, Smith DF, Tissot B, et al. (2008) A novel mechanism for LSECtin binding to Ebola virus surface glycoprotein through truncated glycans. J Biol Chem 283: 593-602.
46. Ji X, Olinger GG, Aris S, Chen Y, Gewurz H, et al. (2005) Mannose-binding lectin binds to Ebola and Marburg envelope glycoproteins, resulting in blocking of virus interaction with DC-SIGN and complement-mediated virus neutralization. J Gen Virol 86: 2535-2542.

CHAPTER 5 – GENERAL DISCUSSION AND FUTURE DIRECTIONS

5.1 Summary of major conclusions

This dissertation contains three chapters exploring the interactions of the Ebola virus (EBOV) glycoprotein (GP) with host cellular and immune responses. In chapter 2 we examined several requirements necessary for GP to induce cytopathology in cells. The most striking conclusion from this chapter is the demonstration that the mucin domain of GP can cause cytopathology when expressed within the context of the irrelevant avian glycoprotein, Tva (Figure 2-1 E and Figure 2-2). The mucin domain potently induced cell rounding, detachment, and the loss of surface staining by flow cytometry in a manner that was nearly indistinguishable from the full-length GP. The mucin domain was previously known to be necessary for these effects, as genetic deletion of this domain abolished GP-induced cytopathology [1,2,3]. However, the determination that this domain was not only necessary, but also sufficient to cause cytopathology represented a quantum step in our understanding of the mechanism of GP-mediated cytopathology. Chapter 2 also provided data indicating that GP was acting in a post-ER step of the secretory pathway and was not acting through a dynamin-dependent pathway. These were incremental advances in our understanding of the biology of cytopathology, but they helped us to focus our attention on the plasma membrane as playing a critical role in this phenomenon. These findings, especially the fact that the mucin domain could be displayed at the cell surface on a heterologous protein and cause cytopathology, lead us to consider a model of steric hindrance, which is the focus of chapter 3.

Chapter 5

Chapter 3 is an in-depth study of the cellular mechanism of EBOV GP-mediated cytopathology. This chapter addresses two basic observations, and then hypothesizes a single model to account for both. The first is the observation that, in cells displaying full detachment from the culture dish, surface staining for GP was dim by flow cytometry (Figure 3-1 B). This was counter-intuitive because such drastic cytopathology seemed likely to occur in cells with the highest level of GP expression. Therefore, we proposed the model that the epitope used in that analysis was occluded from antibody access due to its position at the base of the structure of GP, buried under the mucin domain. We went on to demonstrate that different epitopes on GP displayed different levels of staining by flow cytometry, depending on their position relative to the mucin domain and glycan cap. These experiments served as a proof of concept for our shielding model. We then tested this model in reference to the second observation, which is that by flow cytometry GP appeared to down-modulate host surface proteins. The critical experiment in chapter 3 is found in Figure 3-4 D, in which DTT was used to strip GP_1 subunits off the cell surface. The result of this treatment was the uncovering of previously-shielded epitopes and was direct evidence that GP was occluding surface proteins at the plasma membrane. We then went on to test the next logical hypothesis about the ability of GP to shield at the cell surface: we hypothesized and found that glycosylation on GP played a significant role in steric shielding. Our approach to analyzing surface glycans centered on enzymatic removal of sugars from the cells surface with glycosidases, which again revealed previously-shielded surface proteins (Figure 3-5). The strength of the approaches taken here lie in the fact that cells in which cytopathology had already occurred could be

manipulated to show that surface proteins that had been shielded could be uncovered. These experiments strongly supported our model that GP, by virtue of the highly-glycosylated mucin domain, sterically occluded surface epitopes from antibody recognition. This model also explained our data from chapter 2, suggesting that the mucin domain could provide its steric shield even when expressed on the Tva protein.

The third conceptual study in this dissertation is encompassed by the experiments at the end of chapter 3 and in chapter 4. Here we wanted to further investigate the consequences of steric shielding by GP. One consequence, which had been observed by several previous groups, is that the shielding of integrins had the effect of disrupting adhesion [1,2,3,4,5,6]. Given the observation that major histocompatibility complex class 1 (MHC1) was also shielded by GP, we asked whether this had the functional outcome of disrupting antigen presentation. This hypothesis was supported by our experiments using CD8 T cells that are specifically activated by a tumor cell line displaying an antigenic peptide from the human immunodeficiency virus (HIV) (Figure 3-7). The activation of CD8 T cells was blocked on cells expressing GP, demonstrating another functional consequence of GP-mediated cytopathology.

Finally, we wanted to ask whether our model of shielding by GP applied not just to the cell surface, but to the surface of the virion as well. Chapter 4 begins to address this hypothesis and describes two interesting findings. The first is that the glycan cap- not the mucin domain- seems to be the critical domain in shielding the KZ52 antibody from the cell surface. This was somewhat surprising, as our previous studies found the mucin domain to be necessary and sufficient to shield host surface epitopes (Chapter 2). We

then used this finding to assess potential shielding of this antibody using a form of GP that lacks both the mucin domain and the glycan cap. By removing both of these domains implicated in shielding, we found evidence that GP places steric constraints on the surface of retroviral pseudovirions, which blocks immunoprecipitation (Figure 4-3). Our study went on to suggest that shielding by GP partially prevents the binding of KZ52 antibodies, but failed to find an impact on neutralization sensitivity.

5.2 Relationship of this work to previous studies

The studies presented here describe a novel mechanism for GP-mediated cytopathology that had not been previously considered. In fact, previous studies had implicated other factors in this phenomenon. First, a study by Sullivan and colleagues reported that down-regulation of surface proteins was dependent on the GTPase, dynamin [2]. This makes some conceptual sense because many surface proteins, including β1 integrin, undergo dynamin-dependent endocytosis; although, natural endocytosis of MHC1 is dynamin-independent [7,8,9]. We have directly addressed this report by repeating the experiments conducted by Sullivan *et al*., but found that dynamin had no effect on GP-mediated cytopathology (Figure 2-5). It is our opinion that previous experiments using dominant-negative (DN) dynamin were misinterpreted, due to uneven transfection levels between samples, which gave the appearance of fewer cells showing GP-mediated cytopathology in samples containing DN dynamin.

A second study investigating the mechanism of GP-mediated cytopathology found that the extracellular signal-regulated kinases types 1 and 2 (ERK 1/2) pathway

was important for the loss of host protein surface staining by flow cytometry [10]. This group presents compelling data that expression of the mucin domain decreases the phosphorylation of ERK2. In contrast, another report had found that Ebola virus-like particles (VLPs) activated the ERK pathway, and that this activation was dependent on the mucin domain [11]. Although the interactions between GP and the ERK pathway may be complex, and GP-dependent signaling likely occurs, the initial ERK investigation found that loss of staining by flow cytometry could be enhanced by ERK2 knockdown or reversed by the over expression of constitutively-active ERK2. Again, it is our opinion that these experiments were misinterpreted due to uneven transfection levels among samples.

The issue of signaling raises an important concern when studying GP-mediated cytopathology. Loss of adhesion and cellular detachment may have profound effects on cells that may relate more to the fact that the cells have detached than to the fact that GP is expressed. For example, it has been reported that GP-induced detachment of primary human cardiac microvascular endothelial cells results in apoptotic cell death [12]. This anchorage-dependent apoptosis, or anoikis, likely results from "outside-in" signaling by integrins through the phosphoinositide-3 kinase/AKT and other pathways to begin programmed cell death [13,14,15]. Additionally, upon detachment, integrin signaling at focal adhesions is lost, leading to the inactivation of focal adhesion kinase and the subsequent loss of ERK signaling [16]. This likely explains the previous finding that GP leads to loss of ERK2 activation, and would indicated that GP and ERK interactions are only indirect [10]. Interestingly, different cell types have different dependences on

anchorage for survival. A previous report from our group found that 293T cells transiently expressing GP readily detached from the culture substrate, but remained viable and regained adherence after additional culturing [1]. Taken together, these studies highlight the need for careful consideration when examining the biology of detached cells from adherent lines.

Another area of concern when studying GP-mediated cytopathology is the relative expression level of GP achieved during transient expression compared to GP expression during EBOV infection. It is possible or even likely that GP levels produced during infection can be exceeded by over-expression systems. Moreover, we have observed that GP-induced epitope shielding occurs only when GP expression reaches a certain threshold (discussed in section 2.5), and others have reported that when GP expression is driven by less active vectors, cytopathology is not observed [17]. Is it possible, then, that the phenomenon of GP-mediated cytopathology is simply an artifact of over-expression? Two reports have addressed this issue directly. In the first, 293T cells were infected with EBOV; rounded and floating cells were observed at significant levels at 24 and 48 hours post infection, and loss of integrin and MHC1 staining was observed by 48 hours [17]. The second study compared GP expression levels from an adenoviral expression system to EBOV infection in human umbilical vein endothelial cells, both of which were found to induce cell rounding. This report determined that GP expression levels were equivalent by western blot [3]. These studies indicate that GP-mediated cytopathology occurs during EBOV infection and that GP expression does not have to be driven to non-physiological levels to study these effects. Although the studies in this dissertation were not repeated

using live EBOV, we have used both an Adenoviral expression system and mammalian expression vectors at carefully titrated levels to guard against overt over-expression.

The studies presented in this dissertation benefited greatly from the determination of the crystal structure of the EBOV GP by the Saphire lab, which was published as our work was ongoing [18]. Our hypothesis that the mucin domain and glycan cap might provide a steric shield to nearby epitopes is conceptually supported by the position and size of these domains. The co-crystallization of GP with the KZ52 Fab further supports our model, because the position of this epitope is demonstrated to be beneath the heavily-glycosylated domains of GP. The mucin domain was genetically deleted in the construct used to determine the structure; however, its general position was modeled (Figure 1-4). Of note, the Saphire lab recently presented a low-resolution structure of the mucin domain within soluble, trimeric GP, determined by small-angle X-ray scattering [19]. This structure indicates that the mucin domain extends up and out to the side of the chalice-structured globular core, again supporting the concept that this domain could provide steric shielding to nearby proteins.

Our model of steric hindrance by GP at the cell surface is additionally supported by a recent study that compared surface staining of cells expressing GP using a panel of anti- GP monoclonal antibodies [20]. This study concluded that differences in GP surface staining were due to masking by GP and that this likely applied to other host surface proteins. This study proposes an identical model of steric occlusion to the one presented here, but their evidence is indirect. They do not directly test their model by mapping the epitopes of their monoclonal antibodies to show that epitope shielding occurs relative to

the highly-glycosylated regions. They use immunofluorescence and biochemical membrane fractionation to show that surface levels of affected host proteins are unchanged by GP - a finding that is highly suggestive of shielding - but do not provide direct evidence of the model by uncovering previously-shielded epitopes, as we have done in these studies.

One interesting product of these studies is the development of our primed GP construct. Primed GP mimics the cathepsin processing that occurs during viral entry to expose the receptor-binding domain (RBD) and allow for fusion [21,22,23,24]. Because this is a critical step in the EBOV replication cycle, we have endeavored to characterize primed GP to demonstrate its potential utility as tool for the study of EBOV entry (Figure 4-1). Therefore, it was concerning that Shedlock *et al*., found that cathepsin L-processed GP could not longer be immunoprecipitated by the KZ52 antibody and pseudovirions bearing cathepsin L-processed GP could not be neutralized by KZ52 [25]. This disagreed with our findings that primed GP-bearing pseudovirions could be immunoprecipitated and neutralized by KZ52 (Figures 4-3 and 4-4) and calls into question our claim that our primed GP construct accurately reflects the structure of cathepsin-processed GP. As discussed at length in section 4.5, *in vitro* cathepsin treatment may result in a less stable form of GP that more readily undergoes further conformational rearrangements, which would likely destroy the KZ52 epitope. Alternatively, cathepsin could be proteolytically cleaving at a non-canonical site other than in the disordered loop that connects the glycan cap to the head domain, which would not be reproduced by our primed GP construct. This seems unlikely though, as an in-depth biochemical analysis of the GP products of

cathepsin L processing identified the disordered loop as the only region of proteolysis [23]. Furthermore, that report also found by surface plasmon resonance that the KZ52 antibody could bind soluble cathepsin-processed GP. In separate studies not germane to this dissertation, we have preliminary data suggesting that primed GP also mimics the increased binding and infectivity associated with *in vitro* cathepsin processing of GP [24,26]. Therefore, we re-assert our claim that our primed GP construct accurately reflects the processing of GP by cathepsin L, and that this construct should be of use in the study of EBOV entry.

5.3 Role of GP-mediated cytopathology in EBOV pathogenesis

One major focus of this dissertation was to explore the functional consequences of steric occlusion by GP. We have approached this topic from two angles: the shielding of host surface proteins and the shielding of neutralizing epitopes on GP. It has been appreciated by many groups that GP disrupts cell adhesion [1,2,3,4,5,6]. The fact that the mucin domain is necessary and sufficient for this effect is not entirely surprising, as cellular mucin proteins have long been known to be potent modulators of adhesion through a similar mechanism of steric hindrance [27,28,29,30,31]. However, we also noted that work on mucin proteins in the field of cancer biology has demonstrated that cellular mucin proteins may also act to protect tumor cells from recognition by the immune system [30,32,33]. One particularly intriguing report proposed a model of steric shielding of the cell surface by Muc4, which would then prevent antibody and cytotoxic

lymphocyte recognition of a cancerous cell [32]. Because we have also demonstrated potent shielding of MHC1, we investigated the role of shielding in blocking interactions with cytotoxic T cells (Figure 3-7). Our findings suggest that GP expression could protect infected target cells from cellular immune surveillance in a similar manner to that observed in mucin-expressing cancer cells. It is unknown whether this mechanism occurs during EBOV infection. One could argue that because EBOV induces bystander apoptosis of lymphocytes, an adaptive immune response is not an important factor that has to be directly avoided during infection [34,35,36]. However, these observations are specific to humans and non-human primates, which are non-natural hosts for EBOV. In the natural host to EBOV, possibly fruit bats, the virus may have established an interplay with the immune response in which it is necessary to avoid the killing of infected cells by cytotoxic lymphocytes. Additionally, the disruption of MHC and other cellular adhesion molecules may have the functional consequence of preventing professional antigen presenting cells (APCs) from trafficking or properly stimulating lymphocytes. It is known that monocytes and dendritic cells are early targets of infection and that these cells are functionally compromised by EBOV infection [37,38,39,40]. While the active suppression of the interferon response by EBOV VP24 and VP35 plays a likely role in disrupting APCs' effector functions, GP-mediated disruption of surface protein function may further compromise their activities. Indeed, we have previously shown that PECAM-1, a cell-adhesion molecule critical for leukocyte diapedesis, is shielded by GP in HUVEC cells [1].

The second aspect of GP-mediated cytopathology is the ability to shield

neutralizing epitopes on GP. From this observation, we designed experiments to test whether shielding of the neutralizing KZ52 epitope would affect pseudovirion neutralization (Figure 4-4). Despite our inability to observe such an effect using lentiviral pseudovirions, we have observed that GP places steric constraints on these particles that may prevent antibody binding (Figure 4-3). There is also reason to believe that the glycosylated regions on GP may impact the immune response to EBOV virions. Indirect evidence for this theory can be found in a study in which mice were vaccinated with full-length or cathepsin-processed GP [23]. The authors found that sera from the cathepsin-treated GP samples was 3-fold better at neutralizing GP-bearing lentiviral pseudovirions. This suggests that the mucin domain and glycan cap are partially preventing the immune response from making antibodies to the most potently neutralizing epitopes. It follows, then, that GP lacking these domains might be more easily neutralized during infection. This model is reminiscent of one proposed for HIV, in which N-linked glycans on the envelope protein (Env) serve to protect critical components, including the CD4 receptor-binding domain, from antibody pressure [41]. Indeed, current HIV vaccination strategies involve the modulation of Env glycosylation sites to illicit more protective immune responses [42,43]. Here again, it is likely that the effect of protection of EBOV from neutralizing antibodies may be more vital in the natural host to EBOV, in which the virus may persist for long enough to encounter pressure from a humoral immune response. Interestingly, it has been reported that antibody responses from human survivors of Ebola hemorrhagic fever were primarily directed against the VP40 protein and the nucleoprotein [34]. It seems likely, then, that steric shielding can occur on EBOV

particles, but the contribution of this mechanism on pathogenesis needs to be further characterized.

5.4 Future directions

The studies in this dissertation have elucidated the cellular mechanism of GP-mediated cytopathology. However, significant questions are raised by this work that remain to be addressed. Although our model of steric shielding at the plasma membrane is well supported by the studies in chapter 3, the observation of a threshold requirement for GP to shield surface epitopes could be further explored. It is clear from our work and that of other groups that low levels of GP expression do not cause cell detachment or loss of surface staining by flow cytometry (Figure 2-4 and [17]). What changes occur in cells that have just reached the threshold of GP expression necessary to cause cytopathology? One possibility is that surface GP re-localizes into specific microdomains, such as lipid rafts, at a certain surface density. GP has been suggested to target to lipid rafts during infection; however, in-depth studies have not been conducted [44]. Additionally, our finding that the GP mucin domain causes cytopathology from the transmembrane-anchored, but not GPI-anchored form of Tva suggests the importance of surface microdomains (Figure 2-2). It would be feasible to stain cells for GP, and then sort cells by flow cytometry that do or do not display the required GP expression for cytopathology. These populations could then be fractionated on density gradients to query whether GP has localized into low-density fractions containing lipid raft components.

Another intriguing question left unanswered by these studies is the stoichiometric

requirements for GP-mediated cytopathology. For example, does it take one GP trimer to effectively shield an integrin molecule or does it take 5 or 10 trimers? This question could potentially be answered using quantitative flow cytometry to measure and compare the number of surface molecules of GP to that of an affected host protein. This requires identifying antibodies whose epitopes are not shielded by GP so that an accurate comparison would be made. We and other groups have shown that such un-shielded epitopes can be found on GP; however, our analysis of several MHC1 epitopes suggests this could be more challenging for host surface proteins (Figures 3-3, 3-6 and [20]).

Our observation that MHC1 is functionally shielded by GP so that they cannot be recognized by CD8 T cell receptors raises the possibility that EBOV infected cells would become targets for natural killer (NK) cells (Figure 3-7). However, killing by NK cells requires not only the loss of MHC1, but also the engagement of NK activating ligands [45,46]. Therefore, it would be interesting to ask whether GP also sterically shields surface MICA, MICB and ULBP proteins, which are activating ligands for the NK receptor, NKG2D [47,48]. Effective shielding of these ligands might block the activation and subsequent killing of targets by NK cells.

Our observations that GP may shield the surface of the viral particle require further experimentation in two areas. The first extends from the finding that the GP mucin and glycan cap domains limit the amount of KZ52 antibody bound to pseudovirions, yet do not alter the neutralization profile to this antibody (Figures 4-3 and 4-4). Variations in virion surface density or arrangement of glycoproteins could vary depending on the type of particle used to pseudotype GP. Therefore, filamentous Ebola

VLPs should be used in neutralization assays, as they will more accurately reflect the nature of EBOV virions. It should be noted, though, that production of VLPs gives rise to a heterogeneous population of particles that have different morphologies. Recent work on Marburg virus VLPs demonstrated that filamentous particles exclude host proteins that are often incorporated into more vesicular particles, which co-purify in VLP preparations [49]. Because the presence of host proteins may affect levels of GP incorporation, vesicular particles need to be purified away from filamentous particles.

The finding that GP may shield the particle surface also raises the possibility that this could help protect virions from complement-mediated neutralization. One study has examined the sensitivity of GP-bearing pseudovirions and found them to be sensitive to complement [50]. It would be interesting to ask whether complement sensitivity is altered by the presence of the mucin and glycan cap domains. It is possible that steric shielding could effectively prevent the deposition of complement components, an effect that would perhaps be more pronounced with VLPs.

These additional experiments and future directions will help clarify the mechanism by which GP sterically shields proteins in the surrounding membrane. They will also begin to query the role that GP-mediated cytopathology plays in viral pathogenesis and potentially illuminate new ways in which EBOV counters the immune response. Ultimately, the best method to study the effects of GP-mediated cytopathology will be the creation of EBOV with genetic deletions in the GP mucin domain and glycan cap. This is technically feasible, as a reverse genetic system exists for EBOV [6,51]. However, EBOV containing deletions in the highly-glycosylated domains of GP could

complicate studies of pathogenesis because of the critical roles these domains may play in viral entry.

5.5 References

1. Simmons G, Wool-Lewis RJ, Baribaud F, Netter RC, Bates P (2002) Ebola virus glycoproteins induce global surface protein down-modulation and loss of cell adherence. J Virol 76: 2518-2528.
2. Sullivan NJ, Peterson M, Yang ZY, Kong WP, Duckers H, et al. (2005) Ebola virus glycoprotein toxicity is mediated by a dynamin-dependent protein-trafficking pathway. J Virol 79: 547-553.
3. Yang ZY, Duckers HJ, Sullivan NJ, Sanchez A, Nabel EG, et al. (2000) Identification of the Ebola virus glycoprotein as the main viral determinant of vascular cell cytotoxicity and injury. Nat Med 6: 886-889.
4. Takada A, Watanabe S, Ito H, Okazaki K, Kida H, et al. (2000) Downregulation of beta1 integrins by Ebola virus glycoprotein: implication for virus entry. Virology 278: 20-26.
5. Chan SY, Ma MC, Goldsmith MA (2000) Differential induction of cellular detachment by envelope glycoproteins of Marburg and Ebola (Zaire) viruses. J Gen Virol 81: 2155-2159.
6. Volchkov VE, Volchkova VA, Muhlberger E, Kolesnikova LV, Weik M, et al. (2001) Recovery of infectious Ebola virus from complementary DNA: RNA editing of the GP gene and viral cytotoxicity. Science 291: 1965-1969.
7. Vassilieva EV, Gerner-Smidt K, Ivanov AI, Nusrat A (2008) Lipid rafts mediate internalization of beta1-integrin in migrating intestinal epithelial cells. Am J Physiol Gastrointest Liver Physiol 295: G965-976.
8. Ng T, Shima D, Squire A, Bastiaens PI, Gschmeissner S, et al. (1999) PKCalpha regulates beta1 integrin-dependent cell motility through association and control of integrin traffic. Embo J 18: 3909-3923.
9. Naslavsky N, Weigert R, Donaldson JG (2003) Convergence of non-clathrin- and clathrin-derived endosomes involves Arf6 inactivation and changes in phosphoinositides. Mol Biol Cell 14: 417-431.
10. Zampieri CA, Fortin JF, Nolan GP, Nabel GJ (2007) The ERK mitogen-activated protein kinase pathway contributes to Ebola virus glycoprotein-induced cytotoxicity. J Virol 81: 1230-1240.
11. Martinez O, Valmas C, Basler CF (2007) Ebola virus-like particle-induced activation of NF-kappaB and Erk signaling in human dendritic cells requires the glycoprotein mucin domain. Virology 364: 342-354.
12. Ray RB, Basu A, Steele R, Beyene A, McHowat J, et al. (2004) Ebola virus glycoprotein-mediated anoikis of primary human cardiac microvascular endothelial cells. Virology 321: 181-188.
13. Frisch SM, Screaton RA (2001) Anoikis mechanisms. Curr Opin Cell Biol 13: 555-562.
14. Zhan M, Zhao H, Han ZC (2004) Signalling mechanisms of anoikis. Histol Histopathol 19: 973-983.
15. Frisch SM, Francis H (1994) Disruption of epithelial cell-matrix interactions induces apoptosis. J Cell Biol 124: 619-626.

16. Schlaepfer DD, Hanks SK, Hunter T, van der Geer P (1994) Integrin-mediated signal transduction linked to Ras pathway by GRB2 binding to focal adhesion kinase. Nature 372: 786-791.
17. Alazard-Dany N, Volchkova V, Reynard O, Carbonnelle C, Dolnik O, et al. (2006) Ebola virus glycoprotein GP is not cytotoxic when expressed constitutively at a moderate level. J Gen Virol 87: 1247-1257.
18. Lee JE, Fusco ML, Hessell AJ, Oswald WB, Burton DR, et al. (2008) Structure of the Ebola virus glycoprotein bound to an antibody from a human survivor. Nature 454: 177-182.
19. Saphire EO, Dias JM, Keuhne AI, Abelson DM, Muhammad M, et al. Crystal structure of Sudan GP reveals a shared solution for neturalizing Ebolaviruses; 2010; Tokyo, Japan.
20. Reynard O, Borowiak M, Volchkova VA, Delpeut S, Mateo M, et al. (2009) Ebolavirus glycoprotein GP masks both its own epitopes and the presence of cellular surface proteins. J Virol 83: 9596-9601.
21. Chandran K, Sullivan NJ, Felbor U, Whelan SP, Cunningham JM (2005) Endosomal proteolysis of the Ebola virus glycoprotein is necessary for infection. Science 308: 1643-1645.
22. Dube D, Brecher MB, Delos SE, Rose SC, Park EW, et al. (2009) The primed ebolavirus glycoprotein (19-kilodalton GP1,2): sequence and residues critical for host cell binding. J Virol 83: 2883-2891.
23. Hood CL, Abraham J, Boyington JC, Leung K, Kwong PD, et al. Biochemical and structural characterization of cathepsin L-processed Ebola virus glycoprotein: implications for viral entry and immunogenicity. J Virol 84: 2972-2982.
24. Kaletsky RL, Simmons G, Bates P (2007) Proteolysis of the Ebola virus glycoproteins enhances virus binding and infectivity. J Virol 81: 13378-13384.
25. Shedlock DJ, Bailey MA, Popernack PM, Cunningham JM, Burton DR, et al. Antibody-mediated neutralization of Ebola virus can occur by two distinct mechanisms. Virology 401: 228-235.
26. Schornberg K, Matsuyama S, Kabsch K, Delos S, Bouton A, et al. (2006) Role of endosomal cathepsins in entry mediated by the Ebola virus glycoprotein. J Virol 80: 4174-4178.
27. Wesseling J, van der Valk SW, Hilkens J (1996) A mechanism for inhibition of E-cadherin-mediated cell-cell adhesion by the membrane-associated mucin episialin/MUC1. Mol Biol Cell 7: 565-577.
28. Wesseling J, van der Valk SW, Vos HL, Sonnenberg A, Hilkens J (1995) Episialin (MUC1) overexpression inhibits integrin-mediated cell adhesion to extracellular matrix components. J Cell Biol 129: 255-265.
29. Fukuda M (2002) Roles of mucin-type O-glycans in cell adhesion. Biochim Biophys Acta 1573: 394-405.
30. Hollingsworth MA, Swanson BJ (2004) Mucins in cancer: protection and control of the cell surface. Nat Rev Cancer 4: 45-60.

31. Komatsu M, Carraway CA, Fregien NL, Carraway KL (1997) Reversible disruption of cell-matrix and cell-cell interactions by overexpression of sialomucin complex. J Biol Chem 272: 33245-33254.
32. Komatsu M, Yee L, Carraway KL (1999) Overexpression of sialomucin complex, a rat homologue of MUC4, inhibits tumor killing by lymphokine-activated killer cells. Cancer Res 59: 2229-2236.
33. van de Wiel-van Kemenade E, Ligtenberg MJ, de Boer AJ, Buijs F, Vos HL, et al. (1993) Episialin (MUC1) inhibits cytotoxic lymphocyte-target cell interaction. J Immunol 151: 767-776.
34. Baize S, Leroy EM, Georges-Courbot MC, Capron M, Lansoud-Soukate J, et al. (1999) Defective humoral responses and extensive intravascular apoptosis are associated with fatal outcome in Ebola virus-infected patients. Nat Med 5: 423-426.
35. Sanchez A, Lukwiya M, Bausch D, Mahanty S, Sanchez AJ, et al. (2004) Analysis of human peripheral blood samples from fatal and nonfatal cases of Ebola (Sudan) hemorrhagic fever: cellular responses, virus load, and nitric oxide levels. J Virol 78: 10370-10377.
36. Reed DS, Hensley LE, Geisbert JB, Jahrling PB, Geisbert TW (2004) Depletion of peripheral blood T lymphocytes and NK cells during the course of ebola hemorrhagic Fever in cynomolgus macaques. Viral Immunol 17: 390-400.
37. Geisbert TW, Hensley LE, Larsen T, Young HA, Reed DS, et al. (2003) Pathogenesis of Ebola hemorrhagic fever in cynomolgus macaques: evidence that dendritic cells are early and sustained targets of infection. Am J Pathol 163: 2347-2370.
38. Mahanty S, Hutchinson K, Agarwal S, McRae M, Rollin PE, et al. (2003) Cutting edge: impairment of dendritic cells and adaptive immunity by Ebola and Lassa viruses. J Immunol 170: 2797-2801.
39. Bosio CM, Aman MJ, Grogan C, Hogan R, Ruthel G, et al. (2003) Ebola and Marburg viruses replicate in monocyte-derived dendritic cells without inducing the production of cytokines and full maturation. J Infect Dis 188: 1630-1638.
40. Bray M, Geisbert TW (2005) Ebola virus: the role of macrophages and dendritic cells in the pathogenesis of Ebola hemorrhagic fever. Int J Biochem Cell Biol 37: 1560-1566.
41. Wei X, Decker JM, Wang S, Hui H, Kappes JC, et al. (2003) Antibody neutralization and escape by HIV-1. Nature 422: 307-312.
42. Bolmstedt A, Hinkula J, Rowcliffe E, Biller M, Wahren B, et al. (2001) Enhanced immunogenicity of a human immunodeficiency virus type 1 env DNA vaccine by manipulating N-glycosylation signals. Effects of elimination of the V3 N306 glycan. Vaccine 20: 397-405.
43. Mori K, Sugimoto C, Ohgimoto S, Nakayama EE, Shioda T, et al. (2005) Influence of glycosylation on the efficacy of an Env-based vaccine against simian immunodeficiency virus SIVmac239 in a macaque AIDS model. J Virol 79: 10386-10396.

44. Bavari S, Bosio CM, Wiegand E, Ruthel G, Will AB, et al. (2002) Lipid raft microdomains: a gateway for compartmentalized trafficking of Ebola and Marburg viruses. J Exp Med 195: 593-602.
45. Orange JS, Fassett MS, Koopman LA, Boyson JE, Strominger JL (2002) Viral evasion of natural killer cells. Nat Immunol 3: 1006-1012.
46. Orange JS, Ballas ZK (2006) Natural killer cells in human health and disease. Clin Immunol 118: 1-10.
47. Cosman D, Mullberg J, Sutherland CL, Chin W, Armitage R, et al. (2001) ULBPs, novel MHC class I-related molecules, bind to CMV glycoprotein UL16 and stimulate NK cytotoxicity through the NKG2D receptor. Immunity 14: 123-133.
48. Bauer S, Groh V, Wu J, Steinle A, Phillips JH, et al. (1999) Activation of NK cells and T cells by NKG2D, a receptor for stress-inducible MICA. Science 285: 727-729.
49. Kolesnikova L, Strecker T, Morita E, Zielecki F, Mittler E, et al. (2009) Vacuolar protein sorting pathway contributes to the release of Marburg virus. J Virol 83: 2327-2337.
50. Ji X, Olinger GG, Aris S, Chen Y, Gewurz H, et al. (2005) Mannose-binding lectin binds to Ebola and Marburg envelope glycoproteins, resulting in blocking of virus interaction with DC-SIGN and complement-mediated virus neutralization. J Gen Virol 86: 2535-2542.
51. Neumann G, Feldmann H, Watanabe S, Lukashevich I, Kawaoka Y (2002) Reverse genetics demonstrates that proteolytic processing of the Ebola virus glycoprotein is not essential for replication in cell culture. J Virol 76: 406-410.